An analysis of anticancer activities of drug- and DNA-loaded Nano formulations *in vitro* and *in vivo*

By

Chukhu Muj

(16LTPH03)

Under the supervision of

Prof. Anand Kumar Kondapi

Department of Biotechnology and Bioinformatics

School of Life Sciences

University of Hyderabad

Gachibowli

Hyderabad: 500046

Telangana, India

December 2022

University of Hyderabad

School of Life Sciences

Department of Biotechnology and Bioinformatics

DECLARATION

I, Chukhu Muj, hereby declare that this thesis entitled, **"An analysis of anticancer activities of drug- and DNA-loaded Nano formulations *in vitro* and *in vivo*"** submitted by me under the guidance and supervision of Prof. Anand Kumar Kondapi, is an original and independent research work. I also declare that it has not been submitted previously in part or in full to this University or any other University or Institution for the award of any degree or diploma.

Prof. Anand Kumar Kondapi
(Research Supervisor)

Prof. ANAND K. KONDAPI
Senior Professor
Dept. of Biotechnology & Bioinformatics
School of Life Sciences
University of Hyderabad
Gachibowli, Hyderabad-500 046.

Chukhu Muj
(16LTPH03)
(Research Scholar)

University of Hyderabad

School of Life Sciences

Department of Biotechnology and Bioinformatics

CERTIFICATE

This is to certify that this thesis entitled, **"An analysis of anticancer activities of drug- and DNA-loaded Nano formulations *in vitro* and *in vivo*"** is a record of bona fide work done by Chukhu Muj, a research scholar for the Ph.D. program in Department of Biotechnology and Bioinformatics, School of Life Sciences, University of Hyderabad under my guidance and supervision. The thesis is free from plagiarism and has not been submitted previously in part or in full to this or any other University or Institution for the award of any degree or diploma. Further the student has passed the following courses towards fulfillment of course work required for PhD.

S.No	Course code	Course Name	Credits	Pass/Fail
1.	BT 801	Analytical techniques	4	Pass
2.	BT 802	Research Ethics, data analysis and biostatistics	3	Pass
3.	BT 803	Lab work and Seminar	5	Pass

A. Part of this thesis has been published in the following journals:

1. **Chukhu Muj**, Satyajit Mukhopadhyay, Anand K. Kondapi*. Synergistic action of lactoferrin in enhancing the safety and effectiveness of docetaxel treatment against prostate cancer. (Under review).

B. Part of the work has been presented in the following conferences:

1. **Chukhu Muj** and Prof. Anand Kumar Kondapi. Targeted delivery of combination of doxorubicin and cyclophosphamide through lactoferrin nanoparticles for thetreatment of metastatic cancers. International Conference IABS 2018. Poster presentation, held at IACS, Kolkata.

2. **Chukhu Muj** and Prof. Anand Kumar Kondapi. Target-directed co delivery of combination chemotherapeutics for treatment of metastatic cancer. NANOBIOTECK - 2018 3rd annual conference of ISNM. Poster presentation, held at AIIMS, Delhi.

Head of Department
(DOBB)
HEAD
Dept. of Biotechnology & Bioinformatics
University of Hyderabad
Hyderabad.

Supervisor
Prof. ANAND K. KONDAPI
Senior Professor
Dept. of Biotechnology & Bioinformatics
School of Life Sciences
University of Hyderabad
Gachibowli, Hyderabad-500 046.

Dean
(School of Life Sciences)
DEAN
School of Life Sciences
University of Hyderabad
Hyderabad-500 046.

ACKNOWLEDGEMENTS

I would like to extend my sincere gratitude to my supervisor, **Prof Anand Kumar. Kondapi** for his guidance, support, and encouragement during the course of my PhD.

I offer my sincere thanks to my doctoral committee members, **Prof. Prakash Babu** and **Dr. Prakash Prabhu** for their valuable inputs.

I offer my sincere thanks to the present and former Heads of Dept. of Biotechnology & Bioinformatics, **Prof. J.S.S. Prakash**, **Prof. K.P.M.S.V Padmasree**, **Prof. Anand Kondapi** and **Prof. Niyaz Ahmed** for allowing me to use all research facilities available in the department during my work.

I am thankful to the present and former Deans of the School of Life sciences, **Prof. N. Siva Kumar, Prof. S. Dayananda**, **Prof. K.V.A Ramaiah**, **Prof. P. Reddanna**, for providing the necessary facilities in SLS during my work.

I thank **Prof. Y. Suresh** for the discussion on prostate cancer and helpful suggestions

I thank all the teaching and non-teaching staff of Biotechnology department and life sciences for their extended help during my work.

I thank Ms. Sunitha, Mr. Pankaz & Mr. Durga Prasad for their help during my work with SEM and TEM

I thank Ms.Nalini, Ms Deepti and Dushrath for their help during my work with confocal microscopy

I thank Dr. Mahesh for analysing the histological sections

I would like to thank DBT (**JRF and SRF**) for providing me Fellowship during my work and the other funding bodies of Govt of India to science ICMR, DBT and DST for providing funds to our lab during my work

Part of the work is carried out under UGC UPE-II scheme and DST Nanomission projects Funding from UGC SAP, DST FIST, and DBT Builder was useful for the infrastructure used for the experiments.

I thank my past lab members and present lab members, Dr. Prashant, Dr. Lakshmi, Dr. Hari Kiran, Dr. Kurumurthy, Dr. Kiran, Dr. Akhila, Dr. Jagadeesh, Dr. Suresh, Satyajit,

Neha, Pritikana, Sarita , Vidhya, Ritika , Hema, Tanay, Espita, Pratibha and Nandini for their help, support, and encouragement throughout my PhD journey

I would like to thank Mr. Sreenu for his help in the lab.

I would like to thank Dr. Simhadri Praveen, Dr. Kathy, Dr. Deepak Babu, Dr. Sarath Chandra, Dr. Sangeeta and friends and seniors for their help and valuable suggestions

I offer my sincere thanks to Dr. G.B Madhubabu, Dr. Indira Paddibhatla, Ravi and Dhushyant.

I thank all my friends from HCU, Capstone Church, HCU E.U friends and my friends back at home for brightening up my PhD journey.

I am grateful to my parents, **Mr. Chukhu Tanya** and **Mrs. Chukhu Queen**; my sibling's **Indu Chukhu**; **Chukhu Nyokum**, **Chukhu Nyia Loma** , **Chukhu Nyari** and **Chukhu Liza** and my wife, **Mrs. Nupur Fangaria** for their unconditional love and support.

Finally I thank **God Almighty** with all my heart, whose blessings gave me the strength to complete this journey.

Table of contents -

Abbreviations

Dox: Doxorubicin

Cp: Cyclophosphamide

Lf : Lactoferrin

LfNP : Lactoferrin nanoparticle

nDox: Doxorubicin loaded lactoferrin nanoparticle

nCp: Cyclophosphamide loaded lactoferrin nanoparticle

nDoxCp: Doxorubicin and Cyclophosphamide loaded lactoferrin nanoparticle

MES: Sodium 2-mercaptoethanesulfonate

nDox MES: Doxorubicin loaded MES lactoferrin nanoparticles

DTX-LfNP: Docetaxel loaded lactoferrin nanoparticle

p35-LfNP p53-plasmid loaded lactoferrin nanoparticle

I.V Intravenous

I.P: intraperitoneal

Mat Ly Lu: Rat prostate cancer cell line

A549 Human lung cancer cell line

LDH: Lactate dehydrogenase

AKP: Alkaline phosphatase

TNF alpha: Tumor necrosis factor alpha

IFN-γ: Interferon gamma

FE SEM: Field-emission scanning electron microscopy

TEM: Transmission Electron Microscopy

DLS: Dynamic light Scattering

FT-IR: Fourier transform infrared spectroscopy

ATR: Attenuated total reflectance

HPLC: High-performance liquid chromatography

MTT: 3-(4, 5-dimethylthiazol-2-yl)-2, 5-diphenyltetrazolium)

µg: Microgram

µl: Microlitre

nM: nanomolar

CHAPTER 1

INTRODUCTION

1. Introduction

1.1 Cancer

Cancer is a rapid unimpeded growth of cells and eventually it acquires the ability to spread to different body parts from its primary site. Generally, the uncontrolled cell growth caused by the stimulation of oncogenes and/or the deactivation of tumor suppressor genes (1). Based on tissue localization, Cancer is associated in two forms, namely benign and malignant. In benign tumors, the tumors remain in their original location without invading different sites of the body. However, in malignant tumors, the cells grow and spread to different sites of the body. Through the bloodstream or the lymphatic system, tumors can spread to other body areas. The spreading of the tumors to different body parts is called metastasis (2). Benign and malignant tumors are classified from the cell type they arise. Carcinomas, sarcomas and lymphomas are the main groups where most of the cancers fall into. Of all human cancers carcinomas, which epithelial cell malignancies account for 90% (3). Sarcomas, which are solid tumors that develop connective tissues are found in bone, muscle, fibrous tissue and cartilage (3). Leukemias, which develop from immune system and blood-forming cells, account for 8% of all human cancers (4).

Hanahan and Weinberg (2000) listed the following as the seven characteristics of cancer: - i) growth of tumors are independent of growth signals ii) insensitive to growth inhibitor signals, iii) Eluding apoptosis, iv) Can replicate unlimitedly, v) Angiogenesis is continued for an extended period of time vi) Metastasis and vii) Instability in the genome (5).

Cancer is one of the most catastrophic classes of human diseases which causes death to millions around the world every year (6). It was one of the top causes of mortality in 2020, with an estimated 19.3 million new cases of cancer and 10.3 million fatalities worldwide (7).

The number of cancer-related deaths is anticipated to increase in the near future with more than 10 million new cases each year (8).

1.2 Tumor microenvironment

Tumor microenvironment represents environment in the cells where cancerous cells or tumor cells coexist together. Cancer stem cells are present in tumors and capable of self-renewal and promoting carcinogenesis. Progression of tumor depends on collaboration between malignant and non-malignant cells to create a microenvironment (9–11). Protumorigenic function of non- malignant cells in tumor microenvironment eventuate uncontrolled cells proliferation, whereas the malignant cells intrude healthy tissues and spread through lymphatic and circulatory systems to other body parts (10).

Studies have shown that in the tumor microenvironment expression of lactoferrin was downregulated. Also the data taken from cancer patients revealed that, the high risk breast and colorectal patients group had lower expression of lactoferrin levels in comparison to those of low risk groups (12). Additionally, employing lactoferrin as a delivery vehicle against cancer might have a better impact on the therapy of cancer because lactoferrin receptors are expressed in cancerous cells and the cells associated with the tumor microenvironment (13).

1.3 Cancer metastasis

Cancer metastasis is the outspread of a tumor from its primary site to surrounding tissues, then to distant tissues and organs. It is the primary factor causing cancer-related mortality and morbidity (14). Approximately it accounts for 90% of all cancer deaths (15, 16). For the metastasis to complete the tumor cells must detach from its primary site and must go through the vesicle into the lymphatic systems and circulatory systems , escape the attack from immune cells, extravasate in the far off capillary beds, and proliferate in other bodily organs

(17). Metastasis also helps in maintaining an environment which facilitates the proliferation and development of new blood vessels, thus helps in the formation of secondary malignant tumors (16). The progression of metastasis from solid tumor is divided into the following steps (18).

Step 1 Invasion and migration

Metastatic disease begins when cancer cells invade and migrate across the stromal microenvironment and pass the basement membrane either collectively or individually (18, 19). The cancer cells invade through basement membrane and differentiate from precancerous neoplasia to malignant cancers (18).

Step 2: angiogenesis and intravasation

Angiogenesis of the tumor is defined as the development of young vasculature during the progression of tumor, which enables oxygen and nutrients delivery as well as removal of waste (20). Since the recently formed tumor vasculature is not mature and hyper permeable due to the absence of basement membrane and perivascular covering, it causes the efflux of plasma proteins which helps in the development of new vessels and intravasation of the tumor cells. Angiogenesis also aids in tumor metastasis by allowing the transfer of tumor cells to distant sites through lymphatic systems and vascular (21).

In Intravasation, tumor cells penetrate into the blood or lymphatic system through the basement membrane (22). Intravasation is facilitated by tumor vasculature, where the cells invade the vasculature. It is also a useful step in the development of metastasis to distant sites (23–25).

Step 3: survival in the circulation and attachment to the endothelium

After the intravasation step where some of the cancer cells reaches the lymphatic or blood system, even lesser number of cancer cells are able to survive in the blood vessels due to these factors such as immune stresses and hemodynamic shear forces, and collisions of the red blood cells they encounter there (26). These circulating tumor cells are then arrested in the blood vessels and they are extravasated *via* these two mechanisms: adhesion after and rolling physical occlusion (18).

Step 4 and 5: extravasation and colonization

After the tumor cells are arrested in the blood vessels these cells are then extravasated from the blood vessels to colonize in the new areas (17). In extravasation, the blood vessels where the cancer cells have entered are healthier, and due to the flow of blood in it the cancer cells experience fluid shear stresses (18).

1.4 Treatment options against cancer-

The treatment options against cancer are usually based on the localization of the cancer, type of cancer also based on the patient's health conditions. Surgery and radiation therapy is usually used against the tumor which is confined to a particular area. For metastatic cancer, chemotherapy is usually preferred.

1.4.1 Types of cancer treatment

1.4.1.1 Surgery

Depending on the cancer grade the benign tumor can be surgically removed by either removing the part of tumor or removal of the whole organ (4). Of the many cancers few cancers such as prostate, lung cancer and mastectomy of the breast cancer are the ones where surgery was successful by the removal of the complete organ.

1.4.1.2 Radiation therapy

Radiation therapy uses high radiation dose to destroy tumor cells and also helps in tumor shrinkage (27). By altering the DNA of the tumor cells, it destroys the cancer cells or perhaps inhibits their growth (27, 28). It may take days or weeks of radiation therapy for the cancer cells' DNA to be sufficiently damaged for them to die (27).

When radiation therapy is done in combination with surgery it can be given before doing the surgery to shrink the tumor size so that the tumor can be excised by surgery and reduce the chance of tumor recurrence (29). When it is given during surgery the radiation goes straight to the tumor without passing through the skin. It is also done in combination with chemotherapy before, during or after the course of radiation therapy (30, 31).

1.4.1.3 Gene therapy

Gene therapy is the transfer of a healthy and functional genetic material for the treatment of a disease (32). It treats the diseases either by silencing the overexpressed genes or by replacing the defective genes with a better one, such as in cancer where some of the genes are overexpressed or mutated (33). It has advantages over the chemotherapy to treat against cancer which often have nonspecific toxicity issues (33).

The silencing of the gene can be done by either short antisense oligonucleotides (ODNs) or using siRNA technology where it would silence the genes which are overexpressed in a diseased condition (34, 35). Another approach is the delivery of a functional gene such as p53 gene for the treatment of cancer where the particular gene is mutated in most of the cancer (36).

Nucleic acid delivery systems are of viral and non-viral types (37). Of the two viral vectors are more effective in delivering the nucleic acid due to its high delivery efficiency, but its use is limited due to their immunogenicity, oncogenicity and also that it can carry smaller DNA size (38). Non-viral vectors on the other hand are safer to use, lack immunogenicity, toxicity

is low, cost effective and no size limitation of the DNA to be delivered (39, 40). However, the main limitations of using non-viral systems is that its transfection efficiency is low, though there is an improvement in enhancing its transfection efficiency by different methods (41). There is a significant number of research studies reported on non-viral based gene delivery systems, some of them even entered the clinical trials (41). Some of the non-viral gene based therapy which is under clinical trials are GAP-DMORIE–DPyPE, DOTAP–Cholesterol, CRL1005–Benzalkonium chloride, PEI, PEI–mannose–Dextrose Poloxamer, PEG–PEI–cholesterol and GL67A–DOPE–DMPE–PEG (42).

1.4.1.4 Chemotherapy

Chemotherapy utilizes anticancer drugs for cancer treatment. It works by inhibiting the cancer from division, reducing the tumor burden and thus helping by prolonging the individual's life (43). Various types of chemotherapeutic drugs are used to treat different types of cancer, either used alone or in combination (44, 45). Chemotherapy works to prevent invasion and metastasis by reducing the growth of tumor and cell proliferation (43, 46). Traditional chemotherapy medications generally affect the macromolecular synthesis and interfere function of malignant cells by inhibiting production of DNA, RNA, proteins, or metabolic activity or by compromising the performance of the preformed molecule (46). Even though, chemotherapy is widely used several limitations are there for its use, some of which are toxicity to non-cancerous cells (47), development of resistance to the chemotherapeutic agents (48, 49), low bioavailability, poor solubility of the anticancer drugs (50, 51), off-target toxicity (52) etc.

1.4.1.5 Molecularly targeted therapy

1.4.1.5.1 Antibody drug conjugate

Antibody-drug conjugates are one of the fastest growing targeted delivery therapeutics against cancer (54). It consist of monoclonal antibody (mAbs) which is conjugated to chemotherapeutic drugs, and it work on the principle that it specifically binds to the antigen which is expressed on the target cells though the selected monoclonal antibody (mAbs) (55, 56). Antibody drug conjugates (ADCs) are widely used against the treatment of cancer but its attempt is also made to treat several other diseases such as atherosclerosis, bacteremia, and inflammatory diseases and its research is still going on (57–59). Several ADCs have shown good effect against the treatment of refractory cancers but its use is limited because of its toxicities, limited biomarkers and less understood pathways of drug resistance (59, 60).

1.4.1.6 Target-directed therapy

Target-directed therapy is a mode of treatment where the drug is delivered to a particular gene or protein which is overexpressed in the cancer cell or tissue (61, 62). Its effect lies in the fact that the therapeutics is released in the tumor cells while minimising its effect in the normal cells and tissues (63). Also it increases the therapeutic dose to the target organs (64). Target-directed therapy is important in the treatment of cancer as it requires effective and specific target-specific localization in cancer cells (61).

1.4.1.7 Nanomedicine based drug delivery systems

Nanomedicine based delivery systems are delivery vehicles of dimensions in the nanometre range which are used to deliver the therapeutic agent to the target cells (65). The nanoparticles which are used for the treatment of diseases have specific shapes, sizes and surface characteristics as these aspects have an effect on the efficacy and efficiency of the Nano based drug delivery (66). Nanoparticles in the range of 10 nm to 100 nm are usually

suitable for the treatment of cancer, as they can effectively localize the chemotherapeutic agent to the cancerous cells (67), achieve increased retention effect and (EPR) enhanced permeability (68). The particles in the (1-2nm) range can escape from the normal vasculature to cause damage to the healthy cells and also can be filtered out from the kidneys, whereas the particles having the size more than 100 nm can be cleared from the circulation with the help of phagocytes (66).

1.5 Limitations of current treatment

1.5.1.1 Surgery

Even though surgical removal of the primary or even metastatic tumors help save the patients or even extend their life, its limitation is that it can help in tumor recurrence due to the shedding of cancer cells into the circulation (69). It also upregulates the adhesion molecules to the target organs, allows the survival of the circulatory cells by suppressing the antitumor immunity, and induces changes in the cancer cells and helps in metastasis (69).

1.5.1.2 Radiation therapy

The limitations of using radiation therapy is that it not only kills the tumor cells but also affects the healthy tissues (29). The adverse effects of radiation therapy are classified in the following three types-

a) Acute (early) - The toxicity of radiation therapy observed in the initial weeks after the treatment is given and it is involved usually in the intermitotic cells which are skin and mucosa (70).

b) Consequential effects- Its effects are observed when complications which arose from acute radiation therapy were not treated and it also causes persistent damage (70).

c)Late effects –It complications arise months to years after the initial exposure of the radiation therapy and it is normally involved in the post mitotic cell such as heart, kidney, liver, bone, and muscle (30, 70).

1.5.1.3 Gene therapy

The limitations of the commonly used gene therapy based on viral vectors are –

Adenovirus- insert size being small (71); the immune response lessens the infectivity of the desired target cells (72).

Adeno-associated virus- insert size being low, upon infection the humoral immunity is provoked (73).

Herpes simplex virus- optimal Immune response of the desired target cells (74); possibility of herpes encephalitis (75).

Retrovirus- Infecting frequently short-lived dividing cells, integration of genes at random sites (76), chances in development of dormant diseases, immune related diseases and cancer (38).

1.5.1.4 Chemotherapy

Poorly water soluble

Most of the commonly used chemotherapeutic drugs and also the recently developed small molecule anticancer compounds are highly lipophilic and are poorly soluble in water. However, these chemotherapeutic compounds which are poorly soluble in water are solubilized with the help of surfactants and co- solvents which have adverse detrimental effects (77).

Multi Drug resistance

In Cancer chemotheraphy, multi-drug resistance (MDR) is the cancer cells capacity to survive in the presence of various anti-cancer drugs (78). Increased release of drugs outside of cells may result in the emergence of MDR mechanisms. Consequently, these cells have limited absorption of drugs (49). The various mechanisms for the development of drug resistance are enhance efflux of drugs, which are mainly caused by the overexpression of BCRP (breast cancer resistance protein) and P-gp (P-glycoprotein) (79, 80), elevated xenobiotics mechanism (81), increased capacity DNA repair, growth factors and other genetics factors such as amplification, gene mutation and epigenetic alterations (81).

Lack of target specificity

One of the side effects of chemotherapy is that it is not able to distinguish between the cancerous and the normal cells. The anticancer agents being cytotoxic in nature not only kills the cancerous cells but also the normal cells which causes undesirable side effects in the patients (8).

1.6 Nanoformulations for cancer metastasis, importance of combination of drugs in treatment

Nanoparticles (NPs) help in combating cancer metastasis by targeting the primary cancer site toward different strategies, including triggering tumor cell apoptosis, preventing EMT, targeting cancer stem cells (CSCs), regulating the TME, or eliciting immunological responses. NPs have also been applied to modulate primary TME as a possible method for preventing and treating cancer metastasis. Numerous studies also illustrated that focusing on the activity of cancer stem cells (CSCs) could open the door to the implementation of novel therapeutic techniques with nano-combination formulations for the eradication/suppression of metastatic tumor masses (82).

Combination therapy is a type of treatment that employs two or more anticancer drugs or other therapeutic agents to combat cancer (83). The combination of the anticancer agents increases the efficacy in comparison to when drugs are given alone because of the synergistic action of both the anticancer agents (84, 85). Since, the prolonged usage of mono therapy leads to the development of drug resistance, the combination therapy approach helps in reducing the resistance from anticancer drugs and also offers additional therapeutic advantages such as, reduce in the tumor growth and metastatic potential, inducing apoptosis and reducing the population of cancer stem cells (86, 87). Furthermore, treatment using combination therapy targets multiple pathways which controls progression of disease and also reduces the possibility of cancer cells to transform into malignant and untreatable (87, 88).

1.7 Prostate cancer

Prostate cancer is the second most prevalent cancer and sixth leading cause of mortality for men (89, 90). With an estimated 375,304 fatalities and 1,414,000 new cases of cancer in males worldwide in 2020, it is the fifth greatest cause of cancer death (91). It is an age-dependent disease wherein the risk of incidence of prostate cancer rises with an increase in age (92). Studies have shown that prostate cancer is less prevalent in men below 40 years of age but 80-100% of men above the age of 80 are most susceptible to prostate cancer (93). The global population of prostate cancer is expected to increase to nearly 2.3 million new cases giving rise to a death toll of 740,000 by the year 2040 (94). The cause of prostate cancer are genetic alterations, other etiology risk factors such as intake of processed fat, consumption of red meat, Superfluous nutrients obesity (90, 95).

1.7.1 Treatment options for prostate cancer

Prostate cancer can be broadly characterized into two types, localized and metastatic (96). Surgery and radiation are the only current treatment options for localized prostate cancer (97). When localized cancer progresses to metastatic cancer, then Chemotherapy and Androgen deprivation therapies are employed to treat cancer (98). Androgen deprivation therapy was the first line of treatment for prostate cancer due to the role of the androgen receptor pathway in the disease's progression (99). However, most of the patients who underwent Androgen deprivation therapy developed resistance within a year or more (100). Docetaxel has been used as the standard treatment against hormone-refractory prostate cancer (101). However, the use of docetaxel in therapeutic applications is limited due to its insolubility in water, cytotoxicity, and development of drug resistance (102). To overcome these limitations of docetaxel, there is a requirement to develop a suitable delivery vehicle.

1.8 Lactoferrin role in cancer and prostate cancer

Lactoferrin (Lf), with a molecular weight of 80 kDa is an iron binding glycoprotein (103–105). It belongs to the transferrin family and it is expressed in most of the biological fluids (106, 107). It has protective actions such as antimicrobial, antibacterial, antiviral, antifungal and antiparasitic, to anti-inflammatory and anticancer activities (105). With a 60% sequence homology, Lactoferrin protein structure resembles serum transferrins, and it binds iron (Fe^{3+}) ions reversibly (108, 109). Therefore, lactoferrin comes under the family of transferrin, along with serum transferrin, melanotransferrin and ovotransferrin (110). Lactoferrin increases the body's ability to absorb iron (111), regulates the growth of cells, eliminates dangerous free radicals (112), and prevents the synthesis of hazardous substances. It engages in antibacterial, antiviral, antioxidative, anticancer, and anti-inflammatory activities to control immune responses (113). Numerous *in vivo* studies have shown that

Lactoferrin may have an anticancer effect (114, 115), indicating that oral administration of bovine Lf (bLf) may reduce chemically induced carcinogenesis in rodents and exhibit significant cytotoxic and anti-metastatic action against a variety of cancer cell lines (116). The stimulation of apoptosis in tumor tissues is one of the several methods by which Lf exerts its anticancer effects (117). Lf binds specifically to its receptors i.e (Lf R1, Lf R2) or to transferrin receptors which are expressed on most of the cancer lines (13). Furthermore, lactoferrin receptors are known to express in prostate cancer tissue by which it makes lactoferrin an excellent delivery vehicle for the treatment of cancer (118).

1.9 Nanoformulations for prostate cancer treatment-

Nanotechnology is cutting edge of the development of anticancer drugs, employing nanoparticles (NPs) to expedite the detection and treatment of cancer (66, 67). Nano Drug delivery systems are in high demand and extensively studied in tumor therapy (119). With the help of nanotechnology, a number of problems can be resolved, such as (a) nano-delivery systems due to its ideal size can prevent renal elimination, (b) *In vivo* nano-delivery systems can increase the efficacy, decrease the side effects of chemotherapeutic drugs and prolong the circulation time due to its targeted delivery and sustained release, and (c) It can increases EPR (enhance permeability and retention) effect and the concentrates anticancer drugs at the target site (120).

The various types of nanoparticle for the treatment for prostate cancer are as follows-

1.9.1 Liposomes

Liposomes were the first clinically approved technology for the drug delivery which effectively transformed the pharmaceutical industry (121). It consists of single or multi lipid bilayer, cholesterol and phospholipids are majorly used to encapsulate the hydrophilic drugs and can also encapsulate hydrophobic drugs. Zhang et al., (2022) used liposomes as the

delivery vehicle for co-delivery of docetaxel and resveratrol for treatment of prostate cancer. They have shown that both the drugs were released simultaneously and in sustained manner from the liposomes and also it could be targeted to the PC-3 cells (122). Studies involving liposomes in prostate cancer have few known clinical trials, which includes examination of tumor targeting efficacy of liposomes and studies were conducted only with doxorubicin liposome formulation. (122, 123).

1.9.2 Polymeric nanoparticles

Synthetic and natural polymers are typically used to prepare polymeric nanoparticles. The Diameters of these nanoparticles are less than 1 µm (124, 125). In addition to controlling the pharmacokinetic properties of various active compounds, polymeric nanoparticles can also have an impact on the biodegradability and biocompatibility of the polymers for the preparation of nanoparticles (125, 126). For actively targeting tumors Shitole et al, (2020) established chemically altered polymeric Nano capsules (NCs) , these nano capsules containing mixtures of quercetin (QU) and docetaxel (DTX) for the the treatment of prostate cancer (127).

1.9.3 Magnetic nanoparticles

A growing body of research is being done on magnetic nanoparticles (MNPs) due to their distinctive physical characteristics, biocompatibility, stability, and a variety of other characteristics (128). To precisely target the drugs to the specific location, magnetic nanoparticles can be used as effective delivery systems. As the magnetic nanoparticles interact with external magnetic fields produced by permanent magnet. Ngen et.al, (2019) designed “prostate-specific membrane antigen” targeted MNPs for the treatment of prostate cancer, accumulation of the PSMA targeted MNPs at the tumor site helps in tumor

regression. Even though the use of MNPs was approved by the FDA, the materials used for the preparation can be harmful (130).

1.9.4 Gold nanoparticles

Distinct properties of gold anoparticles (AuNPs), such as fluorescence enhancement and surface plasmon resonance (SPR), make it worthy for drug delivery and targeting, have drawn a lot of attention lately (131).

Luo et al, (2020) developed gold nanoparticles by conjugating PSMA-targeting ligands and gadolinium (Gd) Gd (III) complexes to its surface for MR-guided prostate cancer targeting therapy. The surface modification on the gold nanoparticles increased its binding affinity. They have shown that binding of Gd (III) and gold resulted better efficacy in prostate cancer cells after radiotherapy and increased uptake of AuNPs by PSMA-expressing cancer cells (132).

1.9.5 Mesoporous silica nanoparticles

Mesoporous silica nanoparticles (MSNs) are silicon materials with pores that are in the nanometer size range (133). MSNs, because of its distinctive qualities, including its large surface area, pore size and pore volume, customizable particles, ease of surface modification, high stability, and capacity to efficiently entrap therapeutics molecules, are employed in nano-drug delivery systems (134).

Chaudhary et al. (2019) developed mesoporous silica nanoparticles (MSNs) loaded with resveratrol to improve its anti-proliferative activity and also docetaxel sensitization in hypoxia-induced drug resistant prostate cancer cells (135).

1.9.6 Micelles

Self-assembly of amphiphilic polymers leads to the development of micelles, size ranges from 5 to 100 nm, which contain a hydrophobic core for encapsulating pharmaceuticals that are insoluble in water and a hydrophilic shell on the outside to keep the drug away from the surrounding medium (136, 137).Barve et al. (2020) developed polymeric micelle for targeted delivery of cabazitaxel which is biodegradable as well as enzyme responsive. In comparison to free cabazitaxel its cellular uptake was more in prostate cancer cells. Furthermore, the polymer micelles coupled with ligands showed better efficacy in prostate tumor xenograft mice (138).

1.9.7 Dendritic polymers

High-branched dendritic polymers feature a three-dimensional structure, regulated topologies, numerous terminal functional groups, low melt or solution viscosities, and good solubility (140).Properties like low solution or melt viscosity, nominate it as a potential drug (141) and gene delivery systems (142). They have a lot of potential for medicinal applications delivery (141), gene therapy (142) Lesniak et al. (2019) developed dendrimer Nano carriers using PSMA-targeted Polyamidoamine (PAMAM) functional group. Results from the study showed that the PSMA-targeted Polyamidoamine (PAMAM) dendrimers nanocarriers accumulated more in in PSMA+ PC3 PIP tumors, which also validate that PSMA+ tumor could particularly retain dendrimer nanocarrier (144).

1.9.8 Protein nanoparticles

Proteins are a class of naturally occurring molecules with distinctive properties and prospective application in the biological and material sciences. Due to its amphiphilic nature by which they can interact with both the drug and solvent makes it an ideal material for the preparation of nanoparticles (146, 147). The nanoparticles prepared from natural proteins are

metabolizable, biodegradable, and it is simple to alter its surface so that drugs and targeted ligands can be attached (121, 147). Due to its small size, protein nanoparticles can go through the cell via endocytosis. Protein nanoparticles are useful for drug delivery due to a number of benefits, including surface modification of the particles, biodegradability, stability, ease of controlling particle size, and less toxicity-related difficulties, such as immunogenicity (148). Furthermore, its stability, half-life and activity can be enhanced by protecting the drug from degradation by enzymes and renal clearance (147).

Soll et al., (2020) developed corrole-protein nanoparticles (NPs) for prostate cancer treatment. In human prostate cancer DU-145 cells, it demonstrated antineoplastic action. Additionally, they have shown that Ga/protein NPs are rapidly taken up by cells and that tumor cell necrosis is induced (149).

1.10 Importance of docetaxel and p53 in prostate cancer treatment and current limitations

Docetaxel, an anticancer drug from the taxane family that binds to tubulin and aids in microtubule stabilisation as well as cell cycle arrest and apoptosis (150). DTX showed an improved overall survival when used to treat metastatic castration-resistant prostate cancer, but its usage is constrained by its low solubility and off-target side effects, as well as its limited dose bioavailability (151). Some other limitations of docetaxel is that it causes myelosuppression, thrombosis and hepatotoxicity in many PCA patients, by which it causes most of the patients to discontinue the drug (152).

A mutation in the tumor suppressor gene TP53 is one of the most prevalent genetic abnormalities in cancer which also cause resistance to chemotherapy and radiation therapy (153–155). Recent findings show a surprisingly high incidence of TP53 mutation in both primary and metastatic prostate cancer (156). Current studies from a number of phase II and

phase III trials support the therapeutic benefit of PARP inhibition for overall survival and progression-free in prostate cancer (157–159). However, there is growing evidence that not all prostate cancer patients who are generally considered to have DNA damage repair gene abnormalities benefit from PARP inhibition. Therefore, more molecular markers are required to more precisely describe therapeutic vulnerabilities, treatment resistance, and patient prognosis. TP53, one of the most commonly mutated tumor suppressor genes in human cancer, is often excluded from targeted next-generation sequencing (NGS) panels used in important phase II and III trials to identify patients for PARP inhibitor treatment. (156, 160, 161). Furthermore, P53-mutated tumors often advance more quickly, respond poorly to anticancer therapy, and have a poor prognosis. Therefore, cancer therapy targeting p53 is an attractive strategy (162).

The therapeutic application of gene therapy is hampered due to the various issues associated with its delivery systems, such as non-specificity, swift degradation and clearance in the circulatory system, inability to escape the endosomes, reduced uptake of the therapeutic to the diseased cells and toxic effect of the delivery systems (163). Several delivery vehicles have been used for the delivery of p53 to the tumor site which mainly includes viral and non-viral based delivery. However, the various problems associated with the viral based delivery is the lack of specificity, development of immunogenicity, toxicity to the cells, insertional mutagenesis, restriction in transgenic size capacity (164). Due to the above limitations the emergence of non-viral based delivery has come into effect. The advantages of using non-viral based delivery is it is less immunotoxicity, biosafety, lower cost, no restriction in transgenic size capacity, advances in duration of gene expression, which led to its increased product entering to clinical trials (41, 165). However, the limitation of using non-viral based delivery is poor efficiency in delivery of the therapeutic gene which leads to lower expression of the therapeutic gene (165).

1.11 Overcoming the limitations using nanodelivery

The advantage of using nanoparticles as drug delivery system is that it can incorporate both hydrophilic and hydrophobic drugs, improve the poorly soluble drugs solubility, increase the half-life of the drugs, feasibility in the route of administration, change the drug pharmacokinetics, increase the drug stability, improving the bioavailability of the drug, reducing the side effects of the drugs by targeting the drug to the diseased site (65, 166, 167).

The most important benefit of using nanoparticles for gene delivery is that it protects the therapeutic gene from degradation, as biodegradation is the primary factor affecting the clinical use of nanoparticle-based genes (168, 169). In recent years, Poly (lactic-co-glycolic acid) has been investigated as a gene vector because of its stability and its ability to prevent DNA from being degraded during circulation *in vivo*. The other advantages of using nanoparticle as gene delivery is that it improves the circulation time, enhances the stability, prevent the protein from adsorption, increases the efficacy of gene target *in vivo*, improves in escaping the endosomes, crossing the cellular membrane, and also in nuclear localization (163, 170).

1.12 Rationale of the thesis

When drugs are administered separately, they exhibit differential localization in cells, thus a combination of drug loaded nanoparticles would promote co-delivery of drugs to cells expressing lactoferrin receptors. Thus, conferring intended action by both drugs at the site. Which would also help in higher tolerated doses.

Further, to test whether a cross linking agent would regulate the release of drug form nanoparticles. Also, to understand how a drug or DNA loaded nanoparticle performs in regression of prostate cancer.

1.13 Objectives

1. An analysis of combination nanoformulation of cyclophosphamide and doxorubicin for co-delivery with reduced toxicity

2. Development of a regulated delivery system for delivery of doxorubicin in MES (Sodium 2-mercaptoethanesulfonate) modified lactoferrin nanoparticles in prostate cancer cells

3. Evaluation of efficacy of docetaxel-loaded lactoferrin nanoparticles targeted to prostate cancer *in vitro* and *in vivo*

4. Potentiation of activity of docetaxel with p53 DNA loaded in lactoferrin nanoparticles in treatment of prostate cancer

CHAPTER 2

Materials & Methods

2. Materials and methods

2.1. Materials

2.1.1. Reagents

Lactoferrin (Symbiotics, USA), Olive oil (Leonardo (Italy)), Doxorubicin and Cyclophosphamide (Biochem Pharmaceutical Industries, Pune, India). Docetaxel (TCI (Tokyo chemical industries, catalog no D4102)) and Uranyl Acetate (Spectrochem Pvt Ltd). All reagents used were of analytical grade. Drug loaded Lactoferrin NPs and soluble drug were administered to the mice using oral dosing was done using 22 Standard Wire Gauge needle. The diagnostic kits for determining various parameters for safety evaluation were purchased from Tulip diagnostics Pvt Ltd, Goa, India. Plasmid GFP-p53 (5.2 kb) (Add gene) codes for green fluorescent protein tagged p53 Protein marker for delivery. Proteinase k was purchased from thermo fisher Scientific. Lipofectamine (Invitrogen) used as transfection control. All other reagents were of analytical grade.

2.1.2. Cell lines

Prostate cancer cell line from rat (Mat Ly Lu) was obtained from ATCC and A549 (Lung cancer) cell line was obtained from NCCS, Pune.

2.1.3. Cell culture Reagents

RPMI 1640 media (Gibco), DMEM (Gibco), Fetal bovine serum (Gibco).

2.1.4. Antibodies and Molecular Biology Reagents

Rabbit anti- Cytochrome C antibody (cell signalling and technology, Cat No # 11940S), Rabbit anti-Bax antibody (cell signalling and technology, Cat No 14796), Rabbit anti-Plk1 antibody (ab clonal, Cat No A2548), Mouse anti-p53 antibody (MA5-12453), Mouse anti Vegfr 2 antibody (Cat No 05-554), Rabbit anti-Ki67 antibody (Abcam, Cat No: ab16667),

Rabbit anti-ITLN1 antibody (Lactoferrin receptor) (Thermofisher Scientific, Cat No: PA5-77179), Anti-rabbit Alexa Fluor 594 Secondary Antibody (Thermo Fisher Scientific, Cat No # A-11037), DAPI (Thermo-Fisher Scientific, Cat No #P36935), TNF-alpha and IFN-γ (from rat) Platinum ELISA kit was from Bender MedSystems, Cat No: BMS622 & BMS621).

2.1.5. Instruments

Centrifuge (REMI C30BL and Hermle Z36HK), Vortexer, ultrasonic homogenizer or sonicator was 300V/T (Biologics Inc., Manassas, Virginia, USA), Transmission electron microscope was JEM-2100 (M/S Jeol Limited, Tachikawa, Tokyo, Japan), Zeta sizer (Malvern instrument), HPLC with UV-vis detector (Waters), Gel electrophoresis apparatus, ELISA reader (Teccan).

2.1.6. Animals

CD-1 mice used in this study were approximately 5-6 weeks old and 25-30 mg, obtained from Hylasco biotechnology Pvt. Ltd. Hyderabad. Male Wistar Rats were obtained from Sainath agencies, Hyderabad, India. In our study, mature animals of 2-3 months of age (150-200 g) were used. The Animals were housed at University of Hyderabad animal house facility. All experiments using animals were carried out as per the approval of Institutional Animal Ethics Committee, University of Hyderabad.

2.2. Methods

2.2.1. Preparation of Doxorubicin, cyclophosphamide and their combination loaded Lactoferrin Nanoparticles

Doxorubicin or cyclophosphamide or their combination Doxorubicin and cyclophosphamide loaded lactoferrin nanoparticles (nDox Cp) were prepared using sol-oil method (171, 172). The drug(s) were mixed with lactoferrin at 1:4 (w/w) ratio in 1 ml of phosphate buffer saline

(ice-cold, pH 7.4). The mixture was incubated on ice for one hour and then was gently added to 25 ml of olive oil while vortexing. Then particles were dispersed using sonication at 4°C using a sonicator for 15 minutes at 40 Hz amplitude. The sonicated product was snap frozen in the presence of liquid N2 for 10 min. Then, it was thawed on ice and was pelleted by centrifugation at 6000 rpm for 10 min at 4°C. The pellet was washed thrice with 1 ml of diethyl ether to remove traces of olive oil and non-encapsulated drugs. After washing, the pellet was resuspended in 1X PBS (pH7.4) and stored at 4°C until use.

2.2.2. Preparation of Doxorubicin loaded lactoferrin nanoparticles along with MES incubation

Doxorubicin (Dox) loaded MES-treated lactoferrin nanoparticles (Dox-LfNPs+MES) were prepared by the sol-oil method. Dox and Lf were mixed in 1:4 (w/w) ratios and dissolved in 1ml of ice cold PBS (pH 7.4) and left on ice. After an hour of incubation MES was added to the drug-lactoferrin mixture and incubated up to different time points (5min, 20 min, 40 min, 60 min, 2 hours, 4hours and 6 hours) followed by addition on olive oil. Drug-lactoferrin-MES ratio was optimized my mixing in different ratios (1:4:3, 1:4:6, 1:4:12 and 1:4:20) and preparing nanoparticles following the protocol mentioned earlier.

2.2.3. Preparation of Docetaxel loaded lactoferrin nanoparticles

Docetaxel (DTX) loaded lactoferrin nanoparticles (DTX-LfNPs) were prepared by sol-oil chemistry. DTX was dissolved in DMSO (Dimethyl sulfoxide) (1mg/100 µl) and was mixed with Lf solubilised in PBS at a ratio of 1:4 (w/w). The mixture was then incubated on ice for 1 hour followed by dropwise addition to 20 ml olive oil, while vortexing for phase separation and formation of nanoparticles. The nanoparticles were uniformly dispersed by sonication of the mixture at 4°C using a sonicator for 15 minutes at 40 Hz amplitude with 2 minutes of cooling in ice after every 5 minutes. After sonication, the aggregation of nanoparticles was

inhibited by snap freezing in liquid nitrogen for 10 minutes. The nanoparticles were thawed on ice and were precipitated by centrifugation at 6000 rpm for 10 minutes and the pellet obtained was washed three times using 2 – 3 ml of diethyl ether to remove excess olive oil and the unbound drugs. The pellet was dried and was resuspended in sterile phosphate-buffered saline (PBS).

2.2.4. Determination DNA and lactoferrin molar ration using Gel retardation

Gel retardation assay was performed with increasing concentration of Lactoferrin (0.296, 14.8 ,29.6, 44.4, 59.2, 74, 88.8, 103.6, 118.4, 133.2, 148, 296 pM) along with fixed concentration of GFP-p53 (0.296 pM) , the DNA/Protein mixture were made up to 30 µl using 1x PBS pH-7,4 and incubated for 12 hrs at 4 ℃. The above samples were loaded on to gel using 6x loading dye (Thermofischer scientific) and electrophoresed. The DNA was stained and visualised under UV transilluminator.

2.2.5. Preparation of GFP-p53 DNA loaded lactoferrin nanoparticle

Preparation of Lactoferrin nanoparticles was carried out using the sol-oil method as per (Krishna et.al, 2009) (173). Molar ratio of DNA: Protein (1: 500) was taken and incubated overnight at 4◦C. With an amplitude of 40 and 30 sec on & off pulse for 5 mins, sonication of above mixture has done on ice, the above pattern was repeated for three times then immediately (snap) frozen in liquid nitrogen for 10 mins and later on thawed on ice. The colloidal mixture was pelleted down at 6000 RPM for 10 mins at 4◦C, washed with ether till the removal of oil traces. Lastly dissolved in 1x PBS pH-7.4

2.2.6. Nanoparticle characterization

The dimensions of nanoparticles in terms of size and morphology were analysed using Transmission Electron Microscopy studies. For TEM analysis 20 µl of samples (LfNPs and drug and DNA loaded LfNPs) were layered on a carbon-coated mesh grid and were allowed

to air dry. After the sample was dried, it was stained using 1% uranyl acetate for 45 seconds. The samples were analyzed using a JEM-2100 Transmission Electron Microscope (M/S Jeol Limited, Tachikawa, Tokyo, Japan) as per manufacturer instructions.

2.2.7. Attenuated total reflectance

The ATR-IR spectrum of free drug and Lyophilised Drug loaded NPs was recorded with the help of PLATINUM-ATR, using Bruker OPUS 7.0 software. Lactoferrin powder, lyophilized LfNPs powder, free drug, and lyophilized DTX-LfNPs powder were placed on the ATR diamond probe and IR spectra were obtained. Spectra were generated from the average signal of 32 scans with resolution of 4 cm^{-1} and recorded as transmittance versus wavenumber within a range of 4000-500 cm^{-1}.Background spectra was recorded before scanning the samples.

2.2.8. Determination of drug encapsulation efficiency and drug loading content

Efficiency of encapsulation is defined as the percentage of the amount of drug loaded in nanoparticles. For this purpose, 50 µl of nanoparticles was added in 450 µl of PBS (pH 5.5) and kept for overnight incubation at 25°C on a rocker for drug release. Next day 500 µl of acetonitrile was added for precipitation of the lactoferrin protein. The precipitate was centrifuged for 10 minutes at 12000 rpm and 4°C. A 0.2 micron syringe filter was used for filtration of supernatant. The quantification of drug released from Drug-LfNPs was carried out using reverse phase HPLC (Waters 2695; Waters, MA, USA) with a UV detector (Waters 2487) against a standard curve prepared from known concentrations of pure soluble drug. 10 ul of soluble / nanoparticle released drug was injected into the C-18 column coupled to the HPLC system and was resolved using a mixture of acetonitrile and milliQ water (60:40 V/V) as the mobile phase with 1ml/min flow rate and 10 minutes run time. Drug quantification was done by measuring the absorbances at 252nm and 260 nm for Doxorubicin and

cyclophosphamide respectively. The drug was resolved using the C-18 column. Acetonitrile and Milli Q water (60:40 v/v) were used as mobile phases. Injection volume was 10 µl with a flow rate of 1 ml/min with a run time of 10 minutes. The absorption was kept at 252nm and 260 nm for Doxorubicin and cyclophosphamide respectively. The experiments were performed in triplicates. Encapsulation efficiency and Drug loading content were computed by using the formula-

Encapsulation efficiency (%) = (Weight of drug in NPs/Initial weight of drug used) X 100

Drug loading content (%) = (Weight of drug in NPs/ weight of the nanoparticles) X 100

Encapsulation of DTX in DTX-LfNPs was determined by resuspending 80 µg of nanoparticles in 450 µl of PBS (pH 5.5) and incubated overnight at 25°C in rocking condition. 50 µl of 30% $AgNO_3$ was added to the mixture on the next day for protein precipitation, then 450 µl of Milli Q water was added. The sample was centrifuged at 12000 rpm for 10 minutes at 4°C and the supernatant was collected and filtered using a 0.2 micron syringe filter. The amount of DTX released from DTX-LfNPs was quantified using reverse phase HPLC (Waters). The drug was resolved on a C-18 column connected to the HPLC system. The acetonitrile- Milli Q water mixture (60:40 v/v) was used as mobile phase. The flow rate was 1 ml/min with an injection volume of 10 µl and a run time of 10 minutes. Released DTX from the filtered samples were quantified from their absorbance at 230nm against the standard curve. The experiments were performed in triplicates. Encapsulation efficiency and Drug loading content were calculated by using the above formula.

2.2.9. Loading efficiency/Encapsulation efficiency of p53 DNA

Loading efficiency of particles was calculated by estimating the amount of DNA released after treatment with either proteinase K at 60◦C or Heat treatment for 10 mins at 90◦C or incubating with 1% SDS at room temperature or 1 hr.

Equation for calculating Loading efficiency is -

Loading efficiency = Concentration of DNA released from nanoparticle/Total concentration of DNA used for preparation of nanoparticle X 100.

2.2.10. pH-dependent release studies

DLf-NPs (0.5mg) were mixed with 450 µl of PBS ranging in pH from 2 to 7 and kept for overnight incubation at room temperature on a rocker. After incubation was completed 500 µl of acetonitrile was added in the above mixture to precipitate the lactoferrin protein. It was mixed well and was pelleted by centrifugation at 12000 rpm for 15 min. The supernatant was filtered using 0.2 µm syringe. The amount of drug released from Drug-LfNPs was quantified using Reverse Phase HPLC with a UV detector. The drug was resolved by injecting 10 µl filtered sample using a C-18 column, while acetonitrile-MilliQ water mixture in 60:40 V/V ratio was used as a mobile phase with flow rate of 1 ml/min and 10-minute run time Drug absorbance was measured at 252 nm and 260 nm for Doxorubicin and cyclophosphamide respectively. The experiments were performed in triplicates.

2.2.11. Cell culture

Mat Ly Lu prostate cancer cells were cultured in high glucose RPMI medium and A549 cells were grown in DMEM medium along with 10% fetal bovine serum, and 1% antibiotic (penicillin and streptomycin) in a humidified CO2 incubator at 37 °C temperature, with 5% CO2 and 95% relative humidity.

2.2.12. Cell viability assay

Approximately, $1x10^4$ cells/per well were seeded in 96 well plates and grown up to 70% confluency. Indicated concentrations of DTX and DTX-LfNPs were added and incubated for 48 hours. After that the drug rich media was removed and cells were washed with PBS. MTT dissolved in complete media (5mg/ml) was added to each well to reach a final

concentration of 0.5mg/ml and incubated 4 hours until the purple intracellular formazan crystals were visible under microscope. Then the cells were centrifuged, cell supernatant was discarded and formazan crystals formed were dissolved by addition of 100 µl of DMSO in each well following incubation for 10 min in the dark. Absorbance of solution was recorded at 570 nm in an ELISA plate reader (SM600 microplate reader biomedical LTD).

2.2.13. Biomarker analysis

The Mat Ly Lu cells were s cultured in 60 mm dishes to 60-70% confluency and were exposed to DTX and DTX-LfNPs of desired concentrations. After 48 hours incubation, the treated cells were homogenized in radio-immunoprecipitation assay buffer (RIPA) continuing 50 mM Tris-Cl pH 8.0; 150 mM NaCl, 2 mM EDTA; 1% [w/v] NP-40; 0.5% [w/v] sodium deoxycholate; 0.1% [w/v] SDS containing cocktail of protease inhibitors (Thermo scientific). Then, the homogenized product was centrifuged at 12000 rpm for 15 minutes for removal of the insoluble debris. The protein content of the tissue lysate was estimated by Bradford method. Proteins from the tissue lysate were separated on a 12% SDS PAGE and Western transferred to a nitrocellulose membrane. The membrane was blocked with 5% milk and incubated with primary antibodies (against cytochrome –c, Plk1 and GAPDH) overnight at 4ºC. Afterwards, horseradish peroxidase (HRP) conjugated secondary was added to the membrane and incubated for 2 hrs at room temperature. . The blot was developed using West Pico plus Chemiluminescent substrate (Thermo scientific). The intensity of the GAPDH protein served as a loading control.

2.2.14. To study the Effect of MES when incubated for different time in prostate cancer cells

To study the delayed release effect of MES, Dox+Lf+MES LfNPs were treated to the Mat Ly Lu cells for different time points and different concentrations. 0.3X 10^{6} cells were seeded

in coverslip and were grown in a 35 mm dish. Upon reaching desired confluency Dox+Lf+MES LfNPs were treated to the cells for different time points and in different concentrations of MES and its incubation. After completion of incubation, the cells were fixed with 4% paraformaldehyde for 10 min at 37 °C, then washed with PBS for three times. Further, the cells were counterstained with DAPI, mounted on microscopic slides and visualized under fluorescence microscope.

2.2.15. Lactoferrin receptor expression in A549 and Mat Ly Lu cells

To check the expression of the lactoferrin receptor in A549 and Mat Ly Lu cells, we performed ICC (immunocytochemistry). 0.3X 10^{6} cells were seeded in coverslip and were grown in a 35 mm dish. Upon reaching the desired confluency, the media was removed and the cells were washed thoroughly with sterile PBS. Then 4% paraformaldehyde was added to the cells and incubated for 10 minutes at 37°C for fixation followed by washing with PBS for three times. Cells were blocked with 2%BSA for 30 min at 37 °C followed by three times PBS wash. Anti-Lactoferrin receptor antibody (1:200) was added and incubated at 4°C overnight. Then cells were rinsed with PBS followed by incubation with a secondary antibody conjugated to Alexa Fluor 594 (1:1000) for 30 minutes at dark in room temperature. After removal of secondary antibody cells were washed again with PBS and stained with DAPI. The microscopic slide was visualized under fluorescence microscopy.

2.2.16. Receptor-mediated endocytosis of LfNPs

To explore the function of LfR in the cellular localization of LfNPs, a receptor blocking experiment was conducted to monitor if nanoparticles enter cells through receptor-mediated endocytosis. The Mat Ly Lu cells were cultured in a complete medium containing 1% lactoferrin solution for 12 hours followed by removing the lactoferrin solution and addition of fresh media. After addition of fluorescent Nile red loaded lactoferrin NPs, incubation was

continued for 6 hours. Cells were washed with PBS, mounted on microscopic slides and observed under fluorescent microscopes to detect the localization of fluorescent Nile red. The cells in the absence of lactoferrin were used as the control.

2.2.17. *In-vitro* transfection Assay

Aforementioned cells were seeded in 6 well plates with appropriate media containing 10% FBS. After 50-60% confluency media was replaced with serum free fresh media and transfected with plasmid DNA and plasmid DNA loaded nanoparticles separately. Later after 48 hrs cells were fixed with 4% paraformaldehyde solution, mounted on slides using Gold anti fade DAPI solution (in vitrogen) and observed under fluorescence microscope (Carl-Zeiss).

2.2.18. Animal experiment

Animal experiments were performed using protocol approved by the Institute's Animal Ethics Committee (IAEC) approval. Male CD 1 mice were used for the toxicokinetic studies and male Wistar rats were used for the tumor development and regression studies. Male Wistar rats were obtained from Sainath agencies, Hyderabad, India. The animals were kept in polyethylene cages with stainless steel lids with room temperature maintained at 22 ºC with a 12 h light/dark cycle and free access to food and water. The tumor development and treatment studies were carried out under anaesthesia using intraperitoneal (i.p) injection of a mixture of Ketamine (100 mg kg-1) and xylazine (10 mg kg-1).

2.2.18.1. Toxicokinetic studies

In this study male CD1 mice of age group 5-6 weeks and having weight 25-30 gm were used. Total of 162 mice were used for 27 groups consisting of 6 mice each. First group where no treatments were given to mice were used as control. In sDox and nDox (an equivalent doxorubicin dose of 45, 90, 225, 450 and 900 mg kg^{-1} body weight) were used. For sCp and

nCp (an equivalent cyclophosphamide dose of 70, 140, 275, 650, 1350 mg kg−1 body weight) were used. For sDoxCp and nDoxCp (an equivalent drug dose of Dox-90, CP-135, Dox-180, CP-270 and Dox-360, CP-540 mg kg^{-1} body weight) were used. All the doses were administered to the animals orally with the help of gavage. The animals were observed for a period of seven days. At the end of the study blood samples were collected from the animals using heart puncture method under anaesthetic condition. The animal's organs were collected after the animals were cervically dislocated and processed for Haematoxylin and Eosin staining.

2.2.18.2. Orthotopic tumor development studies

Prostate tumors were developed by orthotopic injection of Mat Ly Lu cells under anaesthetic condition (25). The lower abdominal region was disinfected with 70% alcohol and the hair was removed using a shaving blade. Then lignocaine hydrochloride gel (local anaesthetic gel) was applied in the lower abdominal region. After the application of gel, a 2 cm longitudinal incision was made with a scalpel on the lower abdomen, right above the pubic bone. After finding the bladder, it was pulled to expose the prostate. After finding the prostate, $5x10^5$ Mat Ly Lu cells in 40 µl of 1X PBS was injected into the ventral prostatic lobe of a male Wistar rat using an insulin syringe. The observance of a bleb within the injected prostatic lobe confirms the entry of cells inside the prostate lobe. After injection, the bladder was replaced and the muscle layer was closed using a suture in a simple pattern. The stitched area was applied with betadine using sterile cotton balls and the rat was monitored carefully until they recovered from anaesthesia.

2.2.18.3. *In-vivo* tumor regression studies of DTX LfNPs in prostate cancer orthotopic rat model

Prostate cancer (PCA) orthotopic rat model developed in 18 rats for tumor regression studies *in vivo*. The tumor-bearing rats were randomly divided into 3 treatment groups (n=6), saline, DTX, DTX LfNPs at a dosage of 2.5 mg/kg body weight equivalent of DTX, the drugs were administrated intravenous (100 µl) route on day 12. The animal weight, food, and water intake were measured every day during the experiment. The rat was euthanized by CO_2 inhalation on the 21st day. The prostate tumor tissues were collected and weighed. Using vernier calliper, the prostate tumor's maximum (a) and minimum (b) diameters were measured. The tumor volume was determined using the equation-

Tumor volume (V) =. 0 5 ab2

The levels of p53, cytochrome c, vegfr 2 in rat prostate tissue of 3 groups was analysed using western blot. Briefly, homogenate prepared prostate tumor tissue was processed as mentioned earlier and 20µg of protein was separated on a 12% SDS-polyacrylamide gel, Western transferred to nitrocellulose membrane, then probed with antibody against indicated protein followed by secondary antibody conjugated with horseradish peroxidase, and the blot was developed as described above.

2.2.18.4. Localization of GFP-p53 in Rats using Lactoferrin nanoparticles

Localization study was conducted on male Wistar rats procured from Sainath agencies, Hyderabad. 9 rats were used for the localization studies, classified into 3 groups each group consists of 3 rats (n=3). GFP-p53 (2 mg/kg of body) administered in rats through the tail vein. After 48 hrs of administration rats were sacrificed and organs (Brain, Bladder, Prostate, Lymph node and Heart etc.) were collected and processed for protein and DNA isolation.

Isolated DNA is then used as a template for PCR to check the presence of GFP (GFP-p53) in organs by using primers for GFP

2.2.18.5. Histology and Immunohistochemistry

After the animals were sacrificed, the organs were dissected and stored in 4% paraformaldehyde. Then the prostate tissues were embedded in paraffin wax and sections of approx. 10μm thicknesses were stained with hematoxylin and eosin (H&E) and 20 μm were used for IHC staining. The strained sections were observed under microscope.

The Prostate tissue sections were deparaffinized by incubating the sections in the presence xylene for 5min with 2 washes of xylene, the same was repeated 100% ethanol for 10 min, 95% ethanol for 10 min, and later rehydration was done by washing the sections 2 times in double-distilled water for 5 min each. Following this step, antigen retrieval was carried out by boiling the slides in a 10 mM citrate buffer with 0.05% tween-20 (pH 6.0); and maintaining at a sub–boiling temperature (95-98ºC) for 10 min. The non-specific binding activity was blocked by 1% BSA for 1 hour at room temperature in a humid chamber. The sections were then incubated in primary antibodies (1:200) as indicated for overnight at 4°C. Then, the sections were washed 3 times in TBST (Tris-buffered Saline Tween-20) for 5 min and incubated in secondary antibodies for Alexa fluor 594 (1:1000) in the dark for 1 hour at 25°C. Then, the slides were washed 3 times in TBST for 5 min each and mounted with DAPI. The sections were examined under fluorescent microscope and images were recorded.

2.2.18.6. Bioavailability of DTX-LfNPs

Tumor bearing male Wistar rats were divided (randomly) into 2 treatment groups (n=6) DTX and DTX-LfNPs at a dosage of 10 mg kg−1 body weight equivalent of DTX, the drugs were administrated intravenous (100 μl) route. After 24 h rats were euthanized and prostate tissue was collected and the tissue was homogenized in 1 ml of acetonitrile using a homogenizer.

Later after centrifuging the homogenates at 12000 rpm for 15 min at 4°C, then the supernatant was filtered through 0.2 micrometre syringe filter, and its DTX concentration was determined using HPLC.

2.2.18.7. Estimation of TNF alpha, IFNɣ, LDH, ALP, Creatine and uric acid

Various parameters such as lactate dehydrogenase, alkaline phosphatase, uric acid, urea and creatinine were estimated from the serum collected from the treatment groups. The parameters checked were done using commercially available kits (Tulip diagnostics). The assay was conducted in accordance with the manufacturer's instructions. Similarly, Rat TNF-alpha Platinum ELISA kit (Bender MedSystems, BMS622) and Rat IFN-Platinum ELISA were used to estimate the TNF alpha and IFN in the rat serum as per the instruction supplied in the kit.

2.2.19. Statistical Analysis

The studies were carried out in triplicates in studies reported in the thesis, the data was presented as mean with standard deviation. The data was analysed using Graph Pad Prism 8. The significance of results obtained in differences between treatment groups was analyzed by one-way ANOVA or unpaired Student’s t-test using Graph Pad Prism 8. The significance level was set at $P < 0.05$.

CHAPTER 3

An analysis of combination nanoformulation of cyclophosphamide and doxorubicin for co-delivery with reduced toxicity

3. CHAPTER 3: An analysis of combination nanoformulation of cyclophosphamide and doxorubicin for co-delivery with reduced toxicity

3.1. Introduction

Doxorubicin (Dox) and cyclophosphamide (Cp) along with their combination are among the most widely used anticancer drugs against the treatment of malignant and non-malignant disorders (174, 175). Doxorubicin produces ROS which leads to extensive DNA damage resulting in cell death (176). Cyclophosphamide is an alkylating agent which kills the cells by damaging their DNA (175). The main side effects of doxorubicin and cyclophosphamide include cardiotoxicity and immunosuppression (175, 177). To overcome these side effects, we have used lactoferrin nanoparticles as the delivery vehicle. Nanoparticle-mediated therapy has shown better clinical results due to its ability in retaining the drugs in the body over long periods of time and releasing it slowly such that it has a prolonged effect (171, 178). Nanoparticles can be modified to bind the cancer cells ensuring that higher drug concentrations are localized in these cells. Hence, a targeted nanoparticle drug delivery system helps in reducing toxicity to normal tissues (179). Nanoparticles have been formed by a variety of biomaterials such as lipids, polymers, chitosan and proteins (178). Much interest has been shown in protein-based nanoparticles because of their safety, simple preparation method and also because of their size distribution. Protein can also be modified to improve its functional and targeting abilities (180).

An iron binding 80 kDa glycoprotein, Lactoferrin, belongs to the transferrin family and it is expressed in most of the biological fluids. It has protective actions such as antimicrobial, antibacterial, antiviral, antifungal and antiparasitic, to anti-inflammatory and anticancer activities (105).

Lactoferrin receptors are overexpressed on cancer cells, hence lactoferrin is widely accepted as ligand for recognition of cancer cells and to target Lf-loaded drug nanoparticles for drug localization in cancer cells (181). Rationale of current study is if free drug of Dox and Cp are administered, would get distributed differentially in tissues, thus may not reach target tissue together, thus loosing efficacy of the combination therapy and also exhibit non-target effect, when Dox and Cp are encapsulated into nanoparticles, both drugs will be released together in a target tissue. Thus, lactoferrin nanoparticles facilitate drugs to co-deliver in the lactoferrin receptor expressing metabolically active cancer cells, permitting targeted co-delivery of drugs.

In this study, two anti-cancer drugs, doxorubicin and cyclophosphamide were loaded together in 70 nm lactoferrin nanoparticles with significant drug loading and release kinetics of both doxorubicin and cyclophosphamide at endosomal pH. Further, studies of dose-escalation and toxicokinetic analysis of the combination nanoformulation in CD 1 mice showed that Lf nanoparticles enhanced tolerability of combination drugs along with decreasing dose-limiting toxicities.

3.2. Results

3.2.1. Characterisation of nanoparticles

The preparation of nanoparticles was carried out as explained in methods. TEM analysis in **(Figs 3.1 A)** shows that the average size of blank nLacto is 46 nm, which increases to 74.3 nm in nDox, 74 nm in nCp, and 80 nm nDoxCp. While the zeta potential in **(Fig 3.1B)** of nLacto to be -46.6 mV, nDox -78.2mV, nCp -68.9 mV and of nDoxCp to -62.1 mV, thus suggesting that the Dox and Cp assumed equal proportions in the particles. The encapsulation efficiency was 50.43±1.06 % for nDox, 57.3 ±4.65 % for nCp and 52.88 ±2.88% dox, 62.03±3% Cp for nDoxCp. The drug loading content was 12.6 ±1.06 % for

nDox, 14.32±1.16 % for nCp and 12.81±1 % dox, 15.5±1.2 % Cp for nDoxCp. Thus, suggesting that in combination nanoparticles both doxorubicin and cyclophosphamide were cooperatively loaded, thus the particle size as well as loading efficiency of co-loaded drugs in nanoparticles is similar to that of single drug loaded nanoparticles. The presence of surface negative charge confirms that the particles are stable.

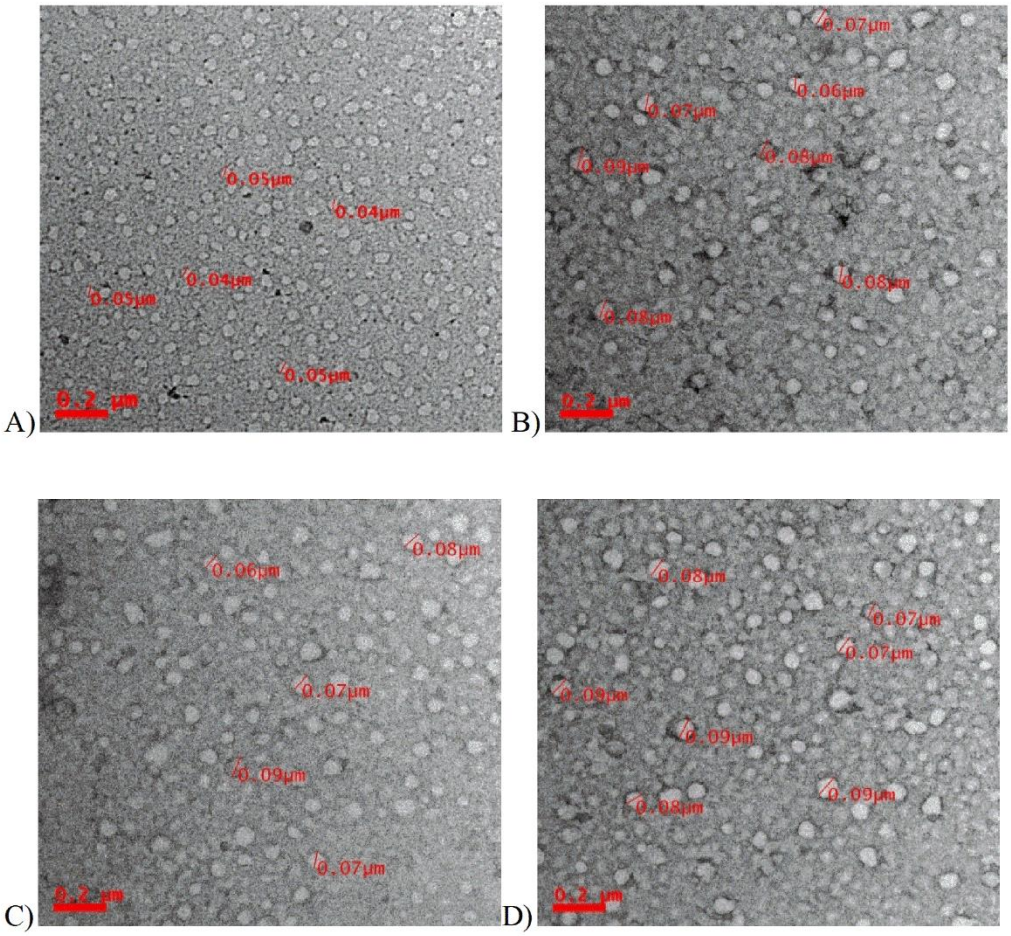

Fig. 3.1 A) TEM analysis of A) nLacto B) nDox C) nCp and D) nDoxCp.

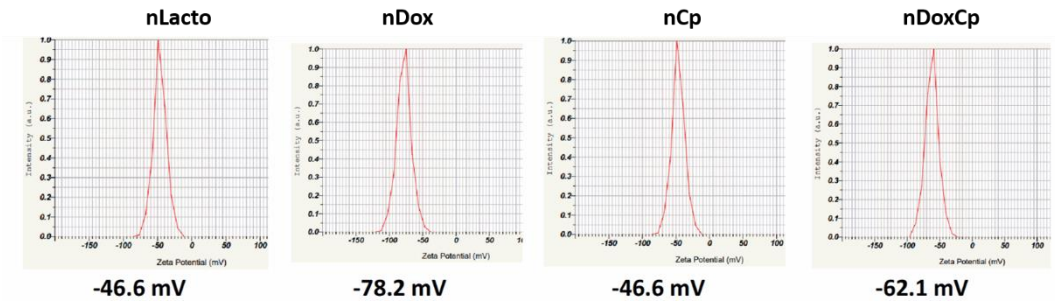

Fig.3.1 B) Zeta potential of A) nLacto B) nDox C) nCp and D) nDoxCp.

3.2.2. Characterization of nanoparticles using ATR (Attenuated total reflectance)

ATR analysis showed that the drugs were intact in the nanoformulations. The bands corresponding to Amide I and Amide II were found in both the pure compound and nano form of Lactoferrin protein. In Pure Lactoferrin **(Fig. 3.2A),** the ATR spectra show Amide I band, Amide II band and C-O-C band were shown to be 1645.97, 1520.19 and 1031 and similarly for nLacto **(Fig.3.2 B)** it were shown to be 1647.81, 1519.01 and 1158.97. For free Dox the ATR spectra of C=O (Ketone) and Amide I were shown to be 1736.61, 1651.42, **(Fig 3.2 C)** and for nDox it was shown to be 1743.36, 1642.72 **(Fig 3.2 D).** For free Cp the ATR spectra of $–CH_2Cl$ and Amide II (N-H bending) were shown to be, 1366.72, 1518.26 and **(Fig 3.2 E)** and for nCp it was shown to be 1372.05, 1540.39 and **(Fig 3.2F).** For free combination (Dox + Cp) the ATR spectra of C=O (Ketone), Amide I, $–CH_2Cl$ and Amide II were shown to be 1722.63, 1649.76, 1368.28 and 1519.37 **(Fig 3.2 G)** and for nDoxCp, it was shown to be 1743.98, 1648.45, 1370.86 and 1516.19 **(Fig 3.2 H).** These results suggest characteristic signals corresponding to Dox and Cp remain unchanged suggesting that the drugs are intact.

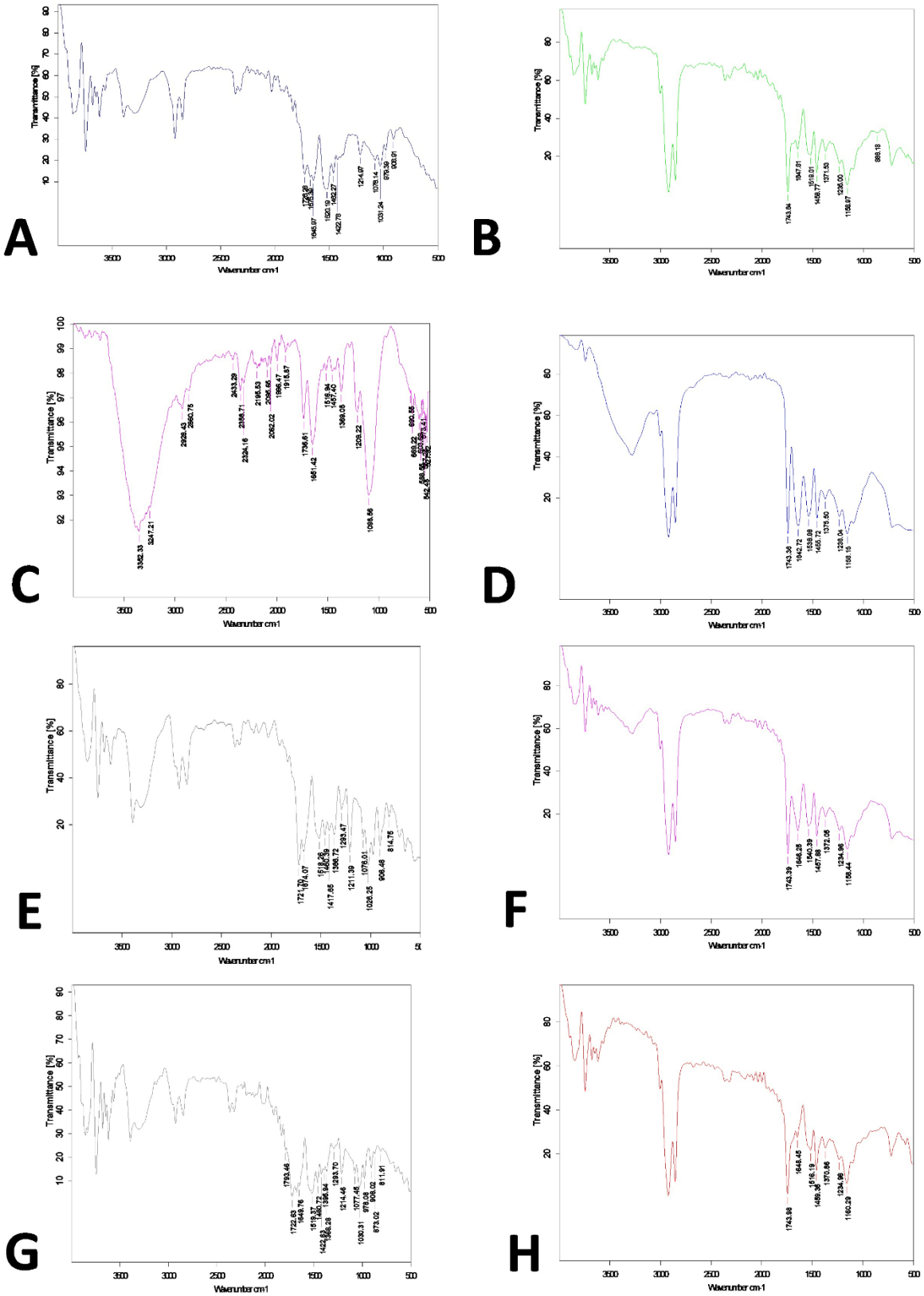

Fig 3.2. ATR analysis of A) Pure lactoferrin , B) nLacto, C) sDox, D) nDox, E) sCp, F) nCp G) sDoxCp and H) nDoxCp. In this analysis it was seen that in Drug loaded LfNPs the drug

was physically entrapped in the Lactoferrin NPs. The Lactoferrin nanoparticles maintained their structural integrity.

3.2.3. pH release studies

Nanoparticles were exposed to different pH conditions released drug was estimated, the results show that drugs are released between pH 5 to 6 **(Fig 3.3)**, furthermore both drugs were released together suggesting that drugs are co-delivered cooperatively between pH 5 to 6. This provide an advantage of co-delivery of drug at site of pH 5 to 6, the pH of endosomes as well as acidic pH gradient in the cancer tissues (182). MRI studies indeed showed the tumors in mouse reaches pH 6 (183). Also, acidic environment has been shown to facilitate evolution of invasive phenotypes of cancer (184). Thus, release of both drugs under acidic pH would promote their action against cancer.

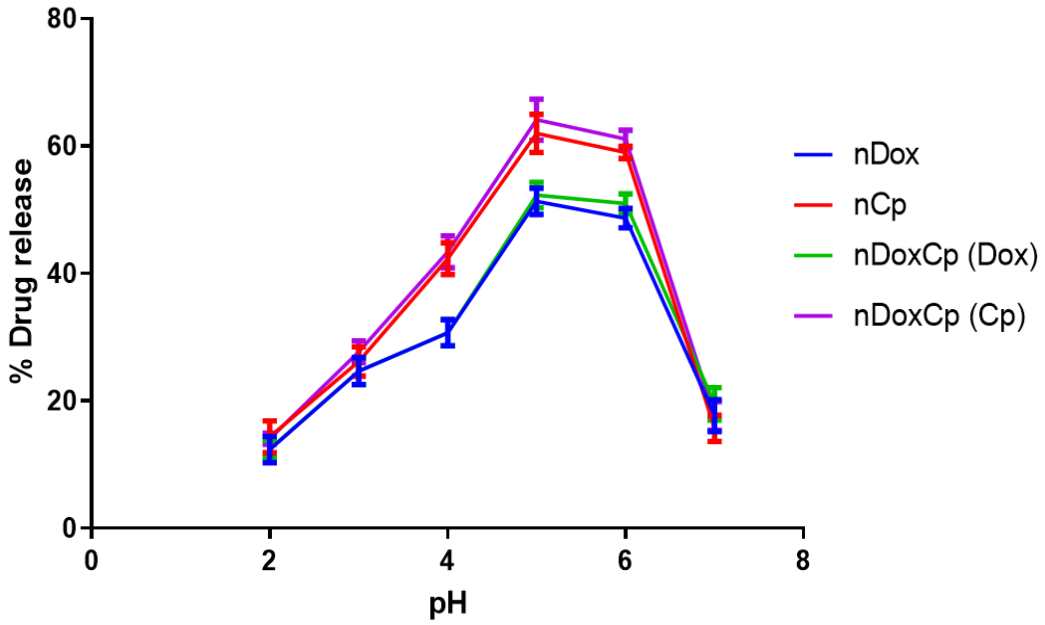

Fig.3.3 The drug release from nanoparticles with increased pH. Maximum drug release was release in between pH 5 to 6. Each data points represent an average of triplicate experiments and presented as Mean ± SD.

3.2.4. Determination of LD_{50}

The animals were made to fast 12 hour prior to administrating dose. The drug loaded nanoparticles were administered orally to male CD-1 mice using oral gavage needle in increasing doses of nDox 46.5, 225, 450, 900 mg/kg body weight **(Fig 3.4 A)**. nCp was given in increasing doses of 70, 140, 650, 1350 mg/kg body weight **(Fig 3.4 B)**. For nDoxCp, the doses Dox-90, CP-135, Dox-180, CP-270, Dox-360, CP-540 mg/kg body weight **(Fig 3.4 C)** were given in increasing order. Similar doses were given for free drugs. The LD_{50} of nDox was found to be 900mg Dox/kg body weight and for free Dox the LD_{50} was found to be 450 mg Dox/kg body weight of doxorubicin. The LD_{50} nCp was found to be 1350 mg Cp/kg body weight, while for Free Cp, the LD_{50} was found to be 650 mg Cp/kg body weight. For combination nanoparticle (nDoxCp) the LD_{50} was found to be 360 mg of Dox/kg bodyweight and 540 mg of Cp/kg body weight and for Free combination (Dox + Cp) the LD_{50} was found to be 180 Dox of mg/kg body weight and 270 mg of Cp/kg body weight. Hence, healthy CD-1 mice were tolerated to 2-fold higher dosage of Doxorubicin and Cyclophosphamide in single or in combination when orally administered through lactoferrin nanoformulations suggesting that a significant reduction in toxicity induced when drugs are delivered in nanoformulations.

Table 1. LD_{50} of free and nano drugs in single and combination.*

Description	**LD_{50} (mg/kg body weight)**	
Formulation	**Free Drug**	**Lactoferrin nanoformulation**
Doxorubicin	450	900
Cyclophosphamide	650	1350
Combination		
Doxorubicin	180	360
Cyclophosphamide	270	540

A

Dose	nDox		Dox	
mg/kg body weight	No of animals	No of animals alive	No of animals	No of animals alive
46.5	6	6	6	6
225	6	6	6	6
450	6	6	6	3
900	6	3	6	0

B

Dose	nCp		Cp	
mg/kg body weight	No of animals	No of animals alive	No of animals	No of animals alive
70	6	6	6	6
140	6	6	6	6
650	6	6	6	3
1350	6	3	6	0

C

Dox	Cp	nDoxCp		DoxCp	
dose mg/kg body weight		No of animals	No of animals alive	No of animals	No of animals alive
90	135	6	6	6	6
180	270	6	6	6	3
360	540	6	3	6	0

Fig 3.4. Healthy CD-1 mice were tolerated to 2-fold higher dosage of doxorubicin and cyclophosphamide and its combination when delivered through lactoferrin nanoparticles compared to soluble suggesting safety advantage of lactoferrin Nanoformulation.

3.2.5. Safety analysis

Both doxorubicin and cyclophosphamide are cardiotoxic and at higher doses they cause fatal haemorrhagic myocarditis (177, 185). Hence, we analysed serum LDH for analysis of effect of free and nanoformulated drug, the results in **Fig 3.5** shows that the levels of LDH were significantly reduced when treated nDoxCp compared free drug combination (sDoxCp). Serum alkaline phosphatase indicate the presence of liver toxicity, Cp when given in higher dose reported to induce acute liver failure. The nDoxCp showed lower levels of alkaline phosphatase in comparison to free DoxCp (**Fig 3.5**) suggesting nanoformulation reduces drug-mediated liver toxicity. High level of serum uric acid and urea is associated with renal disease (186), analysis of uric acid and urea in serum of treated mice showed reduced uric acid and urea in nanoformulation treated mice compared free drug treated mice **(Fig 3.5)** suggesting that the nanoformulation significantly reduces nephrotoxicity of drugs. The results showed that the toxicity of the soluble doxorubicin, cyclophosphamide and their combination to heart, liver, kidney was significantly reduced when drugs and their combination is administered in lactoferrin nanoformulation.

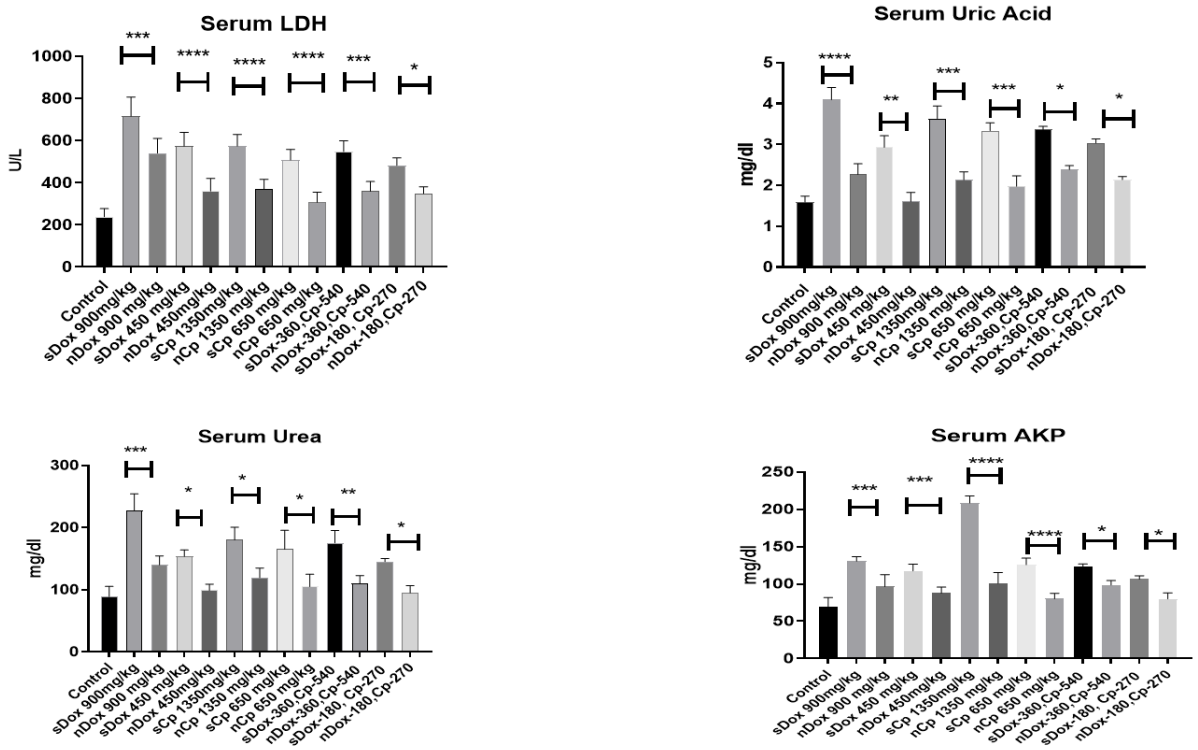

Fig.3.5 Safety analysis of free drug and nano formulations treated mice was done using biochemical kits from the serum collected from the animals. For both the treatment groups, soluble drug and nano formulations equal dose of drug were given orally. Cardiac toxicity was checked using LDH whereas the liver toxicity was assessed using alkaline phosphatase and kidney toxicity was assessed using uric acid and urea. The nanoformulations treated groups showed less toxicity in comparison to soluble drugs.

3.2.6. Histochemical analysis of tissues

In nDox treated mice, the heart showed moderate connective tissue proliferation or fibrosis in external layer of coronary artery in myocardium whereas in the free Dox (sDox) treated mice it was observed the presence of thickening of medial layer of coronary artery **(Fig 3.6 arrow marked).** In nCp treated mice, the heart has moderate pericardial inflammation along with accumulation of inflammatory exudates and inflammatory materials in heart, whereas the

heart tissue of the free Cp (sCp) treated mice showed severe pericarditis with accumulation of inflammatory exudates and inflammatory cells **(Fig 3.6 arrow marked)**.

In the Liver sections of the nDox treated mice, the morphology of hepatocytes was normal in portal, peri portal and centri lobular region of the liver **(Fig. 3.6 arrow marked),** whereas in the free Dox treated mice liver show a mild vacuolar degeneration of hepatocytes in peri portal and centri lobular region **(Fig.3.6 arrow marked).** In nCp treated mice, it was observed the presence of mild peri biliary connective tissue proliferation or fibrosis was observed in multi focal **(Fig.3.6 arrow marked)**, while in free Cp (sCp) treated mice liver showed the foci of centri lobular necrosis with infiltration of inflammatory cells in hepatocytes of liver **(Fig. 3.6 arrow marked)**. In nDoxCp treated mice hepatocytes shown to be normal in portal, peri portal and centri lobular region of the liver sections whereas in the free DoxCp (sDoxCp) treated mice liver sections peri portal/peri biliary infiltration of inflammatory cells was observed **(Fig.3.6 arrow marked).**

In the kidney of nDox, tissue were normal where as in the free Dox (sDox) there was a moderate inflammation with infiltration of inflammatory cells and fibrosis observed near renal pelvis region **(Fig 3.6 arrow marked).** In nCp treated mice, the kidney tissue appeared normal whereas free Cp (sCp) treated mice kidney tissue showed tubular degeneration and haemorrhages were noticed (Fig. 6 arrow marked). In nDoxCp treated mice, the kidney tissue section showed moderate tubular dilatation and tubular degeneration in the collecting duct. In the free DoxCp (sDoxCp) treated mice kidney section also showed moderate tubular dilatation and tubular degeneration were noticed in the collecting duct **(Fig.3.6 arrow marked).**

In the nDoxCp treated mice, the spleen sections showed mild hyperplasia of lymphatic follicles in cortex region, whereas in the free DoxCp (sDoxCp) treated mice showed

moderate hypertrophy of lymphatic follicles in the cortex region of the spleen **(Fig. 3.6 arrow marked)**.

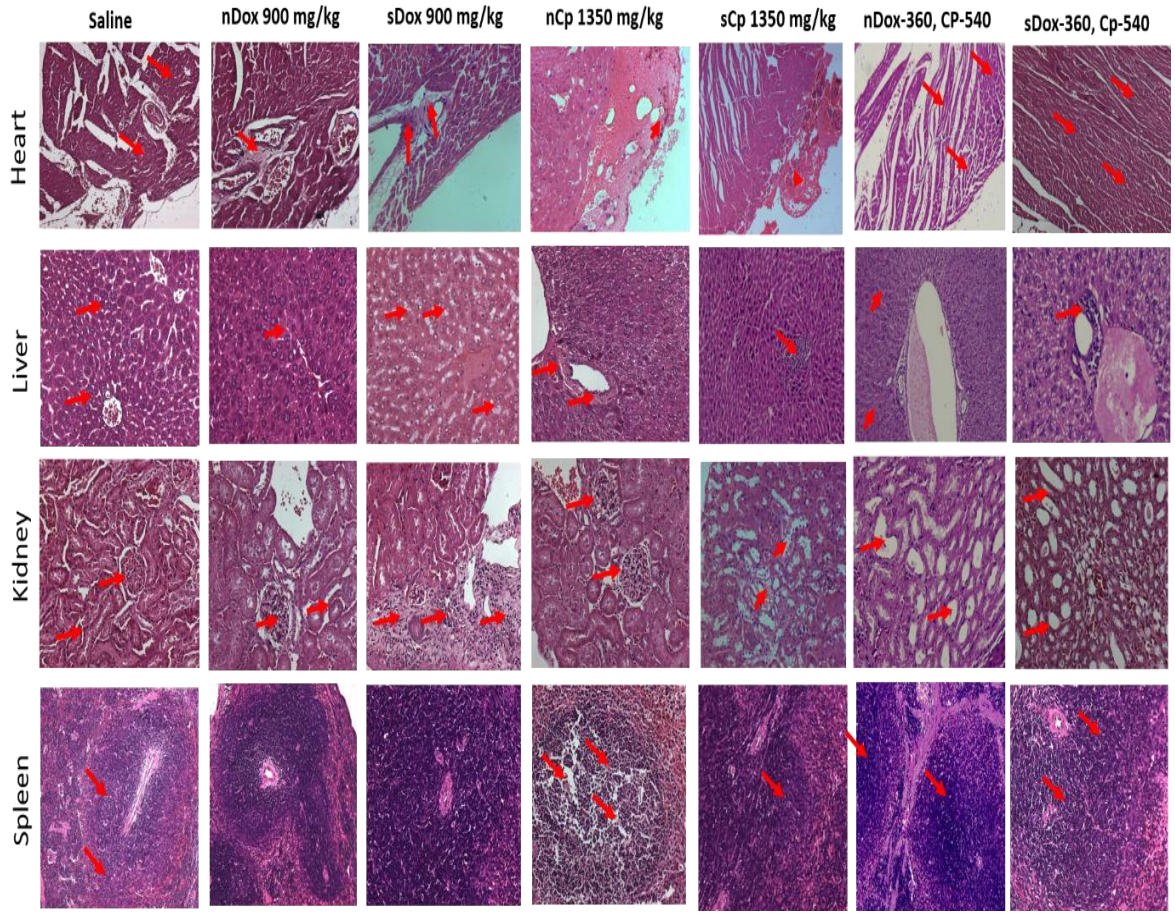

Fig. 3.6 Histopathological analysis of tissues sections. sol Dox (900mg/kg), sol Cp (1350 mg/kg) and Combination (Dox (360) and Cp (540)) were administered orally, it was compared along with the nanoformulations. After the study completion, the organs were collected and processed for paraffin section processing, then stained with Hematoxylin and Eosin (H&E). The results show no significant abnormalities in the above indicated organs, when drugs were delivered through nanoparticle formulation as compared to its soluble form.

3.3. Discussion

Among all the therapeutic designs that have been developed to combat cancer, combination therapy has shown to be most effective. The effectiveness of the combination therapy in comparison to monotherapy is due to the synergistic action of both the drugs (187). Combination therapy also delays or avoids the drug resistance mechanism by intervening the tumor growth pathways (188). Various delivery vehicles such as polymers, lipids, inorganic carriers, polymeric hydrogel was reported to deliver chemotherapeutic agents to the tumor sites. Drug delivery through nanoparticles had higher impact on clinical therapeutics due to its higher efficacy and less toxicity because of its ability to deliver the drug to the tumor sites (189).

The efficacy of combination drugs requires both the drugs to simultaneously act upon the target cells. The complications for the effective delivery of combination drugs at an optimal dose are due to the different bio-distribution of drugs within the body. The above limitations are avoided by the delivery of combination drugs through nanoformulation (190). Furthermore, the nanoparticles have the ability to deliver both hydrophobic and hydrophilic drugs to the cancer cells while causing less toxicity to nearby tissues (191).

In current study, two anti-cancer drugs, doxorubicin and cyclophosphamide were loaded together in lactoferrin nanoparticles using sol-oil method. The benefits of using lactoferrin as a nanoparticle formulation are it is a process of drug encapsulation, do not involve any chemical cross-linking, no cross linking agents are used thus related toxicities are not involved, vehicle itself acts as ligand for target localization along with lactoferrin as an active agent against tumor metastasis.

Furthermore, toxic glutaraldehyde a crosslinker which is used in preparation of several nanoparticle formulations may provide a risk toxicity. Since, lactoferrin is a natural protein

present is body fluids, nanoparticle prepared by it is safe, mice were well tolerated even at high doses (192, 193). The Transmission Electron Microscopy results showed that the dimension of blank lactoferrin nanoparticle was 40 nm and, in the drug-loaded lactoferrin nanoparticle the size was increased to around 70 nm suggesting drug was incorporated in the nanoparticle. The advantage of having smaller sized nanoparticles is that it releases the drug in the optimal dose and it also has the ability to escape the reticuloendothelial system, by which the nanoparticles can stay for longer time in the systemic circulation with higher stability in the blood (193, 194). The Zeta potential of blank lactoferrin is -46 mv and that of doxorubicin and cyclophosphamide was found to be more than -60mv. Neutral or negatively charged nanoparticles have a lower rate of nonspecific cellular uptake and lower plasma protein adsorption (194). Furthermore, nanoparticles having a zetapotential more than +30 mv or –less than 30 mv are stable. Also, the FDA approved nanoparticle formulations having negative charge were reported to possess low toxicity in comparison to the positively charged nanoparticles (195). The drug loading content were 12.6 ±1.06 % for nDox, 14.32±1.16 % for nCp and 12.81±1 % Dox , 15.5±1.2 % Cp for nDoxCp, which was higher than most of the nanoparticles having a low drug loading (less than 10%) (196). The higher drug loading could be due to the interaction of hydrophobic and hydrophilic side chains of lactoferrin protein with the drugs (197). The maximum amount of drug was released from the nanoparticles between the pH of 5-6 which is also the endosomal pH in cancer cells. Furthermore, the FTIR analysis showed that the characteristics peaks corresponding to lactoferrin, doxorubicin and cyclophosphamide were intact in the nanoformulations suggesting that they are stable (192).

Further, dose-escalation and toxicokinetic analysis of the combination nanoformulations were studied in CD 1 mice as it the most widely used mouse strain for toxicological studies (198). The reports have shown that analysing the toxicity of cancer drugs in rodents help in finding

the starting dose in humans and also the toxicity associated with it. The MTDs in humans are often determined firstly by studying in animals. The LD_{50} values helps in estimating the MTDs (199). In this treatment, we choose to deliver the chemotherapeutics drugs in oral route as it is more convenient and less invasive in comparison to the intravenous route with higher patient compliance (200). In our study, the oral LD_{50} of doxorubicin loaded lactoferrin nanoparticles was found to be 900 mg/kg body weight of doxorubicin, LD_{50} of cyclophosphamide loaded lactoferrin nanoparticles was found to be 1350 mg/kg body weight of cyclophosphamide, while combination of doxorubicin and cyclophosphamide loaded lactoferrin nanoparticle formulation LD_{50} was found to be 360 mg/kg body weight of doxorubicin and 540 mg/kg body weight of cyclophosphamide. These results showed a 2-fold increase in tolerability to doxorubicin and cyclophosphamide, this could be due to the co-delivery of both doxorubicin and cyclophosphamide in lactoferrin receptor expressing cells along with protective activity of lactoferrin protein, which will provide an effective treatment advantage of dual drug action in cancer cells as lactoferrin receptors are overexpressed on these cells (201). The Histological studies showed that the tissue was lower damage upon administration of Lactoferrin nanoformulation in comparison to the soluble form of drugs. Indeed a combination of liposomal doxorubicin and cyclophosphamide treatment in a human study reported to decrease cardiotoxicity and increase therapeutic index (202), a combination of both drug indeed would further enable targeted delivery.

In conclusion, doxorubicin and cyclophosphamide can be loaded together in lactoferrin nanoparticles, effective concentration of drugs could be decreased more than two-fold as nanoformulation significantly reduce dose-limiting toxicity of doxorubicin to heart and cyclophosphamide to liver.

CHAPTER 4

Development of a regulated delivery system for delivery of doxorubicin in MES (Sodium 2-mercaptoethanesulfonate) modified lactoferrin nanoparticles in prostate cancer cell

4. CHAPTER 4: Development of a regulated delivery system for delivery of doxorubicin in MES (Sodium 2-mercaptoethanesulfonate) modified lactoferrin nanoparticles in prostate cancer cell

4.1. Introduction

In metastatic cancer, the cells and tissue frequently develop alternative pathways to overcome drug-induced cellular damage, thus becoming resistant to cancer drugs (203). In such conditions, these alternative pathways such as checkpoint protein and DNA repair proteins were inhibited, so that the cancer cells are sensitized to a chemotherapeutic agent. Indeed, a combination of trastuzumab in combination with chemotherapeutic agents such as platin compounds, fluoropyrimidine, epirubicin and docetaxel reported to enhance quality of life and extend survival time in treatment of HER2 positive cancers (204). One of the limitation in practicing the treatment of metastatic cancer is administration of biologicals followed by a wait time before administration of chemotherapeutic agent, for the sensitization of cancer tissue to the anti-cancer agent. Thus, requiring patient admission during the treatment period. Thus, developing a delayed release formulation would help in administering biological along with delayed release from of the chemotherapeutic agent. In this objective, we present some of our results on the development of a delayed release formulation of model drug, doxorubicin.

A regulated release of drug could be achieved by (a) delayed-release or (b) sustained-release, among these in the present context a delayed release to synchronize with the molecular action of biological for affecting alternative pathways may provide the best option. There are various advantages of using controlled drug delivery formulation namely –a) the controlled drug delivery enhances patient compliance, particularly with regard to long-term therapies for chronic disorders; b) It also would help in reducing the dose of the drug and its frequency of

dosing. c) By maintaining the necessary drug concentration in the plasma, drug therapy failure is eliminated, and treatment effectiveness is increased. d) Variations in plasma medication concentration are caused by conventional dose forms (205).

Sodium 2- mercaptoethanesulfonate (MES) is an antioxidant and reported to exhibit cytoprotective effects. It is widely used as a systemic protective agent against toxicity associated with chemotherapy (206). In this study, MES was used for the formation of cross-links between protein and drug during the nanoparticle preparation for achieving the delayed drug release.

Doxorubicin, the widely used in treatment of ovarian cancer, acute lymphocytic leukemia, Kaposi's sarcoma, lymphoma, breast cancer and bladder cancer and many other (207). In this objective, we have used doxorubicin, as model drug for evaluation of the efficiency of MES in delay in its cellular delivery.

Doxorubicin loaded MES lactoferrin nanoparticles (nDox MES) were prepared as explained in the Chapter-2 using sol-oil method. Lf+ Drug+MES was taken in ratio of 4:1:20 w/w. Lactoferrin and drug were incubated for 1 hour followed by MES incubation different concentration (0.3, 0.6, 1.2, 2.0 mg) and time (5, 20, 40, 60 min & 2 hr, 4hr and 6hr). Nanoparticles were characterized using TEM, the results in show a homogenous distribution of particles with the average diameter of blank lactonano is 30 ±10 nm, while the average diameter of DOX-LfNPs + MES was 80 ±10 nm suggesting an increase in average diameter due to the loaded drug.

4.2. Results and Discussion

4.2.1. Characterisation of nanoparticles

The nanoparticles were prepared as explained in methods. TEM analysis in **(Figs 4.1 A and B)** show that the average size of blank nLacto is 46 nm, which increases to 74.3 nm in nDox MES, thus suggesting that the Dox assumed equal proportions in the particles.

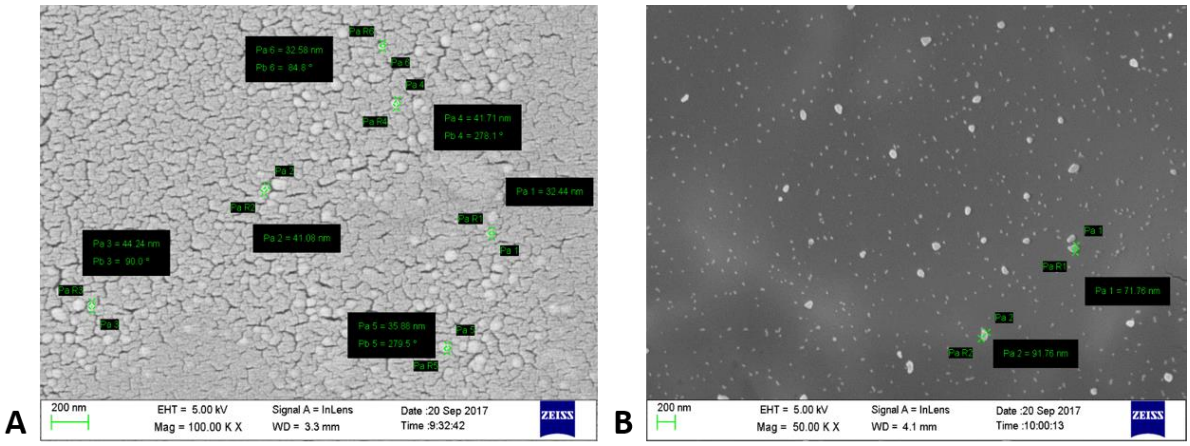

Fig 4.1. SEM analysis of A) LfNPs B) nDox MES

4.2.2.Effect of MES concentrations during nanoparticle preparation on the cellular drug release

When the Doxorubicin loaded MES lactoferrin nanoparticles (nDox MES) were treated to the prostate cancer cells (Mat Ly Lu) in increasing concentrations of (0.3, 0.6, 1.2 mg) of MES a reduction in drug release in 6 hours was observed upon 10 min treatment with 1.2 mg of MES.

Further, significant drug release was observed at 24 hours upon 10 min treatment with 1.2 mg of MES. Furthermore, while the drug release at 48 hours was significant at all concentrations of MES, though higher drug release was observed upon 10 min treatment with 1.2 mg of

MES **(Fig 4.2).**

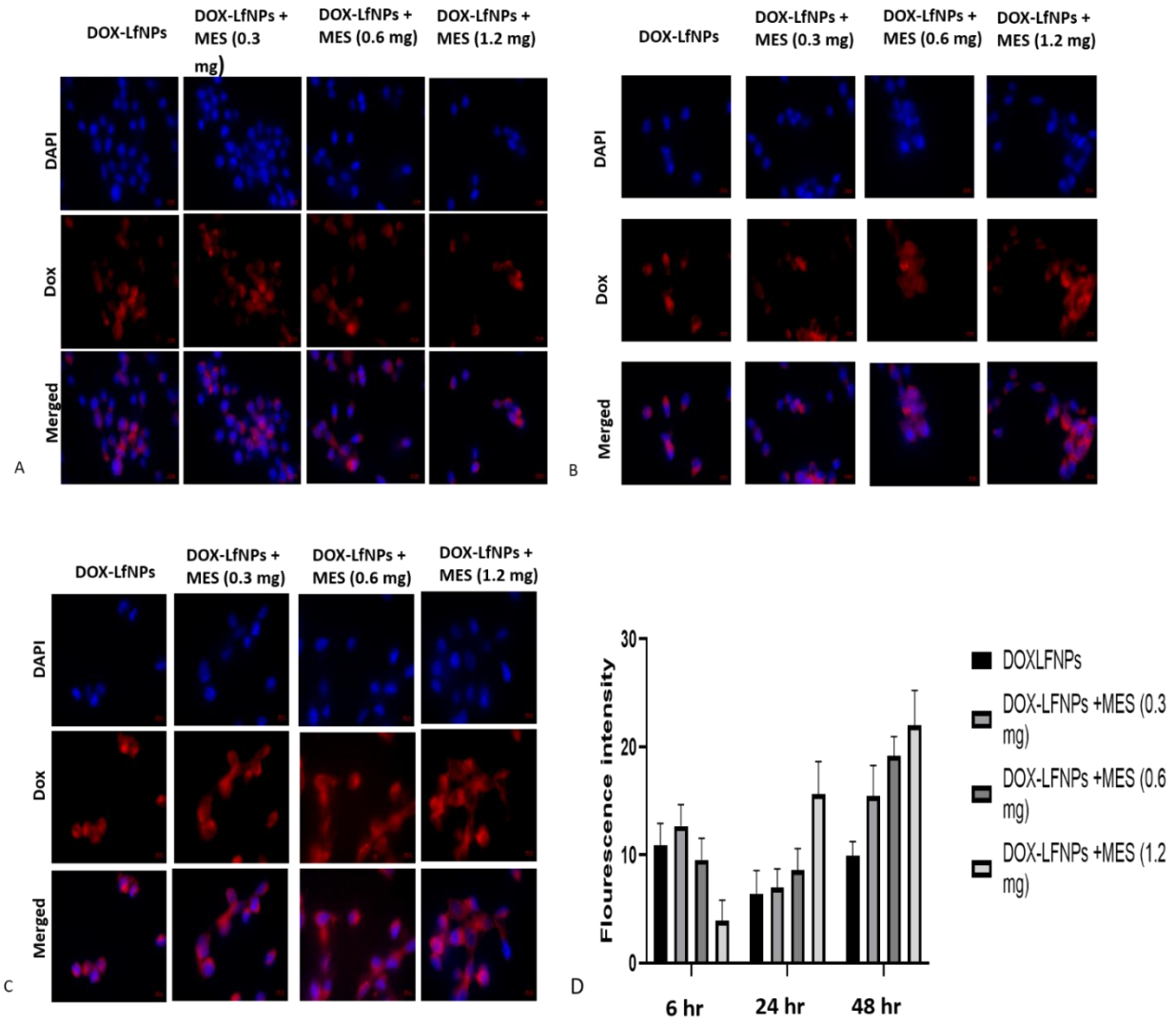

Fig. 4.2. DoxLfNPS+MES was given in 3 different concentrations of MES (0.3, 0.6 and 1.2 mg) where MES was incubated for 10 min. (A) DoxLfNPS+MES was treated to prostate cancer cell line for 6hrs. B) DoxLfNPS+MES was treated to prostate cancer cell line for 24hrs C) DoxLfNPS+MES was treated to prostate cancer cell line for 24hrs. D.) Fluorescent intensity was quantified using Image J software, the results are presented in a bar diagram.

After the time point cells were collected and DAPI was used for staining nucleus and the doxorubicin was observed based on intrinsic fluorescence in red filter. Observed that MES

delayed the release of drug in the highest concentration. MES-treated doxorubicin-loaded lactoferrin nanoparticles showed a concentration-dependent delayed drug release kinetics in prostate cancer cells (Mat Ly Lu).

4.2.3. Effect of MES incubation time during nanoparticle preparation on the cellular drug release

In the above section, we observed that 1.2 mg of MES treatment during drug loaded lactoferrin nanoparticle preparation for 10 minutes could delay drug release for 24 hours. We have analysed the influence of time of incubation with MES during nanoparticle preparation on the drug release kinetics in prostate cancer cells.

We have varied time of incubation at 5, 20 and 60 min during nanoparticle preparation, we have observed an incubation time-dependent delayed drug release, wherein in the 20 and 60 min MES incubation could reduce drug release by 40% when the cells were treated for 6 hours **(Fig 4.3).**

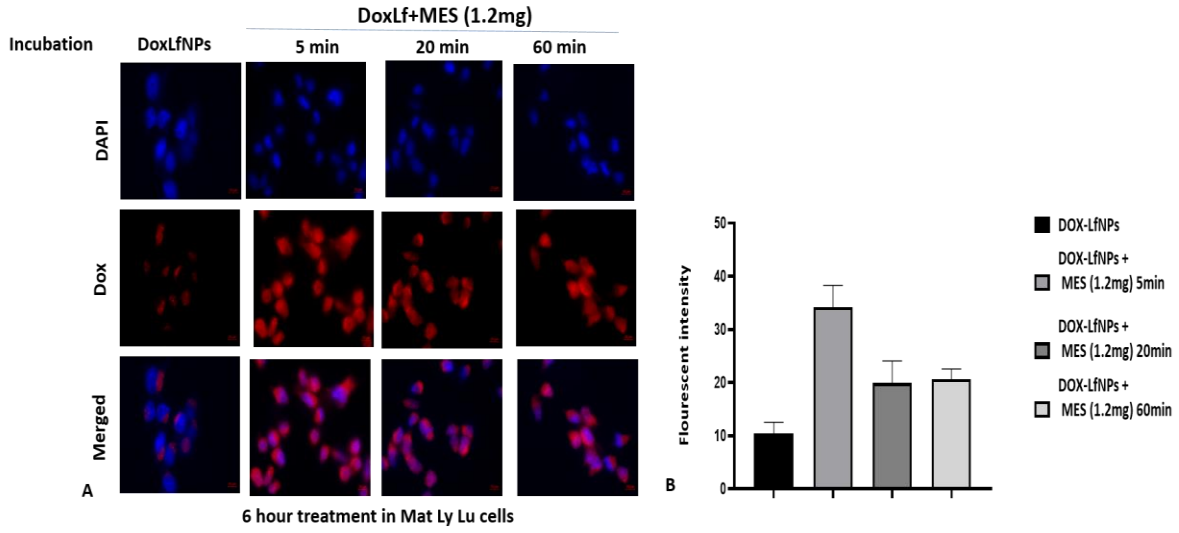

Fig. 4.3. DoxLfNPS+MES where 1.2 mg of MES was used and MES was incubated for 10 min. A) DoxLfNPS+MES was treated to prostate cancer cell line for 6hrs.

B) Quantity of Fluorescent intensity was determined using Image J software and represented as a bar diagram

4.2.4.Drug release in 2 mg MES treated nDOX MES (2 mg) in prostate cancer cells

The above two sections showed that the concentrations of MES and incubation time of MES with lactoferrin-drug mixture determine the time of release. In this section, we have studied effect of 2 mg of MES on drug release kinetics in cells.

Lactoferrin and doxorubicin mixture was incubated with 2 mg of MES for 10 min and nanoparticles were prepared. Intracellular drug release was monitored over 6 hours, the results presented in **(Fig 4.4)** shows that the rlease of drug was completely inhabited for 6 hours.

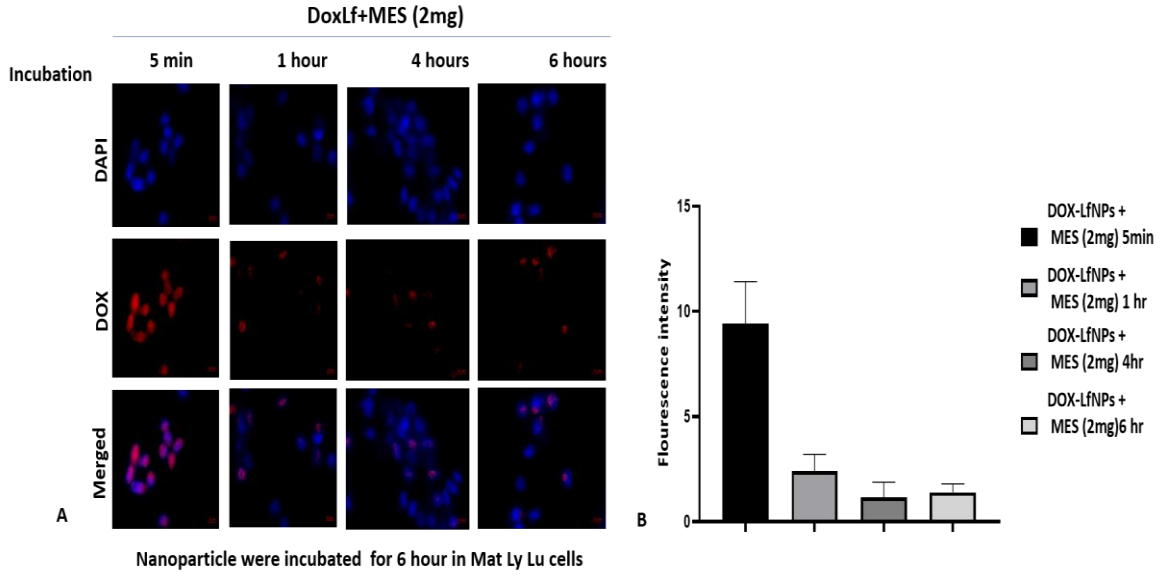

Fig. 4.4. DoxLfNPS+MES where 1.2 mg of MES was used and MES was incubated for 10 min.

A) DoxLfNPS+MES was treated to prostate cancer cell line for 6hrs.

B) Quantification of Fluorescent intensity was carried out using Image J software and shown in a bar diagram

This study show that the treatment of cross linking agent to drug-lactoferrin complexes would induce cross links between drug and protein, thus the nanoparticles formed would regulate the release of drug in cells. The kinetics of intracellular drug release is regulated by the concentration of MES used for treatment of drug-protein complexes and time of incubation of MES with drug-protein complexes before preparation of nanoparticles. Further, MES treated did not affect nanoparticle formation **(Fig 4.1)** and also, the ability of nanoparticle in cellular localization of the drug.

Traditionally drug release is regulated by different type of compositions and polymerization method along with use of cross-linking agents 5-vinyl-1,3-dihydrobenzo[c]thiophene 2,2-dioxide with nitroxide-mediated co-polymerisation in the presence of benzyl acrylate. The process involves use of temperature to 250 °C follow by reduction in the presence of Pd/C. Fills from contact lenses and hydrogel were prepared in imprinting of Hyaluronic acid (HA) on acrylamide (AM), 2-(diethylamino)ethyl methacrylate (DEAEM), nelfilcon A, N-vinyl pyrrolidone (NVP), this allows a 24 hour control release of HA (208). These chemicals possess systemic toxicity, may have limitations in systemic use.

The singlet oxygen-responsive linkers such as thioketal (TK) linkers were used for click-chemistry based cross-linking of polyphosphoesters (PPE) for preparation of poly (thioketal phosphoesters) (TK-PPE) nanoparticles. These nanoparticles after localization in tumors could be activated by exposure to 660nm laser (209). These materials are efficient in localised treatment in solid tumors.

In summary, MES would serve as cross linking agent for delayed release of drug from lactoferrin nanoparticles, drug release time could be controlled by concentration of MES and incubation time. This a simple technique in regulated delivery of drug.

CHAPTER 5

Evaluation of efficacy of docetaxel-loaded lactoferrin nanoparticles against prostate cancer *in vitro* and *in vivo*

5. Chapter 5: Evaluation of efficacy of docetaxel-loaded lactoferrin nanoparticles against prostate cancer *in vitro* and *in vivo*

5.1. Introduction

Prostate cancer is rated to be the second most prevalent cause of cancer among males after lung cancer and is the sixth major cause of death in men worldwide (210)(90). It is an age-dependent disease wherein the risk of incidence of prostate cancer rises with an increase in age (90). When localized cancer progresses to metastatic cancer, then chemotherapy and androgen deprivation therapies are employed to treat prostate cancer (98). Recent phase II clinical study in metastatic prostate cancer treatment using a combination of androgen-receptor inhibitor, darolutamide, androgen-deprivation therapy and docetaxel (DTX) showed promising though the adverse events remains the same (211). Another clinical study for treatment of metastatic prostate adenocarcinoma using a combination of abiraterone, androgen-deprivation therapy and DTX showed promising with toxicity at modest levels (212). Both studies included with DTX, the dose-limiting toxicities myelosuppression, neutropenia, and neurotoxicity, thus requiring a formulated form of DTX for improved safety. In addition, the DTX use is limited due to the limited dosage bioavailability in view of low solubility and non-target effects (151). Studies using nanoformulations using mesoporous CuS (213), poly (lactide-co-glycolide) (PLGA) (214), PEGylated DTX-functionalised titanium nanotubes (215) could achieve sustained release of DTX along with photoactivation capability, though they are devoid of target localization ability. Studies of targeted delivery of DTX involved development of DTX conjugates of mesoporous surface nucleolin binding aptamer AS141115 (216), hyaluronic acid-polyethylene glycol-distearoyl phosphoethanolamine decorated DTX and formononetin co-loaded PLGA-PEG conjugated

with EGFR peptide (GE11) (217), showed interesting results in studies *in vitro* as well as *in vivo*. Being DTX is conjugated in these formulations that limits the concentration of DTX in cellular localization and may exhibit slow release kinetic thus limiting drug bioavailability in prostate cancer tissue.

Lactoferrin, an 80 KDa protein iron containing protein reported to stabilise intestinal mucosal immunity in mice bearing tumors (218, 219). V-ATPase, an ATP-driven proton pump, is present in highly metastatic cancer cells and involved in acidic tumor microenvironment-associated with metastasis and tumor invasion (220). Lactoferrin has been shown to inhibit plasmalemmal V-ATPase associated with metastatic cancer cells leading to alkalisation of extracellular tumor microenvironment and intracellular acidification (221). Higher expression of lactoferrin was correlated with enhanced repair activity in tumors. Lactoferrin overexpression in prostate cancer cells affects Stat-3 expression in Jak/stat pathways and inhibit secretion of tumor-derived GM-CSF, thus dysregulating tumor-associated immunosuppression (222). These studies clearly point out lactoferrin as a potential ligand for targeting prostate cancer tissue both for immune activation and a targeting ligand against cancer (13, 223). Thus, it is an increasing interest in developing formulations containing lactoferrin such as DNA loaded lactoferrin and polyethyleneimine (PEI) conjugated goldnanocages for delivery to prostate cancer cells (224, 225). In this study, DTX was loaded into pure lactoferrin nanoparticle without any chemical modification for delivery of DTX and lactoferrin to prostate cancer cells and tissue. The results show an enhanced drug bioavailability and safety along with an improvement of cancer regression.

5.2. Results and Discussion

5.2.1. DTX-loaded Lf nanoparticle preparation and characterization

Nanoparticles were characterized using TEM, the results in **(Fig 5.1)** show a homogenous distribution of particles with the average diameter of blank lactonano is 30 ±10 nm, while the average diameter of DTX-LfNPs was 60 ±10 nm suggesting an increase in average diameter by 30 nm due to the loaded drug. The process of preparation of DTX-LfNPs do not involve any chemical treatment or conjugation, thus incubation of lactoferrin and docetaxel allow interaction of drug with protein, which upon addition to oil with vigorous stirring would orient the hydrophobic regions of protein to the oil phase leading to phase separation of drug-encapsulated protein multimeric system and protein nanoparticle formation, nanoparticle aggregation was controlled through sonication and followed by snap freezing in liquid nitrogen. Further, higher surface exposure of nanosized particles facilitate the recognition to the receptor for binding thus drug release and providing the ability to escape the reticuloendothelial system for allowing longer resident time in the systemic circulation (193)(194). The entrapment efficiency of DTX in DTX-LfNPs was measured by the estimation of the acidic release of DTX using HPLC, the encapsulation efficiency (EE) of DTX in DTX-LfNPs was determined to be 62.06± 4.07 % (n=3) and the drug loading content was 15.51±1.01 % (n=3).

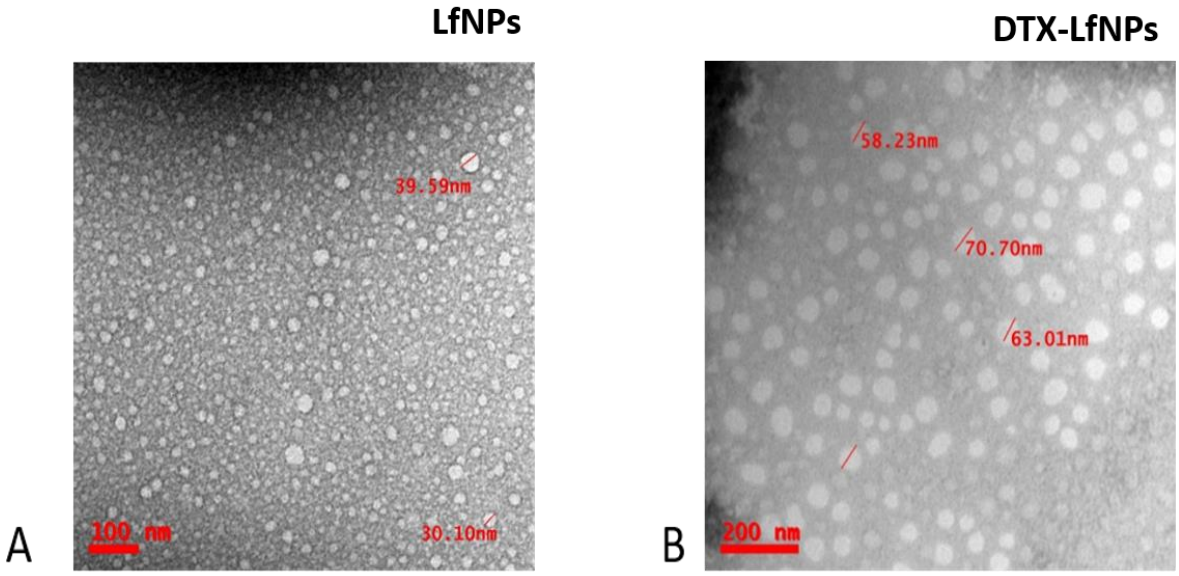

Fig 5.1. Microscopic characterization. A. Nanoparticles were anaysed using TEM, the results show that Lactoferrin nanoparticles size was increased upon DTX loading. LfNPs (A) and DTX-LfNPs (B).

5.2.2. Characterization of nanoparticles using ATR (Attenuated total reflectance)

The structure of drug and lactoferrin in lactoferrin nanoparticle was analysed using ATR to know if drug and protein undergoes any structural changes during nanoparticle formation (226). The results show Amide I bands were positioned around 1634 & 1639 cm^{-1} is corresponding to the characteristic of alpha-helices **(Fig 5.2)**. While Amide II (C-N stretching and N-H bending) were detected at 1513 & 1456 cm^{-1}. The C-O-C stretch was observed around 1074 cm^{-1}& 1091 cm^{-1}. The Amide I and Amide II band positions are sensitive to the secondary structure content present in the protein. The ATR spectrum of DTX and DTX-LfNPs showed bands at 3455 and 3342 cm^{-1} for (νO–H and νN–H), 1450 and 1439 cm−1 (νC=C), 2969 cm−1 (νasCH) and the band assigned to the vibrational mode (νC=0) relative to carbonyl groups of ester at 1737 and 1739 cm^{-1} **(Fig 5.2)**. The presence of characteristic

spectral signature of DTX in DTX-LfNPs confirms that drug structure is intact suggesting that the structure of DTX was unaffected when the drug is loaded in Lf nanoparticles.

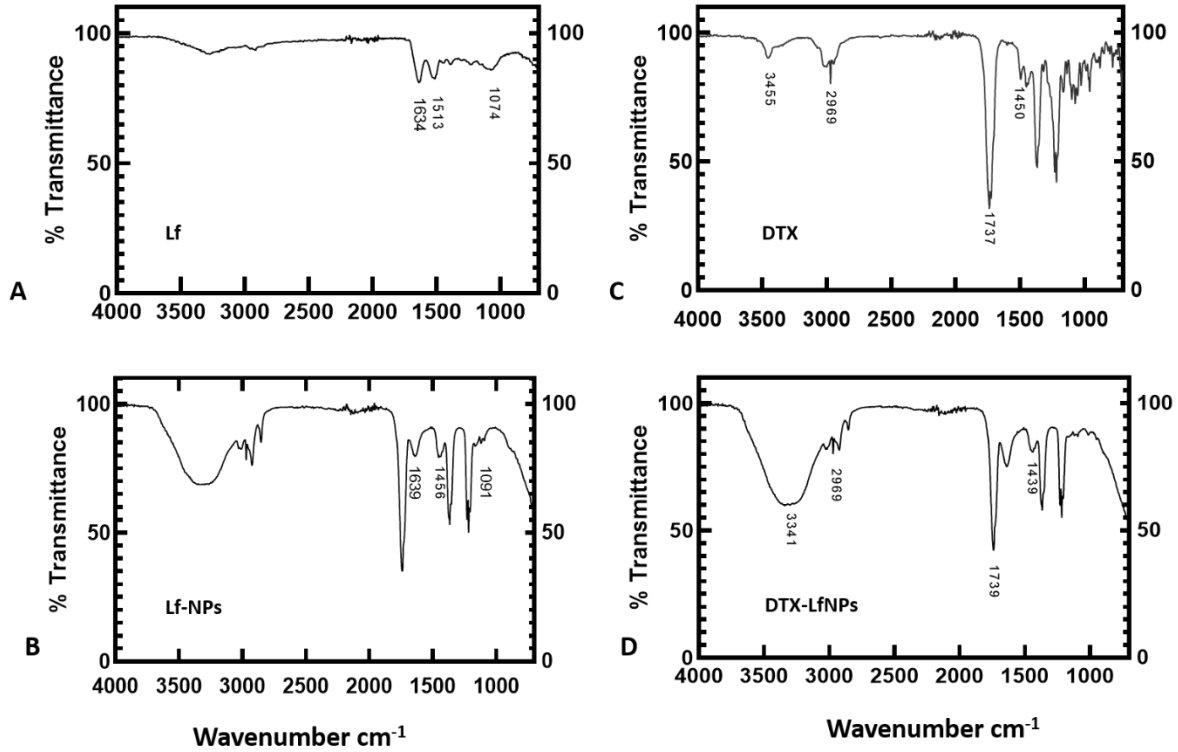

Fig.5.2 ATR spectral analysis. The ATR analysis of Lactoferrin powder (A) LfNPs (B), DTX powder (C), and DTX-LfNPs (D). The results show that DTX in DTX-LfNPs is intact.

5.2.3. Overexpression of lactoferrin receptor in prostate cancer cells

The expression of lactoferrin receptor in a prostate cancer cell line, Mat Ly Lu and lung cancer cell line, A549 was analysed using immunohistochemical (IHC) analysis for reactivity against antibody against lactoferrin receptor, the results in **(Fig 5.3)** show a significant expression in Mat Ly Lu prostate cancer cells, while negligible expression of lactoferrin receptor was observed in A549 cells suggesting that prostate cancer cell significantly express lactoferrin receptor, would serve as potential target for lactoferrin nanoparticles. While no expression of lactoferrin receptors in A549 is supported by the reports that in these cells

transferrin bound iron uptake occurs via TNF alpha and IL1 beta hence these cells do not express lactoferrin receptors (227, 228).

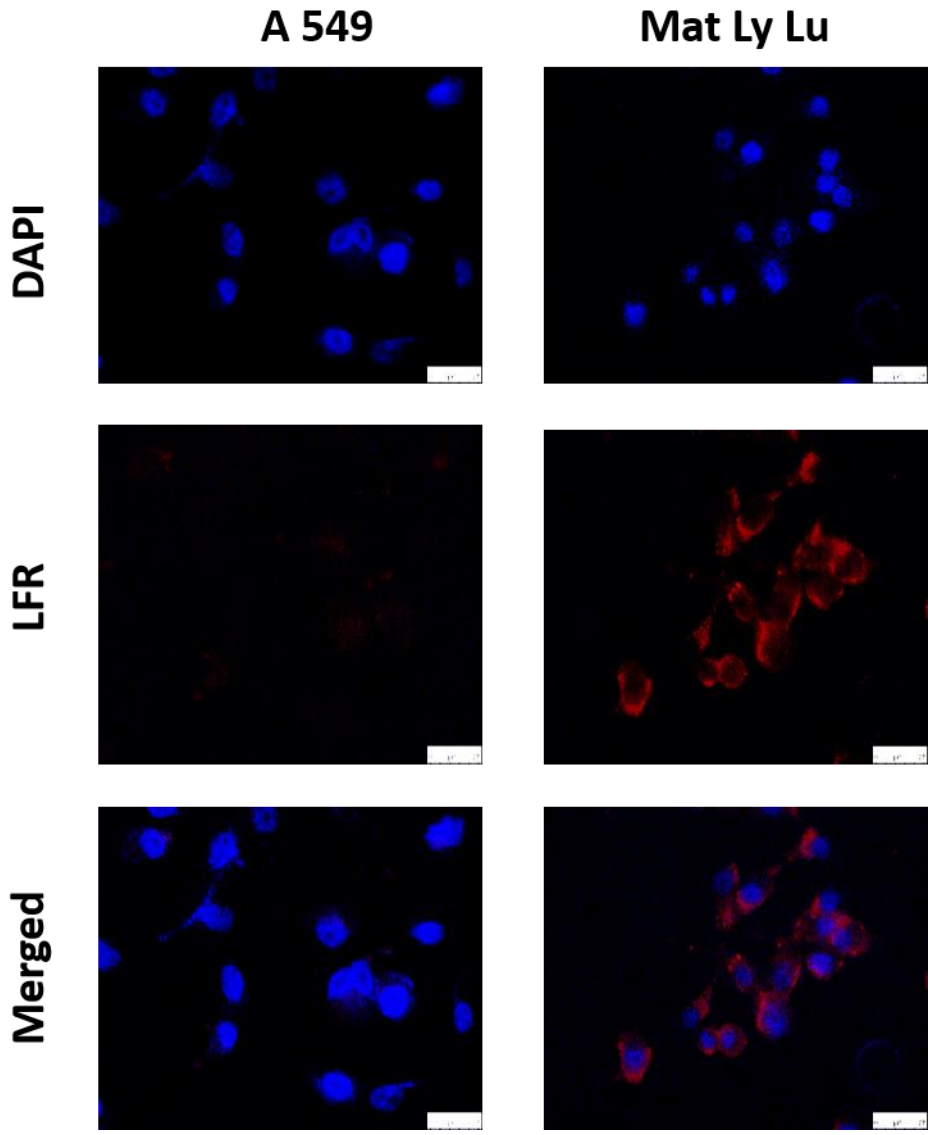

Fig. 5.3. Lactoferrin receptor expression. IHC analysis of the lactoferrin receptor expression in A549 cell line and Mat Ly Lu shows that the lactoferrin receptor was expressed in Mat Ly Lu cells but not in A549 cells. The nucleus was stained using DAPI and the lactoferrin receptor was labelled using Alexa flour 594 secondary antibody. B. LfNP mediated delivery in prostate cancer cells.

5.2.4. Receptor-mediated entry of nanoparticles in Mat Ly Lu cells

The involvement of lactoferrin receptors in the uptake of lactoferrin nanoparticles was analyzed using a competition of soluble lactoferrin with Nile red loaded lactoferrin nanoparticles. The results of these studies presented in **(Fig 5.4)** show that lactoferrin competes out LfNPs-mediated localization of nile red in Mat Ly Lu cells suggesting that the lactoferrin nanoparticle mediated delivery of nile red is through lactoferrin receptor mediated pathway. Further, it was observed that there is a small portion of nile red localization even after competition with lactoferrin, this could be due to intracellular diffusion of smaller size nanoparticles, though it is a minor proportion.

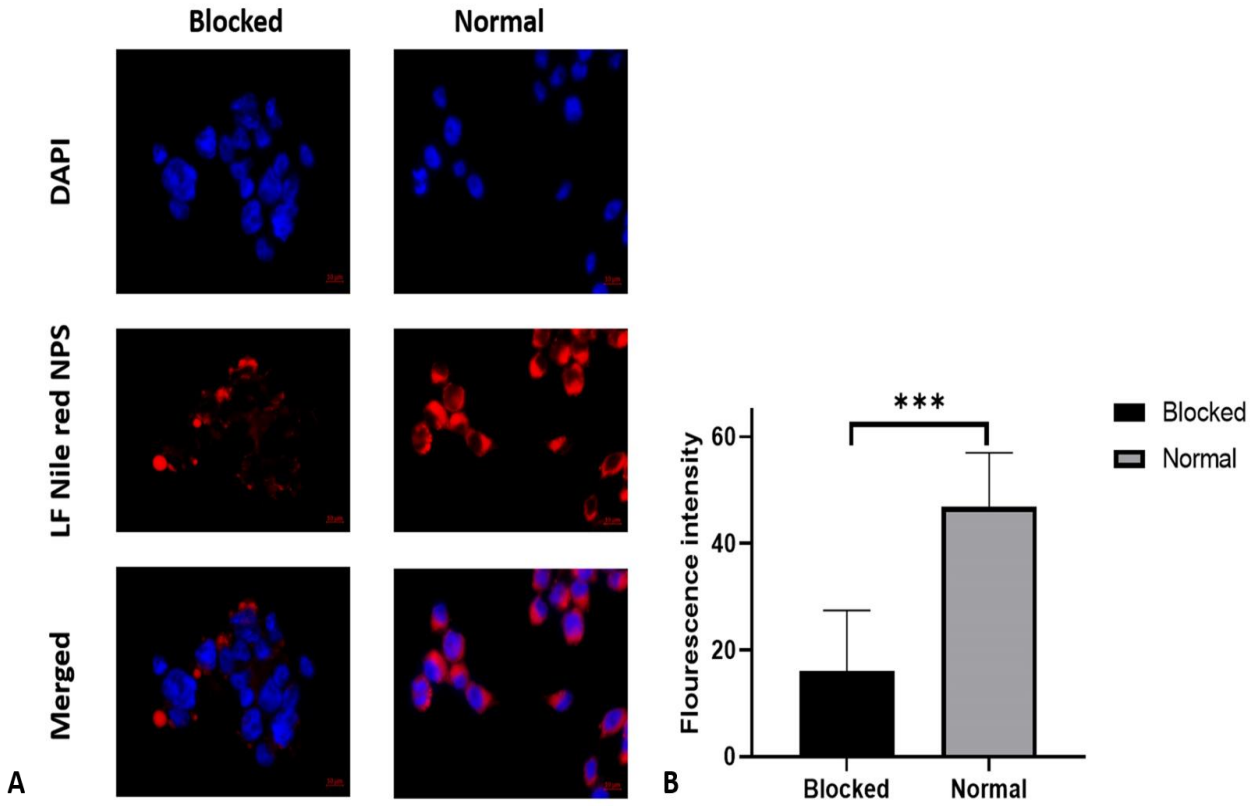

Fig 5.4. Drug delivery. LfNP mediated delivery in prostate cancer cells. The Mat Ly Lu cells were grown in a complete medium containing 1% Lactoferrin solution for 12 h, and then Nile

red-LfNPs were added in treated and untreated cells and kept in incubation for 6 hours and cells were observed under a fluorescence microscope. Images are given in Panel A and fluorescent intensity was quantified using Image J software and presented as a bar diagram in Panel B. The standard deviation is indicated inerror bars. P-values were calculated by using two-tailed unpaired student's *t*-test; * indicates P < 0.05, ** indicates P < 0.01, ***P< 0.001, ****P <0.0001.

5.2.5. Cytotoxicity of drug-loaded nanoparticles

The analysis of cytotoxicity of DTX and DTX-LfNPs was carried out by treatment of cells for 48 hours and estimation on cell viability using MTT assay, the results showed in **(Fig 5.5 A)** suggest that enhanced anti-proliferative activity when treated with DTX-LfNPs compared to DTX. The IC_{50} values of DTX and DTX-LfNPs in Mat Ly Lu cells were found to be 4.29± 0.120 nM and 1.68 ± 0.98 nM. These results suggest that DTX-LfNPs exhibits 2.5 times higher efficacious compared to DTX. The levels of polo-like kinase 1 (Plk-1), a kinase involved in cell division were analysed by western blot, the results showed a decrease in Plk-1 confirming efficacy of DTX-LfNPs **(Fig 5.5 B).** While Bax level increased in DTX-LfNps treated cells compared to DTX **(Fig 5.5 B).** Enhanced efficacy could be due to the increased intracellular retention of DTX upon delivery through LfNPs. This could be facilitated by higher uptake of DTX when loaded with DTX-Lf NPs compared to DTX alone. It has been previously reported that lactoferrin nanoparticles are non-toxic to healthy cells (172).

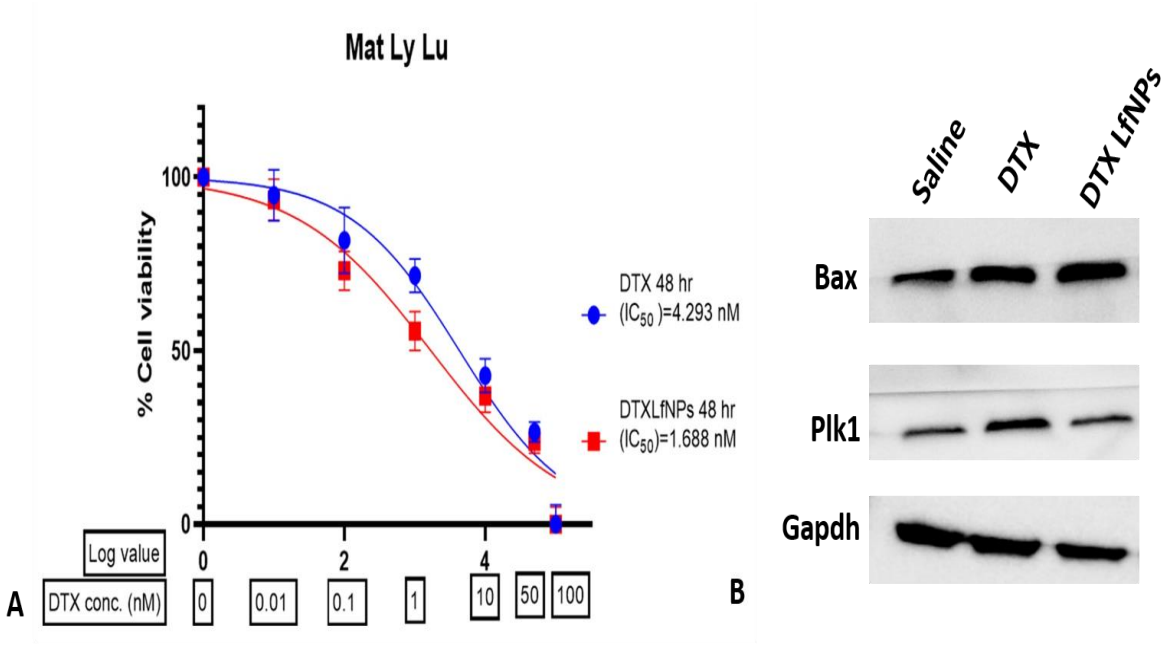

Fig 5.5. Action of DTX-LfNps on cell proliferation of Mat Ly Lu cells. A, Anti-proliferation activity. Action of DTX and DTX-LfNPs on proliferation of prostate cancer cell line Mat Ly Lu cells were incubated for 48 hours in the presence of increasing concentrations of DTX and DTX-LfNPs and viable cells were estimated by MTT assay as described in methods. Each data point represent mean with standard deviation in form of error bars. IC_{50} was calculated at the end of 48 hours from the treatment time. It is observed that IC_{50} of DTX-LfNPs was decreased in comparison to soluble DTX. **B. Analysis of Plk-1 and Bax in DTX and DTX-LfNPs treated cells.** Cells were incubated with DTX and DTX-LfNPs for 48 hours, the treated cells were lysed and protein was estimated. Equal proteins was resolved in SDS-PAGE followed by detection for Plk-1 and Bax using Western blot analysis by ECL reagent. GAPDH was incorporated as loading control.

5.2.6. Orthotopic prostate tumor development

For the prostate tumor development studies, rats were divided into 6 groups where 3 groups were orthotopically injected with 1XPBS into the prostate tissue and in the other 3 groups $5X10^5$ Mat Ly Lu cells were injected into the prostate tissue. Further, both the saline treated as well as Mat Ly Lu cells treated groups were divided into 3 groups i.e, based on the weeks (1^{st}, 2^{nd} and 3^{rd} week) saline or cells was incubated into the prostate tissue. After the end of the time point animal were sacrificed and prostate tissues were collected and analysed using H and E staining. In the rats injected with 1XPBS into the prostate tissue we observed normal morphology of prostate tissue **(Fig.5.6 A, B and C)**, whereas in the rats injected with Mat Ly Lu cells into the prostate tissue metastatic carcinoma was observed **(Fig.5.6 D, E and F)**. Hence, confirming the development of tumor.

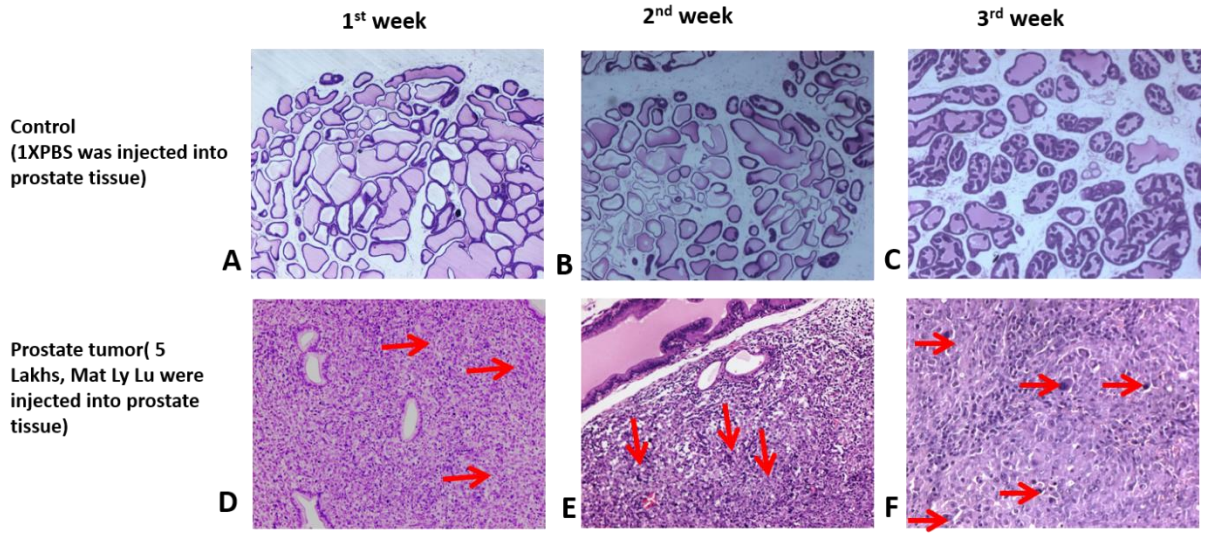

Fig. 5.6 H and E analysis of control prostate and tumor prostate.

A-C) Normal architecture of prostate glands was observed. D) Moderately differentiated neoplastic cells formed nodules [grade- 2] surrounding entire mucosal glands. Extensively invaded adjacent region. – Metastatic adenocarcinoma. E) Moderately differentiated [grade 2] epithelial cells extensively invaded adjacent region – Metastatic adenocarcinoma F)

Moderate differentiated [Grade 2] neoplastic epithelial cells formed a nodules invaded from adjacent region – metastatic carcinoma.

5.2.7. Overexpression of lactoferrin receptor in prostate cancer tissue

We studied the expression of lactoferrin receptor in healthy rat prostate tissue vs prostate cancer tissue of orthotopically cancer induced rat. Tissue sections were IHC analysed using anti-lactoferrin receptor antibody, then probed with secondary antibody conjugated with Alexa flour 549. The results in **(Fig 5.7)** shows a high expression of lactoferrin receptor in prostate cancerous tissue as compared to control prostate tissue suggesting Mat Ly Lu mediated cancer induced in prostate would serve a good model to evaluate efficacy of drug loaded- lactoferrin nanoparticles. Indeed, it has been reported that the levels of circulating intelectin-1, one of the lactoferrin receptor, showed to be higher in prostate cancer patients when compared to the healthy volunteers (229, 230).

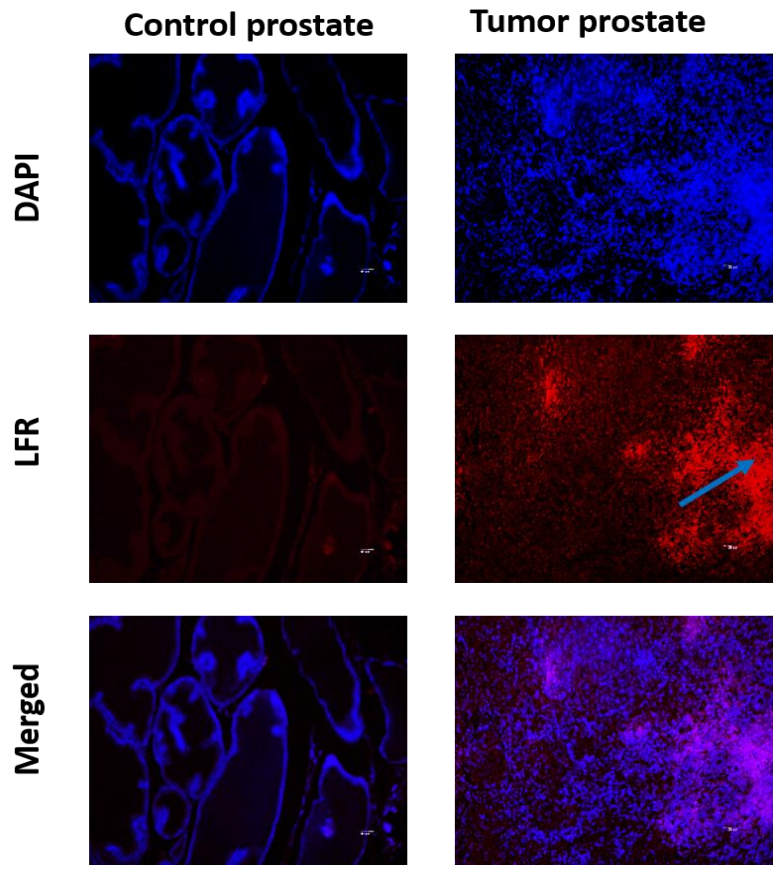

Fig 5.7. Lactoferrin receptor expression in prostate cancer tissue. Tissue sections from prostate tissue from healthy and cancer-bearing rat was analysed for lactoferrin receptor expression using IHC. The results shows that the lactoferrin receptor was over expressed in prostate tumor in comparison to control prostate. The nucleus was stained using DAPI and the lactoferrin receptor was labelled using Alexa flour 594.

5.2.8. Bioavailability of DTX-LfNPs in prostate

Bioavailability studies were conducted by administering a single dose through an intravenous route (bolus) in two groups of Wistar rats (n=6). One group is administered with DTX-LfNPs (equivalent DTX dose of 10 mg/kg body weight) and the second group was administered DTX (10 mg/kg body weight). After 24 hrs treatment, the prostate was collected from the rat, DTX was extracted and estimated using HPLC. The results are presented in **(Fig 5.8)** showed

a 2-fold increase in drug localization in prostate tissue when DTX-LfNPs **(Fig.5.8, grey bar)** compared to DTX.

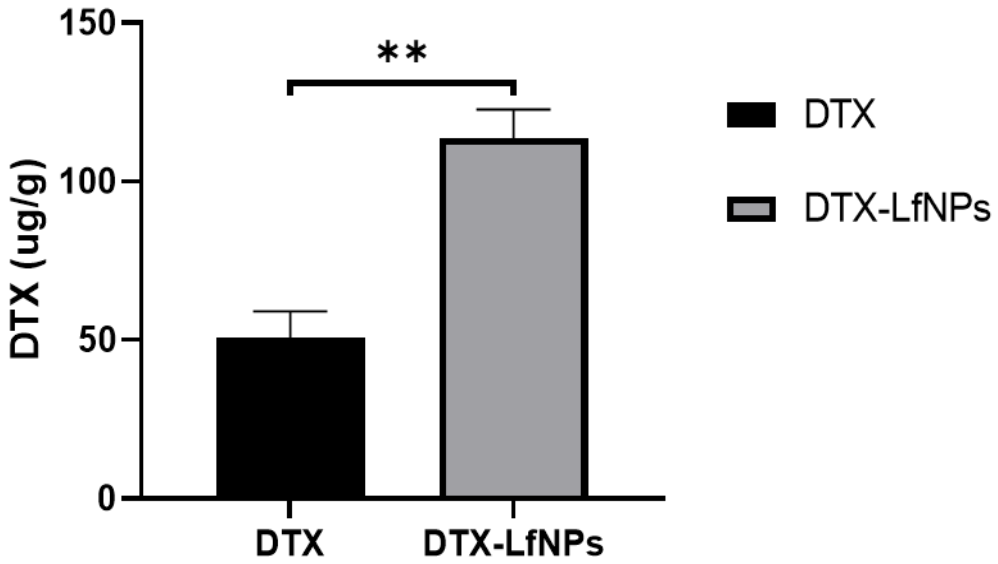

Fig.5.8 Prostate uptake of DTX in male Wistar rat 24 h post injection of DTX and DTX-LfNPs throgh intravenous route with an equivalent dose of 10 mg kg−1. The data was presenred as Mean ±SD, n=6. P-values were calculated by using two tailed unpaired student's t-test; * indicates P < 0.05, ** indicates P < 0.01, ***P< 0.001, ****P <0.0001.

5.2.9. Comparative analysis of DTX and DTX LfNPs in Prostate Cancer

A comparative analysis of activity of DTX and DTX–LfNPs against prostate cancer was studied in a prostate cancer model developed by orthotopic injection of Mat Ly Lu cells in rats as described in the method section. Mat Ly Lu cell line is derived from an anaplastic androgen-independent tumor, hence more relevant model for the analysis of activity of chemotherapeutic agent (231).

Rats were randomly divided into three treatment groups (n = 6), saline, DTX, DTX LfNPs at a dosage of 2.5 mg/kg body weight equivalent of DTX, the drugs were administrated intravenous route on day 12 and the prostate was dissected on the day 21 and processed for histology and other parameters. The tumor masses were excised from orthotopic rat prostate cancer model following treatment with saline or DTX formulations as indicated in **(Fig 5.9 A),** the results show that the tumor dimensions are significantly decreased in DTX LfNPs treated rats compared to DTX **(Fig 5.9).**

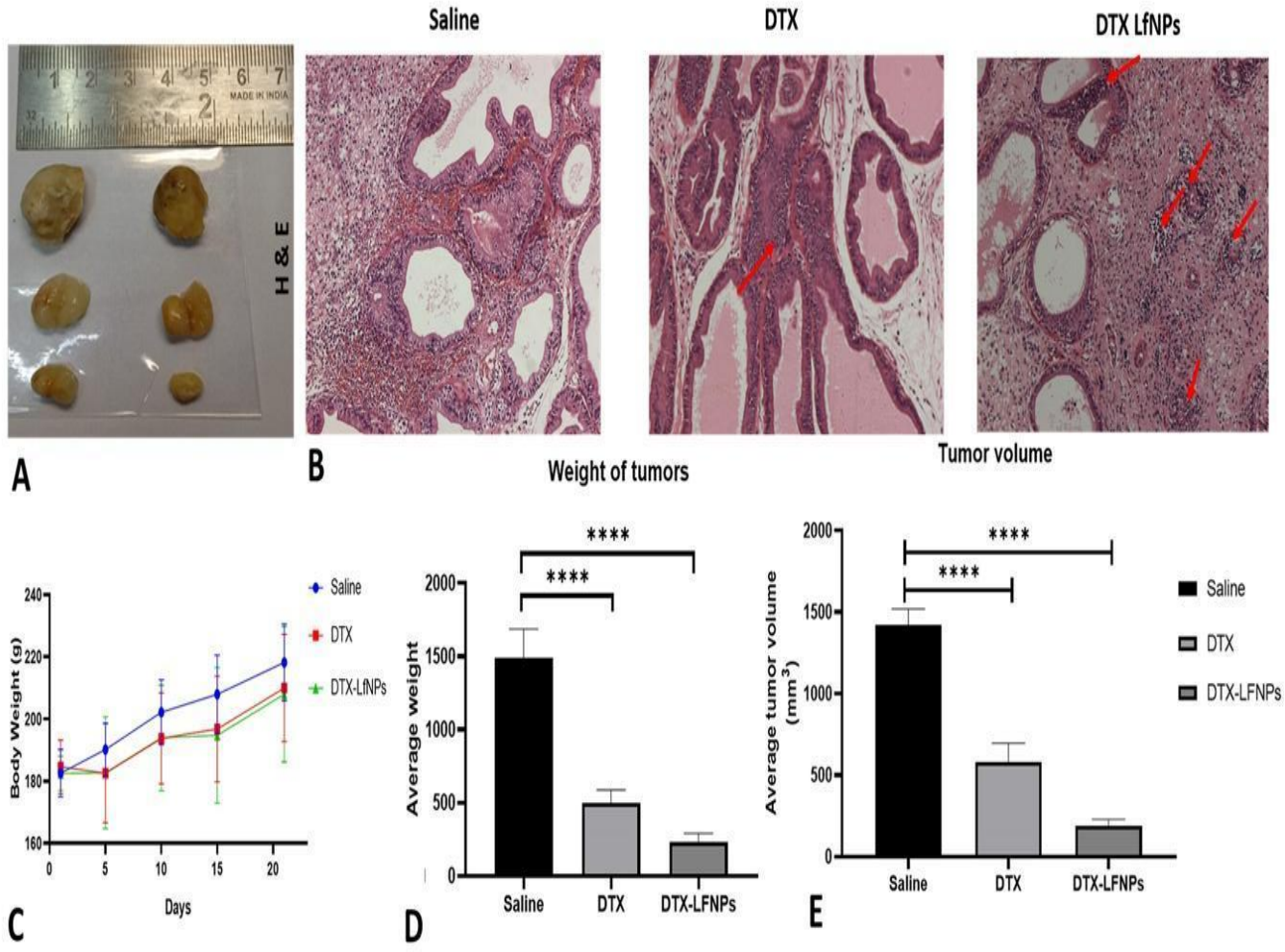

Fig. 5.9 Treatment of tumor. Mat Ly Lu cells were injected on the 1st day, drugs were given on the 12th day and rats were sacrificed on the 3rd week. 2.5 mg/kg body wt of drugs were given *via* tail vein injection (intravenous) for both soluble Docetaxel (DTX) and Docetaxel Lactoferrin nanoparticles (DTX-LfNPs).

A. Photograph of tumor tissues were taken at the end of 3rd week

B. H & E analysis of tumor tissue sections. Histological analysis of prostate tissue sections under two treatment conditions (DTX and DTX-LfNPs) is carried out at 20X magnification, saline treatment is control. Red arrows indicate the site of observation described in the results.

C. Changes in the bodyweight of the animals with the time

D. Weight of the tumors was measured at the end of 3 weeks (n=6).

E. The tumor volume (V) was calculated from the the measurement of maximum diameter (a) and minimum diameter(b) of tumor mass in the whole prostate tissue using vernier calliper and the tumor volume was calculated using the below formula.

Tumor volume (V) = $0.5\ ab^2$

Tumor volumes were calculated at the end of 3 weeks (n=6).

Error bars represent the SD of the deteminnants. P-values were calculated by Tukey's multiple comparison post-test of ANOVA; * indicates P < 0.05, ** indicates P < 0.01, ***P< 0.001, ****P <0.0001.

The tissue sections were analyzed for pathological effects of cancer and the effectiveness of treatment on tissue pathology. The results in **(Figure 5.9B)** shows Hematoxylin and eosin (H & E) staining of sections of tumor tissues in all three groups. The groups which received treatment exhibited necrosis to a certain extent. In the DTX-LfNPs treated cancer tissue, it was observed that severe necrosis and apoptosis of neoplastic mucosal epithelial cells with submucosal accumulation of necrotic materials and fluids, and inflammatory cells **(Fig 5.9B)**, showed with arrow). Thus, the histology results confirm that DTX-LfNPS exhibits higher efficacy in regression of tumor when compared to the free DTX treatment.

Analysis of body weight showed that the body weight decreased in both DTX and DTX-LfNPs treated compared to saline, though there was no notable differences in body weight among the formulations of DTX and DTX-LfNPs. While the prostate tumor weight **(Fig 5.9D)** and tumor volume **(Fig 5.9 E)** show a significant decrease in DTX-LfNPs-treated rats as compared to rats treated with DTX. When tumor regression was calculated based on the average prostate tumor weight in saline-treated rat versus DTX formulation treated rat, the percent decrease tumor weight when treated with docetaxel was 66.40% while it was 84.38 %

when treated with DTX-LfNPs. These results suggest that the DTX-LfNPs confer 18% higher efficacy compared to DTX, which can be correlated with 2 times higher localization of DTX when DTX-LfNPs were administered **(Fig 5.8)**. The relative increase in efficacy of DTX-LfNPs compared to DTX (18%) was higher than that was reported using Docetaxel-loaded aptamer nanoparticles (DTX apt NPs) (16.08%) (232). Also, tumor decrease in DTX-LfNPs treated rats compared to saline-treated one was higher compared to that reported using DTX ap NPs and core-shell lipid-polymer hybrid nanoparticles (CSLPHNPs) in mice (233). The average tumor regression volume of the prostate after treatment with DTX-LfNPs was 13.32 %, while with DTX **(Fig 5.9E)**, it was 40.83% when compared with the group treated with the saline.

5.2.10. Treatment advantage of DTX-LfNPs

The human nuclear protein Ki67 (pKi67) is a protein encoded by the MKI67 gene. pKi67 has been established as a potential predictive marker for disease prognosis in analysis of biopsies from patients with cancer. Further, levels of pKi67 has been well correlated with metastasis and the clinical stage of tumors (234). Higher Ki67 in tumors of patients was correlated with higher Gleason score, progression to advanced tumor stage with increased risk of prostate cancer-associated death compared to other patients (235). Thus, suggesting Ki67 may serve as an important prognostic marker for prostate cancer. In this study, we have monitored expression of Ki67 in cancer tissue sections of Saline, DTX and DTX-LfNPs treated groups using IHC, the results in **(Fig 5.10 A)** show that Ki-67 highly expressed in saline treated suggesting the metastatic cancer, when treated with the DTX LfNPs a very low expression of Ki-67 compared to that DTX suggesting higher efficacy of DTX LfNPs.

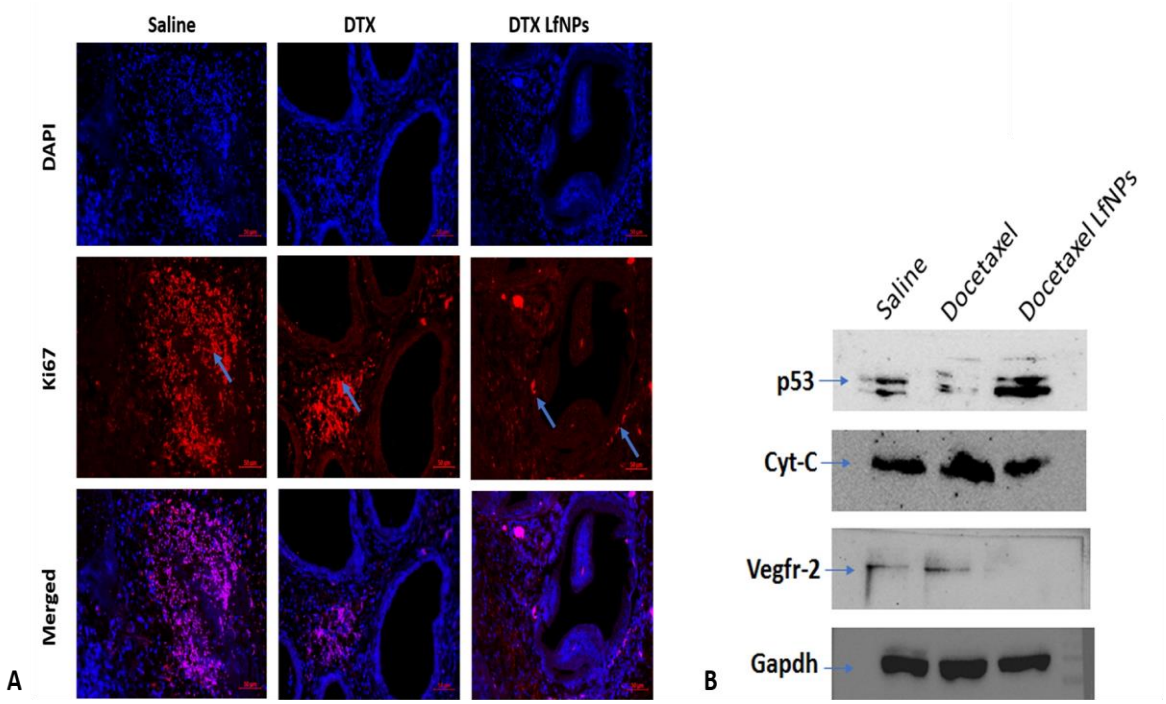

Fig. 5.10 Analysis of tumor tissue: **A. IHC analysis of Ki-67**. The fluorescent intensity of Ki 67 in prostate cancer tissue was treated with saline, DTX, and DTX-LfNPs. In the saline-treated group highest fluorescent intensity of Ki 67 was observed flowed by DTX treated group. DTX-LfNPs treated group showed the least fluorescent of Ki67 among the other two. **B. Analysis of protein expression**. The expression of p53, Cyt C and Vegfr-2 were analysed using western blot as explained in the methods. GAPDH was included as loading control.

The levels of p53, Cyt C and Vegfr-2 were analysed in prostate cancer tissue of control and treatment groups, the results show significant increase of p53 and decrease of Vegfr-2 in DTX-LfNPs compared to DTX groups confirming that DTX LfNPs provide enhanced anti-cancer environment **(Fig 5.10 B)**. In case of Cyt C, it was observed that Cyt C was increased in both DTX and DTX LfNPs compared to control.

5.2.11. Analysis of metastasis

Elevated levels of glycolytic enzyme Lactate dehydrogenase (LDH) is reported to be associated with metabolism of tumor, proliferation, invasion and metastasis (236). A pooled

study included with 54 studies showed that higher LDH levels are frequently associated with poor overall survival (OS) in metastatic prostate cancer patients (237). Based on these studies, LDH was estimated in control and treatment groups, the results in **(Fig 5.11 A)** show that the LDH levels significantly increased in the control group, which upon treatment with DTX show significant decrease, which further decreased when treated with DTX-LfNPs, thus suggesting LfNPs enhances the anti-cancer potency of DTX.

During metastasis of prostate cancer, the osteoblast activity and formation of osteoid in bone tissues could be correlated with alkaline phosphatase (ALP) in serum indicating probable biomarker for bone metastasis (238). A pooled study inferred that the presence of high ALP may significantly associate with poor overall survival (OS), progression-free survival (PFS) of prostate cancer patients (239). Hence, we estimated serum ALP in all the 3 groups, results **(Fig. 5.11 B)** show that ALP is high in untreated rats was significantly decreased in DTX treated rats, which further decreased DTX-LfNPs treated rats (Fig 6B), suggesting LfNPs reduces metastatic activity due to prostate cancer.

Further, we assessed the levels of TNFα, IFNɣ in three treatment groups, and the results in **(Fig. 5.11C and 5.11 D)** show that DTX-LfNPs show a reduction inflammatory response induced due to the metastasis, which could be due to the action of soluble lactoferrin released from the DTX LfNPs after drug release. This is further supported by the significant decrease in lactate dehydrogenase and alkaline phosphatase in LfNPs treated rats indicating the action of lactoferrin in reversal of cancer metastasis, which is well documented in terms of lactoferrin action against plasmalemmal V-ATPase (221) and STAT3 (222).

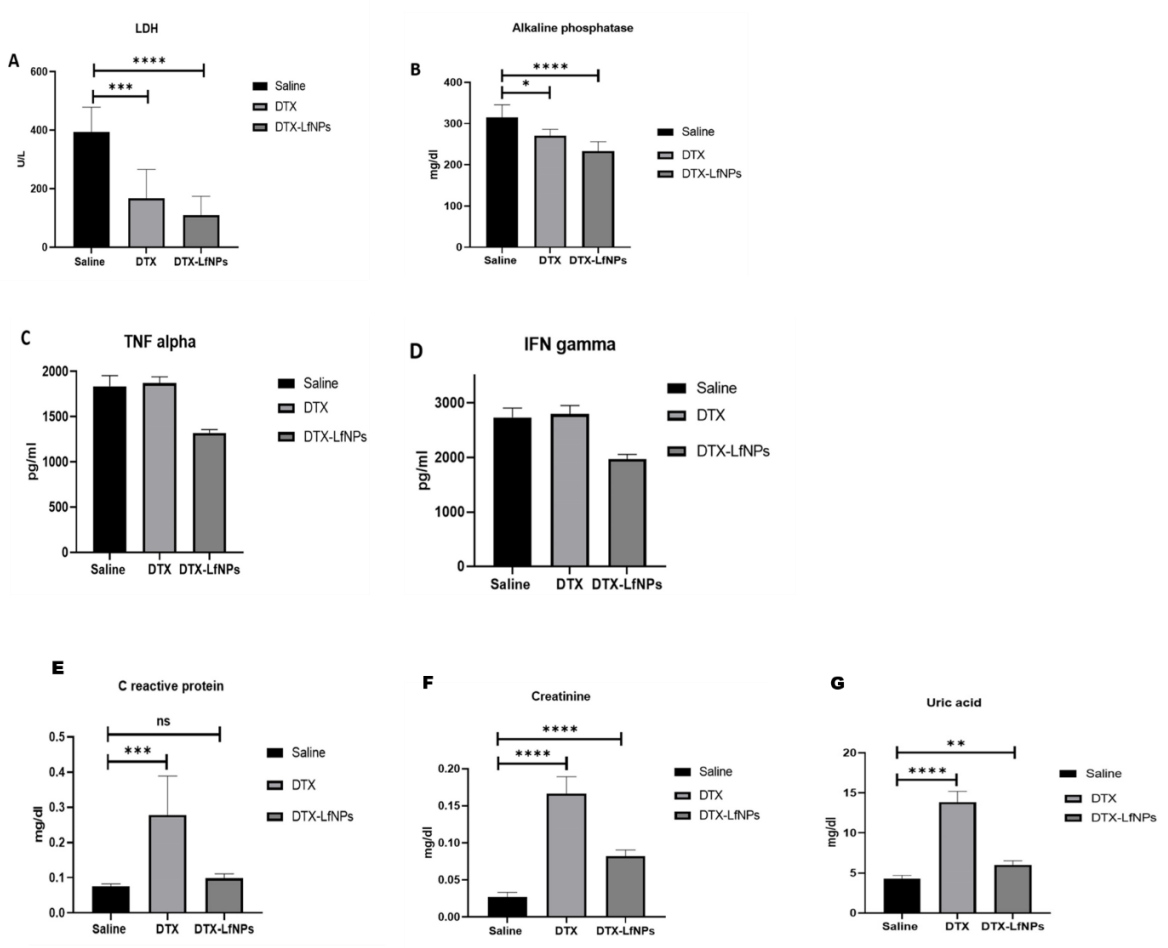

Fig. 5.11 Analysis of metastasis. Serum LDH, ALP, TNFα and IFNɣ, CRP, Creatinine, Uric acid in serum of prostate cancer rats of different treatment groups. A. LDH, B. ALP C. TNFα D. IFNɣ, E. CRP, F. Creatinine, G: Uric acid, Protective activity of DTX-LfNPs from drug induced toxicity. Estimation of C-reactive protein in serum of treatment groups. Sample data were recorded as Mean ±SD, n=6. P-values were calculated by using two tailed unpaired student's *t*-test; * indicates P < 0.05, ** indicates P < 0.01, ***P< 0.001, ****P <0.0001.

The results presented in **(Fig 5.8)** showed a 2-fold increase in drug localization in prostate cancer tissue when DTX-LfNPs **(Fig. 5.8 , grey bar)** compared to DTX. Thus, LfNPs enhance DTX levels in prostate cancer tissue, to see whether such an enhancement of DTX has role in enhancing DTX-mediated toxicity, the treated tissue was analysed for the presence of C-reactive protein (CRP), one of the marker frequently monitored cancer treatment, the

results in **(Fig 5.11 E)** show that the saline treated rats show low level of CRP, when treated with DTX, the CRP level enhanced significantly, which was significantly reduced when treated with DTX-LfNPs suggesting that LfNPs are reducing non-target effects of DTX, which could be confirmed from the histochemical analysis of lymph node, spleen and lungs **(Fig. 5.12)**, the results show neoplastic lymphatic cells are invaded the entire lymph node (indicted with arrow), upon DTX treatment it exhibits a moderate hypertrophy of lymphatic follicles were in cortex region of lymph node (indicated with arrow), when treated with DTX LfNPs, lymph node show normal morphology of lymphatic follicles in the cortex region of lymph node (indicated with arrow), thus suggesting LfNPs reduces DTX-mediated non-target toxicity along with enhanced efficacy. In the spleen tissue, the cancer bearing rats shows lymphatic follicles (indicated by arrow), DTX-treated rats showed increased toxicity compared to DTX-LfNPs **(Fig. 5.12)** suggesting LfNPs reduce DTX mediated toxicity. While in the liver tissue, the hepatocytes showed normal **(Fig. 5.12)** in both treatment groups compared to untreated group. This is also evident is from measurement of creatinine and uric acid **(Fig. 5.11 F and G)**, the results show that the DTX-induced enhancement in creatinine and uric acids could be prevented when administering DTX-LfNPs, these results arer confirmed by histochemical analysis of kidney, wherein the cancer bearing rat showed normal glomerulus and tubules for both treatment groups compared to saline treated rats **(Fig. 5.12)**. Thus, LfNPs mediated delivery of DTX overcome limitations of the DTX and help in reduced toxicity to non-target tissue, while enhancing regression of prostate cancer.

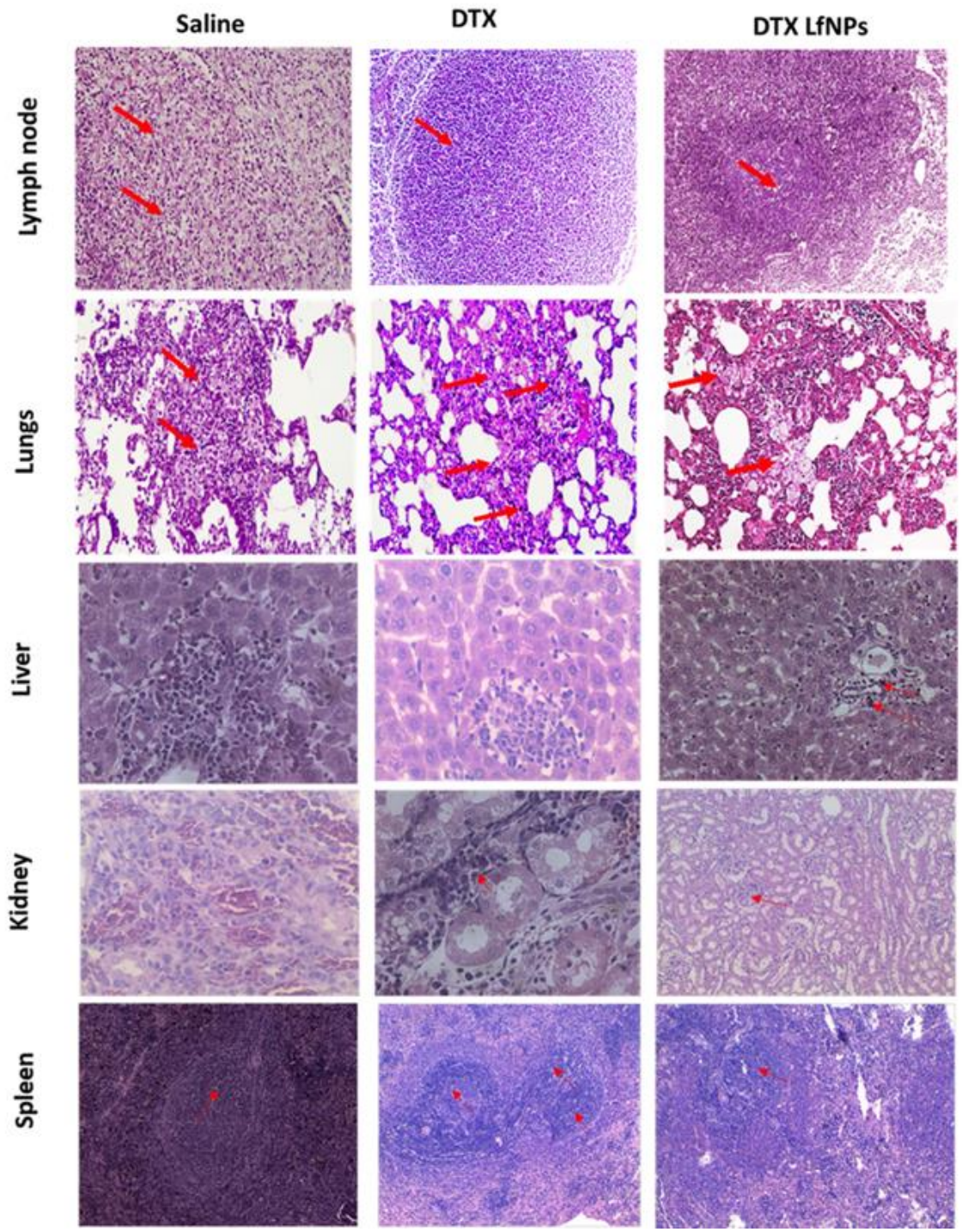

Fig. 5.12 H & E analysis of Lymph node, Lungs, Liver, kidney and spleen. Histological analysis of lymph node, lungs, liver, kidney and spleen sections under two treatment conditions (DTX and DTX-LfNPs) is carried out at 20X and 10X (spleen) magnification, saline treatment is control.

To improve the therapeutic efficacy, anticancer drugs ought to be delivered to the target site of the tumor at optimal concentrations (102). Target tissue location can be achieved by the use of carrier molecules, while encapsulation in nanoparticles will overcome the limitations due to solubility and stability of drugs to some extent (240, 241). The preparation of DTX loaded Lactoferrin nanoparticles were carried out using the sol oil method and the drug was loaded without involving any chemical conjugation. DTX-Lf NPs showed significant localization in prostate cancer cells through receptor-mediated endocytosis. Further, the DTX-Lf NPs showed an improvement of IC_{50} against the proliferation of Mat Ly Lu compared to DTX.

Tumor regression activity of LfNPs was analysed in orthotopic prostate cancer models in rats. When compared to subcutaneous models, orthotopic tumor models are considered to be closely simulate prostate cancer in humans in terms of the development of tumor microenvironment and also to be more relevant to obtain an accurate response to therapies (242).In this study Mat, Ly Lu cells were used to develop prostate cancer in Wistar rats. Since Mat Ly Lu is androgen-independent prostate cancer, this model could be used in simulating treatment of androgen-independent prostate cancer (231). The results of the analysis *in vivo* showed that DTX-LfNPs, when administered intravenously, significantly reduced the size of the prostate tumor in comparison to saline and soluble DTX treated. The tumor regression studies were confirmed by comparing the tumor weight and tumor volume of treatment groups. The results of histological analysis showed higher pathological changes in tumors of DTX NPs-treated groups suggesting that the DTX-LfNPs could deliver higher concentrations of DTX into tumors. The higher efficacy of DTX, when given through Lf NPs could be due to the enhanced cellular localization mediated by lactoferrin through over-expressed lactoferrin receptors in the prostate tissue (118). Further, the lactoferrin release into cells from DTX-LfNPs may provide anti-inflammatory environment along with its known

function in reversal of metastatic status of the cancer (221, 222), which is evident from the reduction of TNFα, IFNɣ, LDH and ALP in DTX LfNPs treated group compared DTX group. Further, DTX LfNPs treatment group shows significant reduction in DTX-induced non-target effects as seen in DTX-treatment group. This could be due to non-availability of free DTX in DTX LfNPs for localization in non-target organs and associated non-specific toxicity, hence the toxicity observed in DTX treatment group may not be exhibited in DTX LfNPs treatment group. In summary, DTX LfNPs are promising in terms of target localization of both DTX and lactoferrin to confer a synergistic activity for regression and cancer metastasis.

5.3. Conclusions

Characterization using TEM and ATR confirms the formation of DTX-LfNPs keeping structure of protein and drug intact. Lactoferrin receptor is significantly expressed in Mat Ly Lu cells and cancer tissue developed using these cells, further DTX-LfNPs localize the drugs into cancer tissue through lactoferrin receptor mediated pathway in these cells. An assessment of anti-proliferative activity showed that DTX-LfNPs performs 2.5-times better than DTX in inhibiting proliferation of cells. Furthermore, the bioavailability studies showed a 2 -fold increase in drug localization in prostate tissue when DTX-LfNPs were given in comparison to DTX. The tumor regression in *vivo* showed higher efficacy of DTX when delivered through lactoferrin nanoparticles. In summary, DTX when delivered via lactoferrin nanoparticles exhibits improved efficacy and safety against prostate cancer due to higher drug localization along with lactoferrin in the prostate cancer tissue.

Chapter 6

Potentiation of activity of docetaxel with p53 DNA loaded in lactoferrin nanoparticles in treatment of prostate cancer

6. Chapter 6: Potentiation of activity of docetaxel with p53 DNA loaded in lactoferrin nanoparticles in treatment of prostate cancer

6.1. Introduction

Gene therapy is recognised as one of the potent therapies for the effective treatment of various genetic disorders by rectifying altered gene by gene editing or replacing genes through administrating corrected gene copies. Gene therapy is categorised into two classes, (a) Germ line genetic manipulation, (b) Somatic gene manipulation (243). The classification is based upon the lineage of target cells for gene therapy. In germ line therapy, eggs and sperms are manipulated by administering gene with high frequency of inheritance to next generations (244), while somatic gene therapy aims manipulation of cell types of different lineage except germ cells, the gene modification may not be inherited to next generations (244). Various physical methods are employed for gene transfer includes biolistic, hydrodynamic injections, ultrasound mediated, electric pulse mediated gene transfer, non-viral gene carriers etc. (245). Though these methods maintain gene integrity, they have certain limitations: biolistic or gene gun uses metal coated particles, has poor penetration capacity which leads to low efficiency and also causes cellular toxicity due to metal accumulation (245). Hydrodynamic injections require very high volume in order to generate pressure to cross the membrane, as a consequence blocks inferior vena cava and causes heart blockage (246). This method is beneficial only for the organs connected to inferior vena cava (mainly Liver) (247). Ultrasound mediated delivery causes cytoskeleton breakdown and DNA trafficking (248), while high frequency electric pulse mediated gene transfer produces holes in the membrane affecting cell viability due to membrane destabilization (249).

The p53 protein is a cell cycle checkpoint and a transcription factor induced upon DNA damage, later activates many genes associated in damage repair, while arresting the cell cycle

(250–253). Profound studies illustrates loss of functional mutation of p53 in 50 % of human cancers (253–260) , extensive mutation in p53 sometimes leads to drug resistance to tumor (261). In our earlier studies, we showed that p53 DNA loaded lactoferrin nanoparticles can potentiate regression of glioma by temozolomide (181). This study aims to deliver of p53 DNA in prostate cancer through lactoferrin nanoparticle mediated delivery, wherein lactoferrin promote localization of DNA in prostate cancer tissue along with its action on the cancer metastasis, while p53 DNA sensitises prostate cancer cells to docetaxel.

6.2. Results

6.2.1. Stoichiometry of DNA and protein

A gel retardation assay was performed with a fixed concentration of DNA and an increasing concentration of lactoferrin. The above mixture was incubated o/n at 4 degrees, then loaded onto 1% agarose gel, and the gel was stained with EtBr and visualized under chemidoc (Bio-Rad) **(Fig. 6.1 A)**. The results in **(Fig 6.1 A)** showed that DNA to protein stoichiometric ratio at 1:500 ratio. This ration was used in nanoparticle preparation.

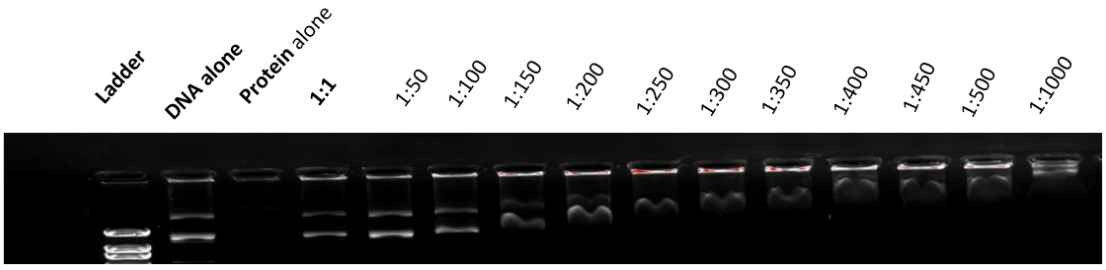

Fig.6.1 Stoichiometry of lactoferrin and DNA binding: The image represents GFP-p53 plasmid and lactoferrin interaction, Gel retardation assay was performed with increasing concentration of Lactoferrin (0.296, 14.8, 29.6, 44.4, 59.2, 74, 88.8, 103.6, 118.4, 133.2, 148, 296 pM) along with fixed concentration of GFP-p53(0.296 pM). Lane 1: Ladder, Lane 2 – Lactoferrin Control (296pM), Lane 3- GFP-p53 (0.296pM), Lane 4- 11 DNA/ Protein mixture.

Image suggests full retardation of DNA by protein, at 1:500 (DNA: Protein) hence 1:500 molar ratio of DNA: protein can be used for preparation of nanoparticles.

6.2.2. Characterization of GFP-p53 loaded Lactoferrin nanoparticles

GFP-p53 loaded Lactoferrin nanoparticles (GFP-p53 LFNPs) were prepared using sol-oil method aforementioned in methods 2.2, prepared particles were then analysed as described in methods using TEM. TEM Images in **(Fig 6.2)** reveals spherical shape particles both blank LFNP and GFP-p53 LFNPs, size range for blank LFNP is 10 ±2 nm **(Fig 6.2A)**, while for GFP-p53 LFNPs is 48 ± 10nm **(Fig 6.2B)**.

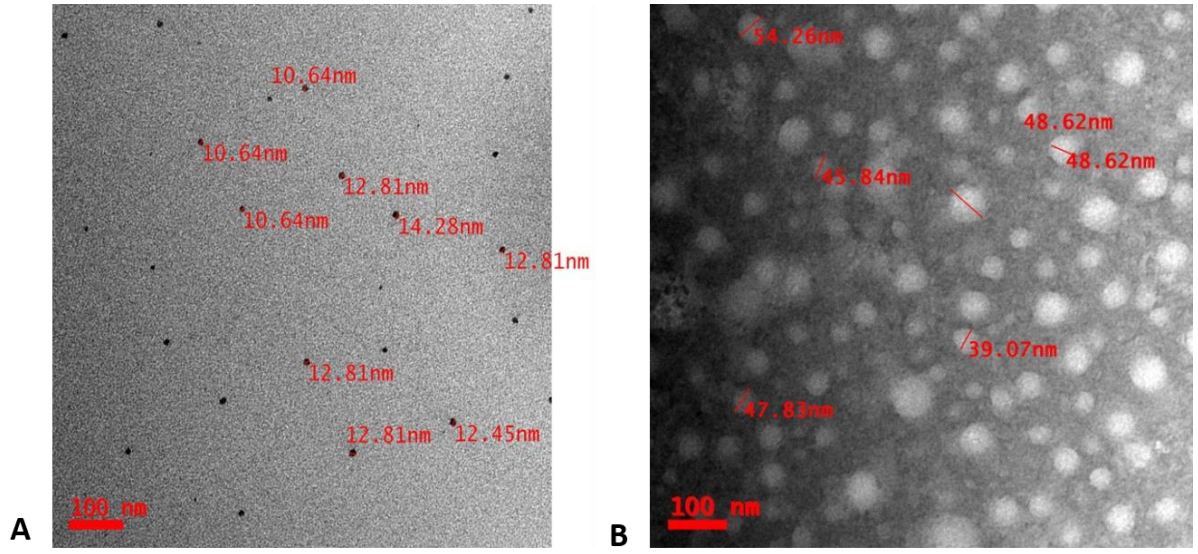

Fig 6.2 A & B: Size estimation of nanoparticles using Transmission electron microscopy. Fig. 6.2A shows size of 10- 13 nm of Blank Lactoferrin nanoparticles while Fig 6.2B shows 39-54 nm size range of GFP-p53 loaded lactoferrin nanoparticles.

6.2.3. Estimation of Loading Efficiency of DNA Loaded Lactoferrin nanoparticles

To estimate the loading efficiency i.e. the amount of DNA loaded into the nanoparticle, GFP-p53 plasmid was crosslinked with acridine orange by exposing with 1% formaldehyde for 1 hr at room temperature. Unbound dye was removed by precipitating the DNA with isopropanol and 100mM ammonium acetate. The recovered dye crosslinked DNA is then

used for the preparation of nanoparticles and later released by treating with proteinase K at 60^{o}C for 10 hrs. The DNA loading efficiency determined to be 42%.

6.2.4.Localization of GFP-p53 *in vitro* in prostate cancer cells

Mat- Ly-Lu cell lines were maintained at 5% CO_2 at 37^{o}C degrees in CO_2 incubator (Eppendrof) in 6 well plates on coverslips (Borosil). At 50-60% confluency, cells were incubated with lipofectamine with GFP-p53 plasmid and GFP-p53 LFNP separately. After 24 hrs and 48 hrs cells were coverslips with the cells were mounted and GFP protein expression was monitored under fluorescence microscope. It was observed that GFP protein expression appeared within 24 hrs of transfection and signal persists until 48 hrs **(Fig. 6.4).**In case of lipofectamine a very low transfection was observed. Thus suggesting lactoferrin exhibited higher efficiency in DNA localization compared to lipofectamine in Mat-Ly-Lu cells. Further, higher expression was seen at 24 hours compared to 48 hours.

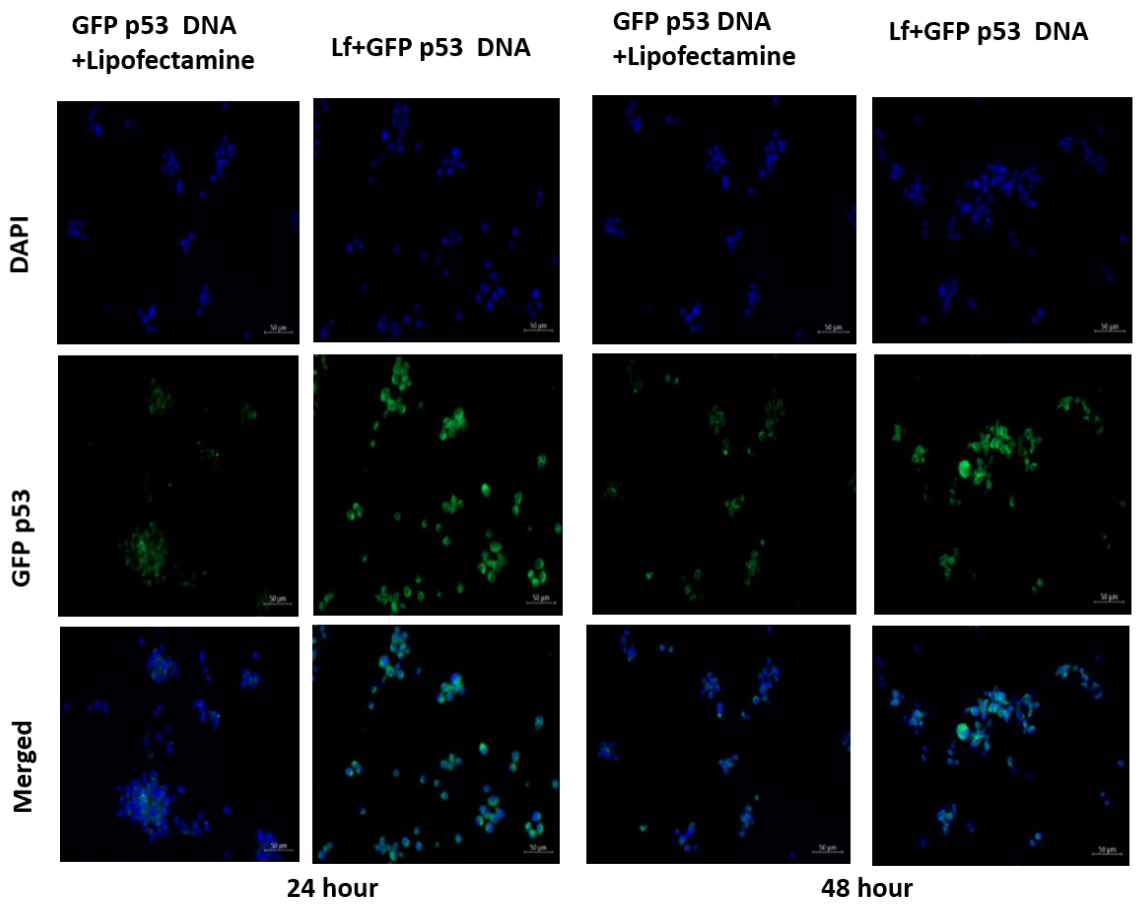

Fig.6.4 Fluorescence image shows GFP-Expression in cells after transfection with lipofectamine Left panel and LfNPs Right panel. While upper, middle and lower panel shows DAPI, GFP and merged image of the cells respectively. Image suggests the expression GFP is more in the cells transfected with Lactoferrin nanoparticles as compared to lipofectamine in both right and left panel and also GFP expression has seen in 24 hrs of transfection and persists in 48 th hr also.

6.2.5. Localization of GFP-p53 in Rats using Lactoferrin nanoparticles

Localization of GFP-p53 in different organs in rats were analysed by administering GFP-p53 loaded lactoferrin nanoparticles through tail vein, the rats were then sacrificed at 48th hr and organs (lymph node, bladder, brain, prostate, spleen, thymus and heart) were collected and DNA was isolated. 20ng of isolated DNA from each organ is used as a template for PCR

amplification of GFP, the results shows that significant localization of GFP-p53 DNA in Bladder, Brain, Prostate, Spleen, while negligible localization found in Lymph node and Thymus while little localization in Heart **(Fig.6.5).**

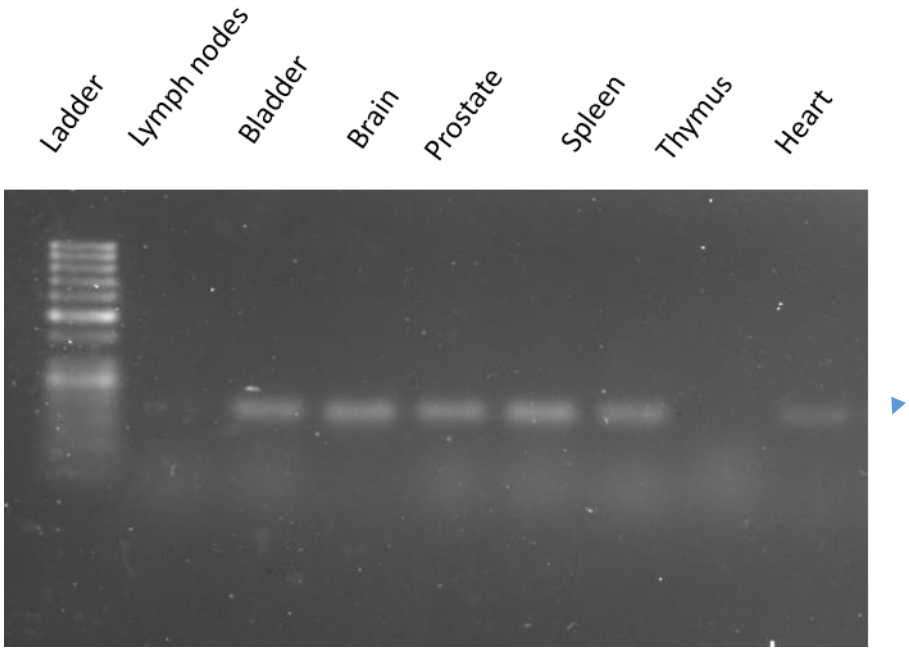

Fig.6.5- Agarose gel image shows the PCR products of GFP, LANE 1: Ladder, PCR product amplified was shown in LANE 2 lymph node, LANE 3 Bladder, LANE 4 Brain, LANE 5 Prostate, LANE 6 spleen, LANE 7 Thymus, and LANE 8 Heart. Image suggests localization of GFP-p53 in Bladder, Brain, Prostate, Spleen and there is no localization found in Lymph node and Thymus while little localization in Heart.

6.2.6. Treatment of Prostate cancer rat model with p53

For development of prostate cancer model 18 Male Wistar rats of age 3 months divided into 3 different groups (n=6). First group was control group given saline, second group was treated with GFP-p53 loaded LfNPs, while third group was administered with GFP-p53 loaded LfNPs followed by treatment with chemotherapeutic drug, docetaxel. Results of these studies given **(Fig 6.6)** show that the tumor weight and volume was significantly reduced in group 3

i.e. treatment with GFP-p53 loaded LfNPs followed by docetaxel. Further, the reduction of tumor weight and tumor volume is higher in group 3 (GFP-p53 loaded LfNPs followed by docetaxel) compared to group 2, which was treated with GFP-p53 loaded LfNPs. Further, histopathological analysis shows that 60 to 70 per cent of neoplastic cells of mucosal epithelial cells are replaced with fibrous tissue and inflammatory cells in GFP-p53 loaded LfNPs rats (Group 2), while Necrosis and lysis of neoplastic cells in mucosal glands was observed in treatment with GFP-p53 loaded LfNPs followed by Docetaxel treated rats (Group 3).

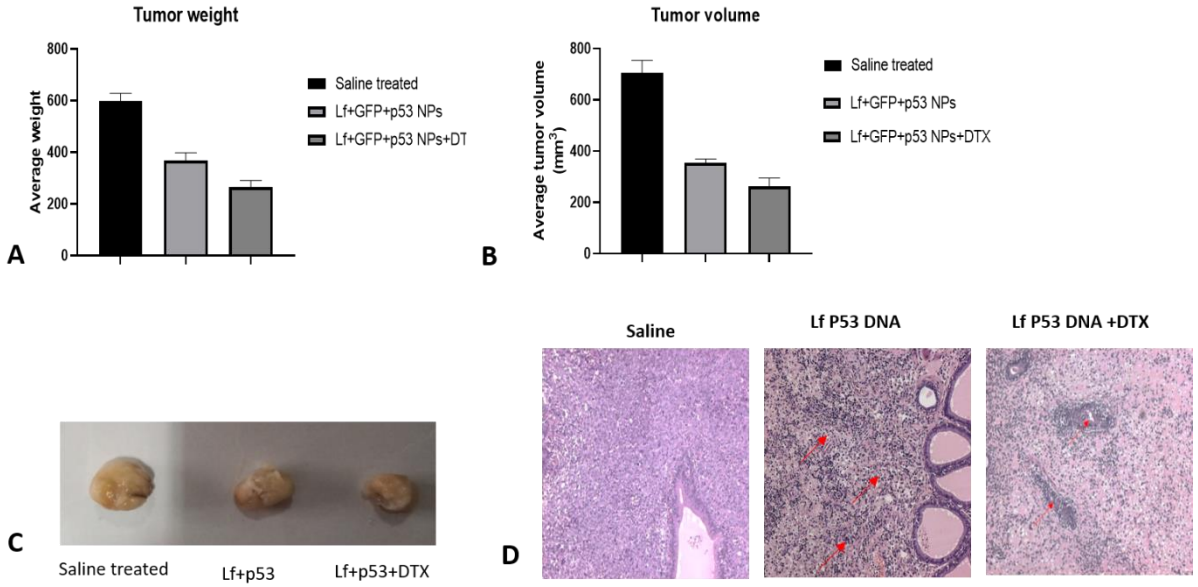

Fig .6.6 A & B: Graph suggest reduction in tumor weight and volume in rats significantly in GFP-p53 LFNP followed by DTX treated rats as compare to GFP-p53 LFNP and there is no reduction observed in saline treated rats.

Fig. 6.6 C.: Image of the prostate tumor of rats after the following treatment: Saline treated, GFP-p53 LfNP, GFP-p53 LfNP followed by DTX treated. Image shows significant reduction in tumor with the rats treated with GFP-p53 LFNP Followed by DTX.

Fig. 6.6 D. Left panel shows 80-90% neoplastic cells while middle panel shows 60 to 70 per cent of neoplastic cells of mucosal epithelial cells are replaced with fibrous tissue and inflammatory cells and the right most panel shows necrosis and lysis of neoplastic cells in mucosal glands

6.3. Discussion

With the advent of non-viral vector-based gene therapy gaining attention in gene and therapies due to the absence of virus-related pathogenesis and other complications (262). The cardinal aspect of the study is to deliver therapeutic DNA stably and efficiently to the prostate cancer. Lactoferrin is a thermodynamically and kinetically stable iron transporter protein might serve as potent vehicle for gene therapy (224, 263). Current study enlightens about the higher levels of lactoferrin receptor expression in cancer cells leads us to design the hypothesis involving lactoferrin protein. p53 protein plays important role as a cell cycle check point (264), mutation in p53 gene would lead to the generation of truncated protein (265). Designating p53 gene as a therapeutic DNA and deliver it to the target cells with the help of lactoferrin nanoparticles is prominence of the current studies, as expressed p53 sensitize cancer cells to chemotherapeutic drug, docetaxel. In this study pGFP-p53 DNA lactoferrin nanoparticles were prepared at molar ratios of 1:500 of DNA to lactoferrin with nanoparticle size of GFP-p53 LfNPs in the range of 39-54 nm. The bioassay for transfection efficacy was conducted, the results showed that pGFP-p53 LfNPs exhibits higher transfection efficiency compared to lipofectamine mediated plasmid delivery. Further, GFP-p53 LfNPs showed protein expression from 24 hours. In vivo localization of GFP-p53 plasmid through LfNPs indicates localization in brain, bladder, spleen and prostate. Treatment strategy was designed for suppression of prostate tumor, the results suggests significant reduction in tumor weight and volume in GFP-p53 LfNPs treatment followed by chemotherapy by docetaxel.

7. Conclusions

- Five different types NP (nDox, nCp, nDoxCp, nDox MES, DTX-LfNPs and p53 LfNPS) have been prepared using sol-oil chemistry.
- The NPs prepared have been characterized using FE-SEM and TEM and the dimension of nanoparticles was in the range of 70-90 nm
- The process showed significant drug loading in terms of the percent encapsulation efficiency (EE %) for each type of NP are as follows, nDox = 50.43±1.06 %, nCp = 57.3 ±4.65 %, nDoxCp (dox- 52.88 ±2.88%, Cp- 62.03±3%), and DTX-LfNPs =62.06 %.
- The ATR data shows that the drug is only physically entrapped inside the nanoparticle without any chemical modifications
- Healthy CD-1 mice were tolerated to 2-fold higher dosage of doxorubicin and cyclophosphamide and its combination when delivered through lactoferrin nanoparticles compared to soluble along with the safety advantage of lactoferrin Nano formulation.
- Drug release in prostate cancer cells could be regulated based on the concentration of MES and time period of incubation of MES with drug and lactoferrin prior to nanoparticle preparation.
- *In vitro* studies shows DTX-LfNPs exhibit an improved anti-proliferative activity by 2.5 times compared to DTX.
- Efficacy studies in prostate cancer model in Wistar rats showed that the docetaxel loaded lactoferrin nanoparticles efficacious compared to soluble docetaxel in terms of tumor weight, tumor volume, immunohistochemistry of prostate for proliferation marker Ki67 and gross histopathology. Further, lactoferrin nanoparticles reduced toxicity to liver, kidney and spleen compared to soluble drug.
- DNA to protein interaction studies showed 1:500 ratio of DNA to protein will be optimum for nanoparticle preparation.

- The *in vitro* cellular localization in prostate cancer cell line showed that the GFP expression was higher when the cells are transfected with Lactoferrin nanoparticles as compared to lipofectamine and also GFP expression is observed within 24 hr of transfection with stable expression until 48th hr.
- Efficacy studies in prostate cancer model in Wistar rats revealed that a higher reduction in tumor burden when combination group GFP-p53 loaded lactoferrin nanoparticles followed by Docetaxel compared to GFP-p53 loaded lactoferrin nanoparticles treated rats, thus suggesting that p53 loaded drug sensitizes prostate cancer cells to docetaxel.

Reference-

1. Sarkar, S., Horn, G., Moulton, K., Oza, A., Byler, S., Kokolus, S., and Longacre, M. (2013) Cancer development, progression, and therapy: an epigenetic overview. *Int. J. Mol. Sci.* **14**, 21087–21113

2. Patel, A. (2020) Benign vs Malignant Tumors. *JAMA Oncol.* **6**, 1488–1488

3. Types of cancer | Cancer Research UK [online] https://www.cancerresearchuk.org/what-is-cancer/how-cancer-starts/types-of-cancer (Accessed December 14, 2022)

4. The Development and Causes of Cancer - The Cell - NCBI Bookshelf [online] https://www.ncbi.nlm.nih.gov/books/NBK9963/ (Accessed October 11, 2022)

5. Idikio, H. A. (2011) Human Cancer Classification: A Systems Biology- Based Model Integrating Morphology, Cancer Stem Cells, Proteomics, and Genomics. *J. Cancer*. **2**, 107–115

6. Upadhyay, A. (2021) ScienceDirect Cancer : An unknown territory ; rethinking before going ahead. *Genes Dis.* **8**, 655–661

7. Debela, D. T., Muzazu, S. G. Y., Heraro, K. D., Ndalama, M. T., Mesele, B. W., Haile, D. C., Kitui, S. K., and Manyazewal, T. (2021) New approaches and procedures for cancer treatment : Current perspectives. 10.1177/20503121211034366

8. Senapati, S., Mahanta, A. K., Kumar, S., and Maiti, P. (2018) Controlled drug delivery vehicles for cancer treatment and their performance. *Signal Transduct. Target. Ther.* 10.1038/S41392-017-0004-3

9. Baghban, R., Roshangar, L., Jahanban-Esfahlan, R., Seidi, K., Ebrahimi-Kalan, A., Jaymand, M., Kolahian, S., Javaheri, T., and Zare, P. (2020) Tumor microenvironment

complexity and therapeutic implications at a glance. *Cell Commun. Signal.* **18**, 1–19

10. Arneth, B. (2020) Tumor Microenvironment. 10.3390/medicina56010015

11. Albini, A., Bruno, A., Gallo, C., Pajardi, G., Noonan, D. M., and Dallaglio, K. (2015) Cancer stem cells and the tumor microenvironment: Interplay in tumor heterogeneity. *Connect. Tissue Res.* **56**, 414–425

12. Wei, L., Zhang, X., Wang, J., Ye, Q., Zheng, X., Peng, Q., Zheng, Y., Liu, P., Zhang, X., Li, Z., Liu, C., Yan, Q., Li, G., and Ma, J. (2020) Lactoferrin deficiency induces a pro-metastatic tumor microenvironment through recruiting myeloid-derived suppressor cells in mice. *Oncogene*. **39**, 122–135

13. Kondapi, A. K. (2020) Targeting cancer with lactoferrin nanoparticles: recent advances. *https://doi.org/10.2217/nnm-2020-0090*. **15**, 2071–2083

14. Welch, D. R., and Hurst, D. R. (2019) Defining the Hallmarks of Metastasis. *Cancer Res.* **79**, 3011

15. Guan, X. (2015) Cancer metastases: Challenges and opportunities. *Acta Pharm. Sin. B.* **5**, 402–418

16. Seyfried, T. N., and Huysentruyt, L. C. (2013) On the Origin of Cancer Metastasis. **18**, 43–73

17. Fares, J., Fares, M. Y., Khachfe, H. H., Salhab, H. A., and Fares, Y. (2020) Molecular principles of metastasis: a hallmark of cancer revisited. *Signal Transduct. Target. Ther.* 10.1038/s41392-020-0134-x

18. Hapach, L. A., Mosier, J. A., Wang, W., and Reinhart-King, C. A. (2019) Engineered models to parse apart the metastatic cascade. *npj Precis. Oncol.* 10.1038/s41698-019-0092-3

19. Cancer Invasion and Metastasis: Molecular and Cellular Perspective - Madame Curie Bioscience Database - NCBI Bookshelf [online] https://www.ncbi.nlm.nih.gov/books/NBK164700/ (Accessed December 15, 2022)

20. Nishida, N., Yano, H., Nishida, T., Kamura, T., and Kojiro, M. (2006) Angiogenesis in cancer. *Vasc. Health Risk Manag.* **2**, 213–219

21. Bielenberg, D. R., and Zetter, B. R. (2015) The Contribution of Angiogenesis to the Process of Metastasis. *Cancer J.* **21**, 267

22. Chiang, S. P. H., Cabrera, R. M., and Segall, J. E. (2020) Tumor cell intravasation. 10.1152/ajpcell.00238.2015

23. Chiang, S. P. H., Cabrera, R. M., and Segall, J. E. (2016) Tumor cell intravasation. 10.1152/ajpcell.00238.2015

24. Sznurkowska, M. K., and Aceto, N. (2022) The gate to metastasis : key players in cancer cell intravasation. **289**, 4336–4354

25. Tsuji, T., Ibaragi, S., and Hu, G. (2009) Epithelial-Mesenchymal Transition and Cell Cooperativity in Metastasis. 10.1158/0008-5472.CAN-09-1618

26. Azevedo, A. S., Follain, G., Patthabhiraman, S., Harlepp, S., and Goetz, J. G. (2015) Metastasis of circulating tumor cells: Favorable soil or suitable biomechanics, or both? *Cell Adhes. Migr.* **9**, 345–356

27. Radiation Therapy for Cancer - NCI [online] https://www.cancer.gov/about-cancer/treatment/types/radiation-therapy (Accessed December 16, 2022)

28. Baskar, R., Dai, J., Wenlong, N., Yeo, R., and Yeoh, K. W. (2014) Biological response of cancer cells to radiation treatment. *Front. Mol. Biosci.* 10.3389/FMOLB.2014.00024

29. Baskar, R., Lee, K. A., Yeo, R., and Yeoh, K. W. (2012) Cancer and Radiation Therapy: Current Advances and Future Directions. *Int. J. Med. Sci.* **9**, 193

30. How Radiation Therapy Is Used to Treat Cancer [online] https://www.cancer.org/treatment/treatments-and-side-effects/treatment-types/radiation/basics.html (Accessed October 11, 2022)

31. Jaffray, D. A., and Gospodarowicz, M. K. (2015) Radiation Therapy for Cancer. *Taehan Uihak Hyophoe Chi.* **6**, 142–146

32. Scheller, E. L., and Krebsbach, P. H. (2009) Gene Therapy: Design and Prospects for Craniofacial Regeneration. *J. Dent. Res.* **88**, 585

33. Das, S. K., Menezes, M. E., Bhatia, S., Wang, X. Y., Emdad, L., Sarkar, D., and Fisher, P. B. (2015) Gene Therapies for Cancer: Strategies, Challenges and Successes. *J. Cell. Physiol.* **230**, 259–271

34. Kher, G., Trehan, S., and Misra, A. (2011) *Antisense Oligonucleotides and RNA Interference*, 10.1016/B978-0-12-384964-9.00007-4

35. Watts, J. K., and Corey, D. R. (2012) Silencing disease genes in the laboratory and the clinic. *J. Pathol.* **226**, 365–379

36. Kher, G., Trehan, S., and Misra, A. (2011) Antisense Oligonucleotides and RNA Interference. *Challenges Deliv. Ther. Genomics Proteomics*. 10.1016/B978-0-12-384964-9.00007-4

37. Nayerossadat, N., Maedeh, T., and Ali, P. A. (2012) Viral and nonviral delivery systems for gene delivery. *Adv. Biomed. Res.* **1**, 27

38. Ghosh, S., Brown, A. M., Jenkins, C., and Campbell, K. (2020) Viral Vector Systems for Gene Therapy: A Comprehensive Literature Review of Progress and Biosafety

Challenges. *Appl. Biosaf.* **25**, 7–18

39. Ramamoorth, M., and Narvekar, A. (2015) Non viral vectors in gene therapy - An overview. *J. Clin. Diagnostic Res.* **9**, GE01–GE06

40. Al-Dosari, M. S., and Gao, X. (2009) Nonviral gene delivery: Principle, limitations, and recent Progress. *AAPS J.* **11**, 671–681

41. Rodriguez, A., del, A., and Angeles, M. (2013) Non-Viral Delivery Systems in Gene Therapy. *Gene Ther. - Tools Potential Appl.* 10.5772/52704

42. Yin, H., Kanasty, R. L., Eltoukhy, A. A., Vegas, A. J., Dorkin, J. R., and Anderson, D. G. (2014) Non-viral vectors for gene-based therapy. *Nat. Rev. Genet.* **15**, 541–555

43. Cancer Chemotherapy - StatPearls - NCBI Bookshelf [online] https://www.ncbi.nlm.nih.gov/books/NBK564367/ (Accessed December 17, 2022)

44. How Does Chemo Work? | Types of Chemotherapy [online] https://www.cancer.org/treatment/treatments-and-side-effects/treatment-types/chemotherapy/how-chemotherapy-drugs-work.html (Accessed October 11, 2022)

45. Cancer Chemotherapy - StatPearls - NCBI Bookshelf [online] https://www.ncbi.nlm.nih.gov/books/NBK564367/ (Accessed October 11, 2022)

46. Nygren, P. (2001) What is cancer chemotherapy? *Acta Oncol. (Madr).* **40**, 166–174

47. Shahidian, A., Ghassemi, M., Mohammadi, J., and Hashemi, M. (2020) Immunotherapy. *Bio-Engineering Approaches to Cancer Diagnosis Treat.* 10.1016/B978-0-12-817809-6.00004-2

48. Alfarouk, K. O., Stock, C. M., Taylor, S., Walsh, M., Muddathir, A. K., Verduzco, D.,

Bashir, A. H. H., Mohammed, O. Y., Elhassan, G. O., Harguindey, S., Reshkin, S. J., Ibrahim, M. E., and Rauch, C. (2015) Resistance to cancer chemotherapy: failure in drug response from ADME to P-gp. *Cancer Cell Int.* 10.1186/S12935-015-0221-1

49. Mansoori, B., Mohammadi, A., Davudian, S., Shirjang, S., and Baradaran, B. (2017) The Different Mechanisms of Cancer Drug Resistance : A Brief Review. *Tabriz Univ. Med. Sci.* **7**, 339–348

50. Narvekar, M., Xue, H. Y., Eoh, J. Y., and Wong, H. L. (2014) Nanocarrier for Poorly Water-Soluble Anticancer Drugs—Barriers of Translation and Solutions. *AAPS PharmSciTech*. **15**, 822

51. Gala, U. H., Miller, D. A., and Williams, R. O. (2020) Harnessing the therapeutic potential of anticancer drugs through amorphous solid dispersions. *Biochim. Biophys. Acta - Rev. Cancer*. **1873**, 188319

52. Lin, A., Giuliano, C. J., Palladino, A., John, K. M., Abramowicz, C., Yuan, M. Lou, Sausville, E. L., Lukow, D. A., Liu, L., Chait, A. R., Galluzzo, Z. C., Tucker, C., and Sheltzer, J. M. (2019) Off-target toxicity is a common mechanism of action of cancer drugs undergoing clinical trials. *Sci. Transl. Med.* 10.1126/SCITRANSLMED.AAW8412

53. Fahmy, S. A., Brüßler, J., Alawak, M., El-Sayed, M. M. H., Bakowsky, U., and Shoeib, T. (2019) Chemotherapy Based on Supramolecular Chemistry: A Promising Strategy in Cancer Therapy. *Pharmaceutics*. 10.3390/PHARMACEUTICS11060292

54. Abdollahpour-Alitappeh, M., Lotfinia, M., Gharibi, T., Mardaneh, J., Farhadihosseinabadi, B., Larki, P., Faghfourian, B., Sepehr, K. S., Abbaszadeh-Goudarzi, K., Abbaszadeh-Goudarzi, G., Johari, B., Zali, M. R., and Bagheri, N. (2019) Antibody–drug conjugates (ADCs) for cancer therapy: Strategies, challenges,

and successes. *J. Cell. Physiol.* **234**, 5628–5642

55. Scott, A. M., Allison, J. P., and Wolchok, J. D. (2012) Monoclonal antibodies in cancer therapy. *Cancer Immun.* [online] /pmc/articles/PMC3380347/ (Accessed December 17, 2022)

56. Thomas, A., Teicher, B. A., and Hassan, R. (2016) Antibody–drug conjugates for cancer therapy. *Lancet. Oncol.* **17**, e254

57. Mahmood, I. (2021) Clinical Pharmacology of Antibody-Drug Conjugates. *Antibodies 2021, Vol. 10, Page 20*. **10**, 20

58. de la Torre, B. G., and Albericio, F. (2021) The Pharmaceutical Industry in 2020. An Analysis of FDA Drug Approvals from the Perspective of Molecules. *Mol. 2021, Vol. 26, Page 627*. **26**, 627

59. Pettinato, M. C. (2021) Introduction to Antibody-Drug Conjugates

60. Drago, J. Z. Unlocking the potential of antibody–drug conjugates for cancer therapy. *Nat. Rev. Clin. Oncol.* **0123456789**, 1–18

61. Padma, V. V. (2015) An overview of targeted cancer therapy. *BioMedicine*. **5**, 1–6

62. Gerber, D. E. (2008) Targeted therapies: A new generation of cancer treatments. *Am. Fam. Physician*. **77**, 311–319

63. J. Boohaker, R., W. Lee, M., Vishnubhotla, P., M. Perez, J. L., and R. Khaled, A. (2012) The Use of Therapeutic Peptides to Target and to Kill Cancer Cells. *Curr. Med. Chem.* **19**, 3794–3804

64. Padma, V. V. (2015) An overview of targeted cancer therapy. *Biomed.* **5**, 1–6

65. Patra, J. K., Das, G., Fraceto, L. F., Campos, E. V. R., Rodriguez-Torres, M. D. P.,

Acosta-Torres, L. S., Diaz-Torres, L. A., Grillo, R., Swamy, M. K., Sharma, S., Habtemariam, S., and Shin, H. S. (2018) Nano based drug delivery systems: recent developments and future prospects. *J. Nanobiotechnology 2018 161*. **16**, 1–33

66. Yao, Y., Zhou, Y., Liu, L., Xu, Y., Chen, Q., Wang, Y., Wu, S., Deng, Y., Zhang, J., and Shao, A. (2020) Nanoparticle-Based Drug Delivery in Cancer Therapy and Its Role in Overcoming Drug Resistance. *Front. Mol. Biosci.* **7**, 1–14

67. Gavas, S., Quazi, S., and Karpiński, T. M. (2021) Nanoparticles for Cancer Therapy: Current Progress and Challenges. *Nanoscale Res. Lett.* **16**, 173

68. Nakamura, Y., Mochida, A., Choyke, P. L., and Kobayashi, H. (2016) Nano-drug delivery: Is the enhanced permeability and retention (EPR) effect sufficient for curing cancer? *Bioconjug. Chem.* **27**, 2225

69. Tohme, S., Simmons, R. L., and Tsung, A. (2017) Surgery for cancer: A trigger for metastases. *Cancer Res.* **77**, 1548–1552

70. Majeed, H., and Gupta, V. (2022) Adverse Effects Of Radiation Therapy. *StatPearls*. [online] https://www.ncbi.nlm.nih.gov/books/NBK563259/ (Accessed December 4, 2022)

71. Lee, C. S., Bishop, E. S., Zhang, R., Yu, X., Farina, E. M., Yan, S., Zhao, C., Zeng, Z., Shu, Y., Wu, X., Lei, J., Li, Y., Zhang, W., Yang, C., Wu, K., Wu, Y., Ho, S., Athiviraham, A., Lee, M. J., Wolf, J. M., Reid, R. R., and He, T. C. (2017) Adenovirus-mediated gene delivery: Potential applications for gene and cell-based therapies in the new era of personalized medicine. *Genes Dis.* **4**, 43

72. Das, S. K., Menezes, M. E., Bhatia, S., Wang, X. Y., Emdad, L., Sarkar, D., and Fisher, P. B. (2015) Gene Therapies for Cancer: Strategies, Challenges and Successes.

J. Cell. Physiol. **230**, 259–271

73. Ghosh, S., Brown, A. M., Jenkins, C., and Campbell, K. (2020) Viral Vector Systems for Gene Therapy : A Comprehensive Literature Review of Progress and Biosafety Challenges. **25**, 7–18

74. Ike, A. C., Onu, C. J., Ononugbo, C. M., Reward, E. E., and Muo, S. O. (2020) Immune Response to Herpes Simplex Virus Infection and Vaccine Development. *Vaccines*. **8**, 1–22

75. He, Q., Liu, H., Huang, C., Wang, R., Luo, M., and Lu, W. (2020) Herpes Simplex Virus 1-Induced Blood-Brain Barrier Damage Involves Apoptosis Associated With GM130-Mediated Golgi Stress. *Front. Mol. Neurosci.* **13**, 2

76. Desfarges, S., and Ciuffi, A. (2010) Retroviral Integration Site Selection. *Viruses*. **2**, 111

77. Narvekar, M., Xue, H. Y., Eoh, J. Y., and Wong, H. L. (2014) Nanocarrier for Poorly Water-Soluble Anticancer Drugs — Barriers of Translation and Solutions. **15**, 822–833

78. Zahreddine, H., and Borden, K. L. B. (2013) Mechanisms and insights into drug resistance in cancer. *Front. Pharmacol.* **4 MAR**, 28

79. Waghray, D., and Zhang, Q. (2018) Inhibit or Evade Multidrug Resistance P-glycoprotein in Cancer Treatment. *J. Med. Chem.* **61**, 5108

80. Xue, X., and Liang, X. J. (2012) Overcoming drug efflux-based multidrug resistance in cancer with nanotechnology. *Chin. J. Cancer*. **31**, 100

81. Bukowski, K., Kciuk, M., and Kontek, R. (2020) Mechanisms of Multidrug Resistance in Cancer Chemotherapy

82. Rani, L., and Piotr, A. (2022) Nanotechnology - aided advancement in the combating of cancer metastasis. *Cancer Metastasis Rev.* **41**, 383–404

83. Mokhtari, R. B., Homayouni, T. S., Baluch, N., Morgatskaya, E., Kumar, S., Das, B., and Yeger, H. (2017) Combination therapy in combating cancer. *Oncotarget*. **8**, 38022

84. Zhao, J., Huang, Y., Liu, D., and Chen, Y. (2015) Two hits are better than one: synergistic anticancer activity of α-helical peptides and doxorubicin/epirubicin. *Oncotarget*. **6**, 1769

85. Jin, C., Li, H., He, Y., He, M., Bai, L., Cao, Y., Song, W., and Dou, K. (2010) Combination chemotherapy of doxorubicin and paclitaxel for hepatocellular carcinoma in vitro and in vivo. *J. Cancer Res. Clin. Oncol.* **136**, 267–274

86. Wang, H., and Huang, Y. (2020) Combination therapy based on nano codelivery for overcoming cancer drug resistance. *Med. Drug Discov.* **6**, 100024

87. Mokhtari, R. B., Homayouni, T. S., Baluch, N., Morgatskaya, E., Kumar, S., Das, B., and Yeger, H. (2017) Combination therapy in combating cancer. *Oncotarget*. **8**, 38022–38043

88. Lopez, J. S., and Banerji, U. (2018) Europe PMC Funders Group Combine and conquer : challenges for targeted therapy combinations in early phase trials. **14**, 57–66

89. Jain, S., Saxena, S., and Kumar, A. (2014) Epidemiology of prostate cancer in India. *Meta Gene*. **2**, 596

90. Rawla, P. (2019) Epidemiology of Prostate Cancer. *World J. Oncol.* **10**, 63–89

91. Wang, L., Lu, B., He, M., Wang, Y., Wang, Z., and Du, L. (2022) Prostate Cancer Incidence and Mortality: Global Status and Temporal Trends in 89 Countries From 2000 to 2019. *Front. public Heal.* 10.3389/FPUBH.2022.811044

92. Rawla, P. (2019) Epidemiology of Prostate Cancer. *World J. Oncol.* **10**, 63

93. De Mulder, P. H. M., Schalken, J. A., and Sternberg, C. N. (2002) Treatment options in hormone resistant prostate cancer. *Ann. Oncol. Off. J. Eur. Soc. Med. Oncol.* **13 Suppl 4**, 95–102

94. Culp, M. B. B., Soerjomataram, I., Efstathiou, J. A., Bray, F., and Jemal, A. (2020) Recent Global Patterns in Prostate Cancer Incidence and Mortality Rates. *Eur. Urol.* **77**, 38–52

95. Gathirua-Mwangi, W. G., and Zhang, J. (2014) Dietary factors and risk for advanced prostate cancer. *Eur. J. Cancer Prev.* **23**, 96–109

96. Cotter, K., Konety, B., and Ordonez, M. A. (2016) Contemporary Management of Prostate Cancer. *F1000Research*. **5**, 1–8

97. Keyes, M., Crook, J., Morton, G., Vigneault, E., Usmani, N., and Morris, W. J. (2013) Treatment options for localized prostate cancer. *Can. Fam. Physician*. **59**, 1269

98. Litwin, M. S., and Tan, H. J. (2017) The diagnosis and treatment of prostate cancer: A review. *JAMA - J. Am. Med. Assoc.* **317**, 2532–2542

99. Harris, W. P., Mostaghel, E. A., Nelson, P. S., and Montgomery, B. (2009) Androgen deprivation therapy: progress in understanding mechanisms of resistance and optimizing androgen depletion. *Nat. Clin. Pract. Urol.* **6**, 76

100. Banerjee, P. P., Banerjee, S., Brown, T. R., and Zirkin, B. R. (2018) Androgen action in prostate function and disease. *Am. J. Clin. Exp. Urol.* **6**, 62–77

101. Petrylak, D. P. (2003) Docetaxel for the treatment of hormone-refractory prostate cancer. *Rev. Urol.* **5 Suppl 3**, S14-21

102. Kulhari, H., Pooja, D., Singh, M. K., Kuncha, M., Adams, D. J., and Sistla, R. (2015) Bombesin-conjugated nanoparticles improve the cytotoxic efficacy of docetaxel against gastrin-releasing but androgen-independent prostate cancer. *Nanomedicine*. **10**, 2847–2859

103. Lönnerdal, B., and Iyer, S. (1995) Lactoferrin: molecular structure and biological function. *Annu. Rev. Nutr.* **15**, 93–110

104. Vogel, H. J. (2012) Lactoferrin, a bird's eye view. *Biochem. Cell Biol.* **90**, 233–244

105. González-Chávez, S. A., Arévalo-Gallegos, S., and Rascón-Cruz, Q. (2009) Lactoferrin: structure, function and applications. *Int. J. Antimicrob. Agents*. 10.1016/j.ijantimicag.2008.07.020

106. Superti, F. (2020) Lactoferrin from Bovine Milk: A Protective Companion for Life. *Nutrients*. **12**, 1–26

107. Adlerova, L., Bartoskova, A., and Faldyna, M. (2008) Lactoferrin: A review. *Vet. Med. (Praha).* **53**, 457–468

108. Baker, E. N., Baker, H. M., and Kidd, R. D. (2002) Lactoferrin and transferrin: functional variations on a common structural framework. *Biochem. Cell Biol.* **80**, 27–34

109. Wally, J., and Buchanan, S. K. (2007) A structural comparison of human serum transferrin and human lactoferrin. *Biometals*. **20**, 249

110. Lambert, L. A., Perri, H., Halbrooks, P. J., and Mason, A. B. (2005) Evolution of the transferrin family : Conservation of residues associated with iron and anion binding. **142**, 129–141

111. Hu, P., Zhao, D., Zhao, F., Wang, J., and Zhu, W. (2019) The Effects of the

Combination of Oral Lactoferrin and Iron Injection on Iron Homestasis, Antioxidative Abilities and Cytokines Activities of Suckling Piglets. *Anim. an Open Access J. from MDPI*. 10.3390/ANI9070438

112. Wang, B., Timilsena, Y. P., Blanch, E., and Adhikari, B. (2017) Lactoferrin: Structure, function, denaturation and digestion. *https://doi.org/10.1080/10408398.2017.1381583*. **59**, 580–596

113. Actor, J. K., Hwang, S.-A., and Kruzel, M. L. (2009) Lactoferrin as a Natural Immune Modulator. *Curr. Pharm. Des.* **15**, 1956

114. Cutone, A., Rosa, L., Ianiro, G., Lepanto, M. S., Di Patti, M. C. B., Valenti, P., and Musci, G. (2020) Lactoferrin's Anti-Cancer Properties: Safety, Selectivity, and Wide Range of Action. *Biomolecules*. 10.3390/BIOM10030456

115. Rascón-Cruz, Q., Espinoza-Sánchez, E. A., Siqueiros-Cendón, T. S., Nakamura-Bencomo, S. I., Arévalo-Gallegos, S., and Iglesias-Figueroa, B. F. (2021) Lactoferrin: A Glycoprotein Involved in Immunomodulation, Anticancer, and Antimicrobial Processes. *Molecules*. 10.3390/MOLECULES26010205

116. Cutone, A., Rosa, L., Ianiro, G., Lepanto, M. S., Di Patti, M. C. B., Valenti, P., and Musci, G. (2020) Lactoferrin's Anti-Cancer Properties: Safety, Selectivity, and Wide Range of Action. *Biomolecules*. 10.3390/BIOM10030456

117. PAN, S., WENG, H., HU, G., WANG, S., ZHAO, T., YAO, X., LIAO, L., ZHU, X., and GE, Y. (2021) Lactoferrin may inhibit the development of cancer via its immunostimulatory and immunomodulatory activities (review). *Int. J. Oncol.* **59**, 1–11

118. Altwaijry, N., Somani, S., Parkinson, J. A., Tate, R. J., Keating, P., Warzecha, M., Mackenzie, G. R., Leung, H. Y., and Dufès, C. (2018) Regression of prostate tumors

after intravenous administration of lactoferrinbearing polypropylenimine dendriplexes encoding TNF-α, TRAIL, and interleukin-12. *Drug Deliv.* **25**, 679–689

119. Thakur, A. (2021) Advances in Cancer Biology - Metastasis Nano therapeutic approaches to combat progression of metastatic prostate cancer. *Adv. Cancer Biol. - Metastasis*. **2**, 100009

120. Zhao, J., Zhang, C., Wang, W., Li, C., Mu, X., and Hu, K. (2022) Biomedicine & Pharmacotherapy Current progress of nanomedicine for prostate cancer diagnosis and treatment. *Biomed. Pharmacother.* **155**, 113714

121. Bulbake, U., Doppalapudi, S., Kommineni, N., and Khan, W. (2017) Liposomal Formulations in Clinical Use: An Updated Review. *Pharm. 2017, Vol. 9, Page 12*. **9**, 12

122. Zhang, L., Lin, Z., Chen, Y., Gao, D., Wang, P., Lin, Y., Wang, Y., Wang, F., Han, Y., and Yuan, H. (2022) Co-delivery of Docetaxel and Resveratrol by liposomes synergistically boosts antitumor efficiency against prostate cancer. *Eur. J. Pharm. Sci.* **174**, 106199

123. Kroon, J., Metselaar, J. M., Storm, G., and van der Pluijm, G. (2014) Liposomal nanomedicines in the treatment of prostate cancer. *Cancer Treat. Rev.* **40**, 578–584

124. Rochín-Wong, S., Rivas, I. V., Rochín-Wong, S., and Rivas, I. V. (2022) Lipid and Polymeric Nanocapsules. *Drug Carriers*. 10.5772/INTECHOPEN.103906

125. Karlsson, J., Vaughan, H. J., and Green, J. J. (2018) Biodegradable Polymeric Nanoparticles for Therapeutic Cancer Treatments. *Annu. Rev. Chem. Biomol. Eng.* **9**, 105

126. Łukasiewicz, S., Szczepanowicz, K., Podgórna, K., Błasiak, E., Majeed, N., Ogren, S.

O. Ö., Nowak, W., Warszyński, P., and Dziedzicka-Wasylewska, M. (2016) Encapsulation of clozapine in polymeric nanocapsules and its biological effects. *Colloids Surfaces B Biointerfaces*. **140**, 342–352

127. Shitole, A. A., Sharma, N., Giram, P., Khandwekar, A., Baruah, M., Garnaik, B., and Koratkar, S. (2020) LHRH-conjugated, PEGylated, poly-lactide-co-glycolide nanocapsules for targeted delivery of combinational chemotherapeutic drugs Docetaxel and Quercetin for prostate cancer. *Mater. Sci. Eng. C.* **114**, 111035

128. Lima-Tenório, M. K., Gómez Pineda, E. A., Ahmad, N. M., Fessi, H., and Elaissari, A. (2015) Magnetic nanoparticles: In vivo cancer diagnosis and therapy. *Int. J. Pharm.* **493**, 313–327

129. Liu, J. F., Jang, B., Issadore, D., and Tsourkas, A. (2019) Use of Magnetic Fields and Nanoparticles to Trigger Drug Release and Improve Tumor Targeting. *Wiley Interdiscip. Rev. Nanomed. Nanobiotechnol.* **11**, e1571

130. Ngen, E. J., Benham Azad, B., Boinapally, S., Lisok, A., Brummet, M., Jacob, D., Pomper, M. G., and Banerjee, S. R. (2019) MRI Assessment of Prostate-Specific Membrane Antigen (PSMA) Targeting by a PSMA-Targeted Magnetic Nanoparticle: Potential for Image-Guided Therapy. *Mol. Pharm.* **16**, 2060–2068

131. Arvizo, R., Bhattacharya, R., and Mukherjee, P. (2010) Gold nanoparticles: Opportunities and Challenges in Nanomedicine. *Expert Opin. Drug Deliv.* **7**, 753

132. Luo, D., Johnson, A., Wang, X., Li, H., Erokwu, B. O., Springer, S., Lou, J., Ramamurthy, G., Flask, C. A., Burda, C., Meade, T. J., and Basilion, J. P. (2020) Targeted Radiosensitizers for MR-Guided Radiation Therapy of Prostate Cancer. *Nano Lett.* **20**, 7159–7167

133. Isa, E. D. M., Ahmad, H., and Rahman, M. B. A. (2019) Optimization of synthesis parameters of mesoporous silica nanoparticles based on ionic liquid by experimental design and its application as a drug delivery agent. *J. Nanomater.* 10.1155/2019/4982054

134. Niculescu, V. C. (2020) Mesoporous Silica Nanoparticles for Bio-Applications. *Front. Mater.* **7**, 36

135. Chaudhary, Z., Subramaniam, S., Khan, G. M., Abeer, M. M., Qu, Z., Janjua, T., Kumeria, T., Batra, J., and Popat, A. (2019) Encapsulation and Controlled Release of Resveratrol Within Functionalized Mesoporous Silica Nanoparticles for Prostate Cancer Therapy. *Front. Bioeng. Biotechnol.* **7**, 1–9

136. Kabanov, A. V., Batrakova, E. V., Melik-Nubarov, N. S., Fedoseev, N. A., Dorodnich, T. Y., Alakhov, V. Y., Chekhonin, V. P., Nazarova, I. R., and Kabanov, V. A. (1992) A new class of drug carriers: micelles of poly(oxyethylene)-poly(oxypropylene) block copolymers as microcontainers for drug targeting from blood in brain. *J. Control. Release*. **22**, 141–157

137. Atanase, L. I. (2021) Micellar Drug Delivery Systems Based on Natural Biopolymers. *Polym. 2021, Vol. 13, Page 477*. **13**, 477

138. Barve, A., Jain, A., Liu, H., Zhao, Z., and Cheng, K. (2020) Enzyme-responsive polymeric micelles of cabazitaxel for prostate cancer targeted therapy. *Acta Biomater.* **113**, 501–511

139. Ma, Y., Mou, Q., Wang, D., Zhu, X., and Yan, D. (2016) Dendritic Polymers for Theranostics. *Theranostics*. **6**, 930

140. Ma, Y., Mou, Q., Wang, D., Zhu, X., and Yan, D. (2016) Dendritic Polymers for

Theranostics. *Theranostics*. **6**, 930

141. Khandare, J., and Calderón, M. (2015) Dendritic polymers for smart drug delivery applications. *Nanoscale*. **7**, 3806–3807

142. Xu, L., and Yang, H. (2019) Folate-decorated polyamidoamine dendrimer nanoparticles for head and neck cancer gene therapy. *Methods Mol. Biol.* **1974**, 393–408

143. El-Betany, A. M. M., Kamoun, E. A., James, C., Jangher, A., Aljayyoussi, G., Griffiths, P., McKeown, N. B., and Gumbleton, M. (2020) Auto-fluorescent PAMAM-based dendritic molecules and their potential application in pharmaceutical sciences. *Int. J. Pharm.* **579**, 119187

144. Lesniak, W. G., Boinapally, S., Banerjee, S. R., Behnam Azad, B., Foss, C. A., Shen, C., Lisok, A., Wharram, B., Nimmagadda, S., and Pomper, M. G. (2019) Evaluation of PSMA-Targeted PAMAM Dendrimer Nanoparticles in a Murine Model of Prostate Cancer. *Mol. Pharm.* **16**, 2590–2604

145. Verma, D., Gulati, N., Kaul, S., Mukherjee, S., and Nagaich, U. (2018) Protein Based Nanostructures for Drug Delivery. *J. Pharm.* **2018**, 1–18

146. Hong, S., Choi, D. W., Kim, H. N., Park, C. G., Lee, W., and Park, H. H. (2020) Protein-Based Nanoparticles as Drug Delivery Systems. *Pharmaceutics*. **12**, 1–28

147. Lohcharoenkal, W., Wang, L., Chen, Y. C., and Rojanasakul, Y. (2014) Protein Nanoparticles as Drug Delivery Carriers for Cancer Therapy. *Biomed Res. Int.* 10.1155/2014/180549

148. Hong, S., Choi, D. W., Kim, H. N., Park, C. G., Lee, W., and Park, H. H. (2020) Protein-Based Nanoparticles as Drug Delivery Systems. *Pharmaceutics*. **12**, 1–28

149. Soll, M., Chen, Q., Zhitomirsky, B., Lim, P. P., Assaraf, Y. G., Gross, Z., Termini, J., and Gray, H. B. (2020) Protein-coated corrole nanoparticles for the treatment of prostate cancer cells. *Cell Death Discov.* 10.1038/s41420-020-0288-x

150. Montero, A., Fossella, F., Hortobagyi, G., and Valero, V. (2005) Docetaxel for treatment of solid tumors : a systematic

151. Franke, R. M., Carducci, M. A., Rudek, M. A., Baker, S. D., and Sparreboom, A. (2010) Castration-Dependent Pharmacokinetics of Docetaxel in Patients With Prostate Cancer. *J. Clin. Oncol.* **28**, 4562

152. Li, K., Zhan, W., Chen, Y., Jha, R. K., and Chen, X. (2019) Docetaxel and doxorubicin codelivery by nanocarriers for synergistic treatment of prostate cancer. *Front. Pharmacol.* **10**, 1–16

153. Rivlin, N., Brosh, R., Oren, M., and Rotter, V. (2011) Mutations in the p53 Tumor Suppressor Gene: Important Milestones at the Various Steps of Tumorigenesis. *Genes Cancer*. **2**, 466

154. Bertheau, P., Espié, M., Turpin, E., Lehmann, J., Plassa, L. F., Varna, M., Janin, A., and De Thé, H. (2008) TP53 status and response to chemotherapy in breast cancer. *Pathobiology*. **75**, 132–139

155. Olivier, M., Hollstein, M., and Hainaut, P. (2010) TP53 Mutations in Human Cancers: Origins, Consequences, and Clinical Use. *Cold Spring Harb. Perspect. Biol.* 10.1101/CSHPERSPECT.A001008

156. Miriam Teroerde, M., Cathleen Nientiedt, M., Anette Duensing, M., Markus Hohenfellner, M., Albrecht Stenzinger, M., and Stefan Duensing, M. (2021) Revisiting the Role of p53 in Prostate Cancer. *Exon Publ.*

10.36255/EXONPUBLICATIONS.PROSTATECANCER.P53.2021

157. Beatson, E. L., Chau, C. H., Price, D. K., and Figg, W. D. (2022) PARP inhibitors on the move in prostate cancer: spotlight on Niraparib & update on PARP inhibitor combination trials. *Am. J. Clin. Exp. Urol.* **10**, 252

158. Xia, M., Guo, Z., and Hu, Z. (2021) The Role of PARP Inhibitors in the Treatment of Prostate Cancer: Recent Advances in Clinical Trials. *Biomolecules*. 10.3390/BIOM11050722

159. Teyssonneau, D., Margot, H., Cabart, M., Anonnay, M., Sargos, P., Vuong, N. S., Soubeyran, I., Sevenet, N., and Roubaud, G. (2021) Prostate cancer and PARP inhibitors: progress and challenges. *J. Hematol. Oncol.* **14**, 1–19

160. Sharma, B., Ma, W., Adjei, I. M., Panyam, J., Dimitrijevic, S., and Labhasetwar, V. (2011) Nanoparticle-mediated p53 gene therapy for tumor inhibition. *Drug Deliv. Transl. Res.* **1**, 43

161. Mateo, J., Carreira, S., Sandhu, S., Miranda, S., Mossop, H., Perez-Lopez, R., Nava Rodrigues, D., Robinson, D., Omlin, A., Tunariu, N., Boysen, G., Porta, N., Flohr, P., Gillman, A., Figueiredo, I., Paulding, C., Seed, G., Jain, S., Ralph, C., Protheroe, A., Hussain, S., Jones, R., Elliott, T., McGovern, U., Bianchini, D., Goodall, J., Zafeiriou, Z., Williamson, C. T., Ferraldeschi, R., Riisnaes, R., Ebbs, B., Fowler, G., Roda, D., Yuan, W., Wu, Y.-M., Cao, X., Brough, R., Pemberton, H., A'Hern, R., Swain, A., Kunju, L. P., Eeles, R., Attard, G., Lord, C. J., Ashworth, A., Rubin, M. A., Knudsen, K. E., Feng, F. Y., Chinnaiyan, A. M., Hall, E., and de Bono, J. S. (2015) DNA-Repair Defects and Olaparib in Metastatic Prostate Cancer. *N. Engl. J. Med.* **373**, 1697–1708

162. Hu, J., Cao, J., Topatana, W., Juengpanich, S., Li, S., Zhang, B., Shen, J., Cai, L., Cai, X., and Chen, M. (2021) Targeting mutant p53 for cancer therapy: direct and indirect

strategies. *J. Hematol. Oncol.* **14**, 1–19

163. Chen, J., Guo, Z., Tian, H., and Chen, X. (2016) Production and clinical development of nanoparticles for gene delivery. *Mol. Ther. - Methods Clin. Dev.* **3**, 16023

164. Nayerossadat, N., Maedeh, T., and Ali, P. A. (2012) Viral and nonviral delivery systems for gene delivery. **1**, 1–11

165. Biological, K. (2015) Non Viral Vectors in Gene Therapy- An Overview. **9**, 1–6

166. Español, L., Larrea, A., Andreu, V., Mendoza, G., Arruebo, M., Sebastian, V., Aurora-Prado, M. S., Kedor-Hackmann, E. R. M., Santoro, M. I. R. M., and Santamaria, J. (2016) Dual encapsulation of hydrophobic and hydrophilic drugs in PLGA nanoparticles by a single-step method: drug delivery and cytotoxicity assays. *RSC Adv.* **6**, 111060–111069

167. Gelperina, S., Kisich, K., Iseman, M. D., and Heifets, L. (2005) Pulmonary Perspective The Potential Advantages of Nanoparticle Drug Delivery Systems in Chemotherapy of Tuberculosis. **172**, 1487–1490

168. Zhang, J., and Marksaltzman, W. (2013) Engineering biodegradable nanoparticles for drug and gene delivery. *Chem. Eng. Prog.* **109**, 25

169. Dizaj, S. M., Jafari, S., and Khosroushahi, A. Y. (2014) A sight on the current nanoparticle-based gene delivery vectors. *Nanoscale Res. Lett.* **9**, 1–9

170. Xiao, Y., Shi, K., Qu, Y., Chu, B., and Qian, Z. (2019) Engineering Nanoparticles for Targeted Delivery of Nucleic Acid Therapeutics in Tumor. *Mol. Ther. Methods Clin. Dev.* **12**, 1–18

171. Golla, K., Cherukuvada, B., Ahmed, F., and Kondapi, A. K. (2012) Efficacy, Safety and Anticancer Activity of Protein Nanoparticle-Based Delivery of Doxorubicin

through Intravenous Administration in Rats. *PLoS One*. 10.1371/journal.pone.0051960

172. Kumari, S., Ahsan, S. M., Kumar, J. M., Kondapi, A. K., and Rao, N. M. (2017) Overcoming blood brain barrier with a dual purpose Temozolomide loaded Lactoferrin nanoparticles for combating glioma (SERP-17-12433). *Sci. Rep.* **7**, 1–13

173. Thomas, M., and Klibanov, A. M. (2002) Enhancing polyethylenimine's delivery of plasmid DNA into mammalian cells. *Proc. Natl. Acad. Sci. U. S. A.* **99**, 14640–14645

174. Ravel, D., Dubois, V., Quinonero, J., Meyer-Losic, F., Delord, J. P., Rochaix, P., Nicolazzi, C., Ribes, F., Mazerolles, C., Assouly, E., Vialatte, K., Hor, I., Kearsey, J., and Trouet, A. (2008) Preclinical toxicity, toxicokinetics, and antitumoral efficacy studies of DTS-201, a tumor-selective peptidic prodrug of doxorubicin. *Clin. Cancer Res.* 10.1158/1078-0432.CCR-07-1165

175. Fraiser, L. H., Kanekal, S., and Kehrer, J. P. (1991) Cyclophosphamide Toxicity: Characterising and Avoiding the Problem. *Drugs*. 10.2165/00003495-199142050-00005

176. Arnold, W. R., and Das, A. (2018) An Emerging Pathway of Doxorubicin Cardiotoxicity Mediated through CYP2J2. *Biochemistry*. 10.1021/acs.biochem.8b00337

177. Chatterjee, K., Zhang, J., Honbo, N., and Karliner, J. S. (2010) Doxorubicin cardiomyopathy. *Cardiology*. 10.1159/000265166

178. Kumari, S., and Kondapi, A. K. (2017) Lactoferrin nanoparticle mediated targeted delivery of 5-fluorouracil for enhanced therapeutic efficacy. *Int. J. Biol. Macromol.* 10.1016/j.ijbiomac.2016.10.110

179. Haley, B., and Frenkel, E. (2008) Nanoparticles for drug delivery in cancer treatment.

Urol. Oncol. Semin. Orig. Investig. 10.1016/j.urolonc.2007.03.015

180. Lohcharoenkal, W., Wang, L., Chen, Y. C., and Rojanasakul, Y. (2014) Protein nanoparticles as drug delivery carriers for cancer therapy. *Biomed Res. Int.* 10.1155/2014/180549

181. Kumari, S., and Kondapi, A. K. (2018) Receptor-mediated targeted delivery of DNA using Lactoferrin nanoparticles. *Int. J. Biol. Macromol.* 10.1016/j.ijbiomac.2017.11.160

182. Webb, B. A., Chimenti, M., Jacobson, M. P., and Barber, D. L. (2011) Dysregulated pH: A perfect storm for cancer progression. *Nat. Rev. Cancer*. **11**, 671–677

183. Zhang, X., Lin, Y., and Gillies, R. J. (2010) Tumor pH and its measurement. *J. Nucl. Med.* **51**, 1167–1170

184. Andreucci, E., Peppicelli, S., Ruzzolini, J., Bianchini, F., Biagioni, A., Papucci, L., Magnelli, L., Mazzanti, B., Stecca, B., and Calorini, L. (1959) The acidic tumor microenvironment drives a stem-like phenotype in melanoma cells Abbreviations CAIX Carbonic anhydrase IX CSC Cancer stem cells ELDA Extreme limiting dilution analysis EMT Epithelial-to-mesenchymal transition TIC Tumor-initiating cells

185. Dhesi, S., Chu, M. P., Blevins, G., Paterson, I., Larratt, L., Oudit, G. Y., and Kim, D. H. (2013) Cyclophosphamide-Induced Cardiomyopathy. *J. Investig. Med. High Impact Case Reports*. 10.1177/2324709613480346

186. Nakagawa, T., Mazzali, M., Kang, D. H., Sánchez-Lozada, L. G., Herrera-Acosta, J., and Johnson, R. J. (2006) Uric acid - A uremic toxin? *Blood Purif.* 10.1159/000089440

187. Mokhtari, R. B., Homayouni, T. S., Baluch, N., Morgatskaya, E., Kumar, S., Das, B., and Yeger, H. (2017) Combination therapy in combating cancer. *Oncotarget*.

10.18632/oncotarget.16723

188. Yardley, D. A. (2013) Drug Resistance and the Role of Combination Chemotherapy in Improving Patient Outcomes. *Int. J. Breast Cancer*. 10.1155/2013/137414

189. Senapati, S., Mahanta, A. K., Kumar, S., and Maiti, P. (2018) Controlled drug delivery vehicles for cancer treatment and their performance. *Signal Transduct. Target. Ther.* 10.1038/s41392-017-0004-3

190. Miao, L., Guo, S., Lin, C. M., Liu, Q., and Huang, L. (2017) Nanoformulations for combination or cascade anticancer therapy. *Adv. Drug Deliv. Rev.* 10.1016/j.addr.2017.06.003

191. Gurunathan, S., Kang, M. H., Qasim, M., and Kim, J. H. (2018) Nanoparticle-mediated combination therapy: Two-in-one approach for cancer. *Int. J. Mol. Sci.* 10.3390/ijms19103264

192. Kumari, S., Ahsan, S. M., Kumar, J. M., Kondapi, A. K., and Rao, N. M. (2017) Overcoming blood brain barrier with a dual purpose Temozolomide loaded Lactoferrin nanoparticles for combating glioma (SERP-17-12433). *Sci. Rep.* 10.1038/s41598-017-06888-4

193. Athmakur, H., and Kondapi, A. K. (2018) Carmustine loaded lactoferrin nanoparticles demonstrates an enhanced antiproliferative activity against glioblastoma in vitro. *Int. J. Appl. Pharm.* 10.22159/ijap.2018v10i6.28004

194. Alexis, F., Pridgen, E., Molnar, L. K., and Farokhzad, O. C. (2008) Factors affecting the clearance and biodistribution of polymeric nanoparticles. in *Molecular Pharmaceutics*, 10.1021/mp800051m

195. Honary, S., and Zahir, F. (2013) Effect of zeta potential on the properties of nano-drug

delivery systems - A review (Part 1). *Trop. J. Pharm. Res.* 10.4314/tjpr.v12i2.19

196. Shen, S., Wu, Y., Liu, Y., and Wu, D. (2017) High drug-loading nanomedicines: Progress, current status, and prospects. *Int. J. Nanomedicine*. 10.2147/IJN.S132780

197. Senapathi, J., Bommakanti, A., Mallepalli, S., Mukhopadhyay, S., and Kondapi, A. K. (2020) Sulfonate modified Lactoferrin nanoparticles as drug carriers with dual activity against HIV-1. *Colloids Surfaces B Biointerfaces*. 10.1016/j.colsurfb.2020.110979

198. Annas, A., Bengtsson, C., and Törnqvist, E. (2013) Group housing of male CD1 mice: Reflections from toxicity studies. *Lab. Anim.* 10.1177/0023677213476278

199. Aston, W. J., Hope, D. E., Nowak, A. K., Robinson, B. W., Lake, R. A., and Lesterhuis, W. J. (2017) A systematic investigation of the maximum tolerated dose of cytotoxic chemotherapy with and without supportive care in mice. *BMC Cancer*. 10.1186/s12885-017-3677-7

200. Mahay, H. (2009) Oral chemotherapy: Patient advantages and challenges. *Pharm. Times*

201. Kondapi, A. K. (2020) Targeting cancer with lactoferrin nanoparticles: Recent advances. *Nanomedicine*. 10.2217/nnm-2020-0090

202. Batist, G., Ramakrishnan, G., Rao, C. S., Chandrasekharan, A., Gutheil, J., Guthrie, T., Shah, P., Khojasteh, A., Nair, M. K., Hoelzer, K., Tkaczuk, K., Youn Choi Park, and Lee, L. W. (2001) Reduced cardiotoxicity and preserved antitumor efficacy of liposome-encapsulated doxorubicin and cyclophosphamide compared with conventional doxorubicin and cyclophosphamide in a randomized, multicenter trial of metastatic breast cancer. *J. Clin. Oncol.* 10.1200/JCO.2001.19.5.1444

203. Housman, G., Byler, S., Heerboth, S., Lapinska, K., Longacre, M., Snyder, N., and

Sarkar, S. (2014) Drug Resistance in Cancer: An Overview. *Cancers (Basel).* **6**, 1769

204. Bilici, A. (2014) Treatment options in patients with metastatic gastric cancer: Current status and future perspectives. *World J. Gastroenterol.* **20**, 3905

205. Rajesh, T. (2016) Controlled Release Drug Formulation In Pharmaceuticals: A Study On Their Application and Properties. *World J. Pharm. Res.* **5**, 1704–1720

206. Yilmaz, E. R., Kertmen, H., Gürer, B., Kanat, M. A., Arikok, A. T., Ergüder, B. I., Hasturk, A. E., Ergil, J., and Sekerci, Z. (2012) The protective effect of 2-mercaptoethane sulfonate (MESNA) against traumatic brain injury in rats. *Acta Neurochir. 2012 1551*. **155**, 141–149

207. Tacar, O., Sriamornsak, P., and Dass, C. R. (2013) Doxorubicin: an update on anticancer molecular action, toxicity and novel drug delivery systems. *J. Pharm. Pharmacol.* **65**, 157–170

208. Ali, M., and Byrne, M. E. (2009) Controlled release of high molecular weight hyaluronic Acid from molecularly imprinted hydrogel contact lenses. *Pharm. Res.* **26**, 714–726

209. Zhou, J., Sun, C., and Yu, C. (2020) Highly-controllable drug release from core cross-linked singlet oxygen-responsive nanoparticles for cancer therapy. *RSC Adv.* **10**, 19997

210. Jain, S., Saxena, S., and Kumar, A. (2014) Epidemiology of prostate cancer in India. *Meta Gene*. **2**, 596–605

211. Smith, M. R., Hussain, M., Saad, F., Fizazi, K., Sternberg, C. N., Crawford, E. D., Kopyltsov, E., Park, C. H., Alekseev, B., Montesa-Pino, Á., Ye, D., Parnis, F., Cruz, F., Tammela, T. L. J., Suzuki, H., Utriainen, T., Fu, C., Uemura, M., Méndez-Vidal, M. J., Maughan, B. L., Joensuu, H., Thiele, S., Li, R., Kuss, I., and Tombal, B. (2022)

Darolutamide and Survival in Metastatic, Hormone-Sensitive Prostate Cancer. *N. Engl. J. Med.* **386**, 1132–1142

212. Fizazi, K., Foulon, S., Carles, J., Roubaud, G., McDermott, R., Fléchon, A., Tombal, B., Supiot, S., Berthold, D., Ronchin, P., Kacso, G., Gravis, G., Calabro, F., Berdah, J. F., Hasbini, A., Silva, M., Thiery-Vuillemin, A., Latorzeff, I., Mourey, L., Laguerre, B., Abadie-Lacourtoisie, S., Martin, E., El Kouri, C., Escande, A., Rosello, A., Magne, N., Schlurmann, F., Priou, F., Chand-Fouche, M. E., Freixa, S. V., Jamaluddin, M., Rieger, I., and Bossi, A. (2022) Abiraterone plus prednisone added to androgen deprivation therapy and docetaxel in de novo metastatic castration-sensitive prostate cancer (PEACE-1): a multicentre, open-label, randomised, phase 3 study with a 2 × 2 factorial design. *Lancet*. **399**, 1695–1707

213. Chen, L., Zhou, L., Wang, C., Han, Y., Lu, Y., Liu, J., Hu, X., Yao, T., Lin, Y., Liang, S., Shi, S., and Dong, C. (2019) Tumor-Targeted Drug and CpG Delivery System for Phototherapy and Docetaxel-Enhanced Immunotherapy with Polarization toward M1-Type Macrophages on Triple Negative Breast Cancers. *Adv. Mater.* **31**, 1904997

214. Rafiei, P., and Haddadi, A. (2017) Docetaxel-loaded PLGA and PLGA-PEG nanoparticles for intravenous application: pharmacokinetics and biodistribution profile. *Int. J. Nanomedicine*. **12**, 935

215. About the Influence of PEG Spacers on the Cytotoxicity ofTitanate Nanotubes-Docetaxel Nanohybrids against a ProstateCancer Cell Line.pdf

216. Dai, L., Wei, D., Zhang, J., Shen, T., Zhao, Y., Liang, J., Ma, W., Zhang, L., Liu, Q., and Zheng, Y. (2021) Aptamer-conjugated mesoporous polydopamine for docetaxel targeted delivery and synergistic photothermal therapy of prostate cancer. *Cell Prolif.* **54**, e13130

217. Dong, Z., Wang, Y., Guo, J., Tian, C., Pan, W., Wang, H., and Yan, J. (2022) Prostate Cancer Therapy Using Docetaxel and Formononetin Combination: Hyaluronic Acid and Epidermal Growth Factor Receptor Targeted Peptide Dual Ligands Modified Binary Nanoparticles to Facilitate the in vivo Anti-Tumor Activity. *Drug Des. Devel. Ther.* **16**, 2683–2693

218. Wang, W. P., Iigo, M., Sato, J., Sekine, K., Adachi, I., and Tsuda, H. (2000) Activation of Intestinal Mucosal Immunity in Tumor-bearing Mice by Lactoferrin. *Jpn. J. Cancer Res.* **91**, 1022

219. Asian Pacific Journal of Cancer Prevention [online] http://journal.waocp.org/?sid=Entrez:PubMed&id=pmid:12716300&key=2000.1.4.277 (Accessed September 10, 2022)

220. Luis Bermudez, by E., Martinez-Zaguilán Stephanie Filleur Jose Perez-Zoghbi Accepted Thomas A Pressley, R. F., and Bermudez, L. E. (2010) V-ATPase at the cell surface in highly metastatic Prostate Cancer cells. [online] https://ttu-ir.tdl.org/handle/2346/ETD-TTU-2010-12-1286 (Accessed September 10, 2022)

221. Guedes, J. P., Pereira, C. S., Rodrigues, L. R., and Côrte-Real, M. (2018) Bovine milk lactoferrin selectively kills highly metastatic prostate cancer PC-3 and osteosarcoma MG-63 cells in vitro. *Front. Oncol.* **8**, 200

222. Zhao, Q., Cheng, Y., and Xiong, Y. (2021) LTF Regulates the Immune Microenvironment of Prostate Cancer Through JAK/STAT3 Pathway. *Front. Oncol.* **11**, 1–12

223. Elzoghby, A. O., Abdelmoneem, M. A., Hassanin, I. A., Abd Elwakil, M. M., Elnaggar, M. A., Mokhtar, S., Fang, J. Y., and Elkhodairy, K. A. (2020) Lactoferrin, a multi-functional glycoprotein: Active therapeutic, drug nanocarrier & targeting ligand.

Biomaterials. **263**, 120355

224. Almowalad, J., Somani, S., Laskar, P., Meewan, J., Tate, R. J., Mullin, M., and Dufès, C. (2021) Lactoferrin-Bearing Gold Nanocages for Gene Delivery in Prostate Cancer Cells in vitro . *Int. J. Nanomedicine*. **16**, 4391–4407

225. Almowalad, J., Laskar, P., Somani, S., Meewan, J., Tate, R. J., and Dufès, C. (2022) Lactoferrin- and Dendrimer-Bearing Gold Nanocages for Stimulus-Free DNA Delivery to Prostate Cancer Cells. *Int. J. Nanomedicine*. **17**, 1409–1421

226. Kumar, P., Lakshmi, Y. S., Bhaskar, C., Golla, K., and Kondapi, A. K. (2015) Improved safety, bioavailability and pharmacokinetics of Zidovudine through lactoferrin nanoparticles during oral administration in rats. *PLoS One*. 10.1371/journal.pone.0140399

227. Smirnov, I. M., Bailey, K., Flowers, C. H., Garrigues, N. E. D. W., Wesselius, L. J., Igor, M., Bailey, K., Flowers, C. H., Garrigues, N. W., and Wesselius, L. J. (2022) Effects of TNF- ⎵ and IL-1 ☒ on iron metabolism by A549 cells and influence on cytotoxicity

228. Elfinger, M., Maucksch, C., and Rudolph, C. (2007) Characterization of lactoferrin as a targeting ligand for nonviral gene delivery to airway epithelial cells. **28**, 3448–3455

229. Uyeturk, U., Sarıcı, H., Kın Tekce, B., Eroglu, M., Kemahlı, E., Uyeturk, U., and Gucuk, A. (2014) Serum omentin level in patients with prostate cancer. *Med. Oncol.* **31**, 6–10

230. Fryczkowski, M., Bułdak, R. J., Hejmo, T., Kukla, M., and Zwirska-Korczala, K. (2018) Circulating Levels of Omentin, Leptin, VEGF, and HGF and Their Clinical Relevance with PSA Marker in Prostate Cancer. *Dis. Markers*. 10.1155/2018/3852401

231. Bannerji, R., Rosenthal, F. M., Heston, W. D. W., Fair, W. R., Gansbacher, B., and Gilboa, E. (1994) Immunotherapy of Prostate Cancer in the Dunning Rat Model: Use of Cytokine Gene Modified Tumor Vaccines. *Cancer Res.* **54**, 1760–1765

232. Chen, Z., Tai, Z., Gu, F., Hu, C., Zhu, Q., and Gao, S. (2016) Aptamer-mediated delivery of docetaxel to prostate cancer through polymeric nanoparticles for enhancement of antitumor efficacy. *Eur. J. Pharm. Biopharm.* **107**, 130–141

233. Wang, Q., Alshaker, H., Böhler, T., Srivats, S., Chao, Y., Cooper, C., and Pchejetski, D. (2017) Core shell lipid-polymer hybrid nanoparticles with combined docetaxel and molecular targeted therapy for the treatment of metastatic prostate cancer. *Sci. Rep.* **7**, 1–8

234. Li, L. T., Jiang, G., Chen, Q., and Zheng, J. N. (2015) Predic Ki67 is a promising molecular target in the diagnosis of cancer (Review). *Mol. Med. Rep.* **11**, 1566–1572

235. Hammarsten, P., Josefsson, A., Thysell, E., Lundholm, M., Hägglöf, C., Iglesias-Gato, D., Flores-Morales, A., Stattin, P., Egevad, L., Granfors, T., Wikström, P., and Bergh, A. (2019) Immunoreactivity for prostate specific antigen and Ki67 differentiates subgroups of prostate cancer related to outcome. *Mod. Pathol.* **32**, 1310–1319

236. Koukourakis, M. I., Giatromanolaki, A., Sivridis, E., Gatter, K. C., and Harris, A. L. (2006) Lactate dehydrogenase 5 expression in operable colorectal cancer: Strong association with survival and activated vascular endothelial growth factor pathway - A report of the tumor angiogenesis research group. *J. Clin. Oncol.* **24**, 4301–4308

237. Li, F., Xiang, H., Pang, Z., Chen, Z., Dai, J., Chen, S., Xu, B., and Zhang, T. (2020) Association between lactate dehydrogenase levels and oncologic outcomes in metastatic prostate cancer: A meta-analysis. *Cancer Med.* **9**, 7341

238. Ren, H. Y., Sun, L. L., Li, H. Y., and Ye, Z. M. (2015) Prognostic significance of serum alkaline phosphatase level in osteosarcoma: A meta-analysis of published data. *Biomed Res. Int.* 10.1155/2015/160835

239. Li, D., Lv, H., Hao, X., Hu, B., and Song, Y. (2018) Prognostic value of serum alkaline phosphatase in the survival of prostate cancer: evidence from a meta-analysis. *Cancer Manag. Res.* **10**, 3125

240. Rosenblum, D., Joshi, N., Tao, W., Karp, J. M., and Peer, D. (2018) Progress and challenges towards targeted delivery of cancer therapeutics. *Nat. Commun. 2018 91*. **9**, 1–12

241. Din, F. ud, Aman, W., Ullah, I., Qureshi, O. S., Mustapha, O., Shafique, S., and Zeb, A. (2017) Effective use of nanocarriers as drug delivery systems for the treatment of selected tumors. *Int. J. Nanomedicine*. **12**, 7291

242. Zhang, W., Fan, W., Rachagani, S., Zhou, Z., Lele, S. M., Batra, S. K., and Garrison, J. C. (2019) Comparative Study of Subcutaneous and Orthotopic Mouse Models of Prostate Cancer: Vascular Perfusion, Vasculature Density, Hypoxic Burden and BB2r-Targeting Efficacy. *Sci. Rep.* **9**, 11117

243. Matthews, Q. L., and Curiel, D. T. (2007) Gene therapy: human germline genetic modifications--assessing the scientific, socioethical, and religious issues. *South. Med. J.* **100**, 98–100

244. Bank, A. (1996) Human somatic cell gene therapy. *Bioessays*. **18**, 999–1007

245. Villemejane, J., and Mir, L. M. (2009) Physical methods of nucleic acid transfer: general concepts and applications. *Br. J. Pharmacol.* **157**, 207

246. Zhang, G., Gao, X., Song, Y. K., Vollmer, R., Stolz, D. B., Gasiorowski, J. Z., Dean,

D. A., and Liu, D. (2004) Hydroporation as the mechanism of hydrodynamic delivery. *Gene Ther. 2004 118*. **11**, 675–682

247. Wolff, J. A., and Budker, V. (2005) The Mechanism of Naked DNA Uptake and Expression. *Adv. Genet.* **54**, 1–20

248. Changes in microtubules and microfilaments due to a combined effect of ultrasound and cytostatics in HeLa cells - PubMed [online] https://pubmed.ncbi.nlm.nih.gov/11508858/ (Accessed December 8, 2022)

249. Davalos, R. V., Mir, L. M., and Rubinsky, B. (2005) Tissue Ablation with Irreversible Electroporation. *Ann. Biomed. Eng. 2005 332*. **33**, 223–231

250. Freeman, E. C., Weiland, L. M., and Meng, W. S. (2013) Modeling the proton sponge hypothesis: examining proton sponge effectiveness for enhancing intracellular gene delivery through multiscale modeling. *J. Biomater. Sci. Polym. Ed.* **24**, 398–416

251. Sionov, R. V., and Haupt, Y. (1999) The cellular response to p53 : the decision between life and death

252. Vousden, K. H., and Lu, X. (2002) Live or let die: the cell's response to p53. *Nat. Rev. Cancer 2002 28*. **2**, 594–604

253. Lacroix, M., Toillon, R. A., and Leclercq, G. (2006) p53 and breast cancer, an update. *Endocr. Relat. Cancer*. **13**, 293–325

254. Ozaki, T., and Nakagawara, A. (2011) Role of p53 in Cell Death and Human Cancers. *Cancers (Basel).* **3**, 994

255. Baker, S. J., Fearon, E. R., Nigro, J. M., Hamilton, S. R., Preisinger, A. C., Jessup, J. M., Vantuinen, P., Ledbetter, D. H., Barker, D. F., Nakamura, Y., White, R., and Vogelstein, B. (1989) Chromosome 17 deletions and p53 gene mutations in colorectal

carcinomas. *Science*. **244**, 217–221

256. Nigro, J. M., Baker, S. J., Preisinger, A. C., Jessup, J. M., Hosteller, R., Cleary, K., Bigner, S. H., Davidson, N., Baylin, S., Devilee, P., Glover, T., Collins, F. S., Weslon, A., Modali, R., Harris, C. C., and Vogelstein, B. (1989) Mutations in the p53 gene occur in diverse human tumor types. *Nature*. **342**, 705–708

257. Takahashi, T., Nau, M. M., Chiba, I., Birrer, M. J., Rosenberg, R. K., Vinocour, M., Levitt, M., Pass, H., Gazdar, A. F., and Minna, J. D. (1989) p53: a frequent target for genetic abnormalities in lung cancer. *Science*. **246**, 491–494

258. Vogelstein, B. (1990) A deadly inheritance. *Nat. 1990 3486303*. **348**, 681–682

259. Hollstein, M. C., Metcalf, R. A., Welsh, J. A., Montesano, R., and Harris, C. C. (1990) Frequent mutation of the p53 gene in human esophageal cancer. *Proc. Natl. Acad. Sci. U. S. A.* **87**, 9958–9961

260. Hollstein, M., Sidransky, D., Vogelstein, B., and Harris, C. C. (1991) p53 mutations in human cancers. *Science*. **253**, 49–53

261. Absence of p53 gene mutations in primary neuroblastomas - PubMed [online] https://pubmed.ncbi.nlm.nih.gov/8221661/ (Accessed December 8, 2022)

262. Ramamoorth, M., and Narvekar, A. (2015) Non Viral Vectors in Gene Therapy- An Overview. *J. Clin. Diagn. Res.* **9**, GE01

263. García-Montoya, I. A., Cendón, T. S., Arévalo-Gallegos, S., and Rascón-Cruz, Q. (2012) Lactoferrin a multiple bioactive protein: An overview. *Biochim. Biophys. Acta. Gen. Subj.* **1820**, 226

264. Chen, J. (2016) The Cell-Cycle Arrest and Apoptotic Functions of p53 in Tumor Initiation and Progression. *Cold Spring Harb. Perspect. Med.*

10.1101/CSHPERSPECT.A026104

265. Rivlin, N., Brosh, R., Oren, M., and Rotter, V. (2011) Mutations in the p53 Tumor Suppressor Gene: Important Milestones at the Various Steps of Tumorigenesis. *Genes Cancer*. **2**, 466

Part of this thesis has been published in the following journals:

1. **Chukhu Muj**, Satyajit Mukhopadhyay, Anand K. Kondapi*. Synergistic action of lactoferrin in enhancing the safety and effectiveness of docetaxel treatment against prostate cancer. (Under review).

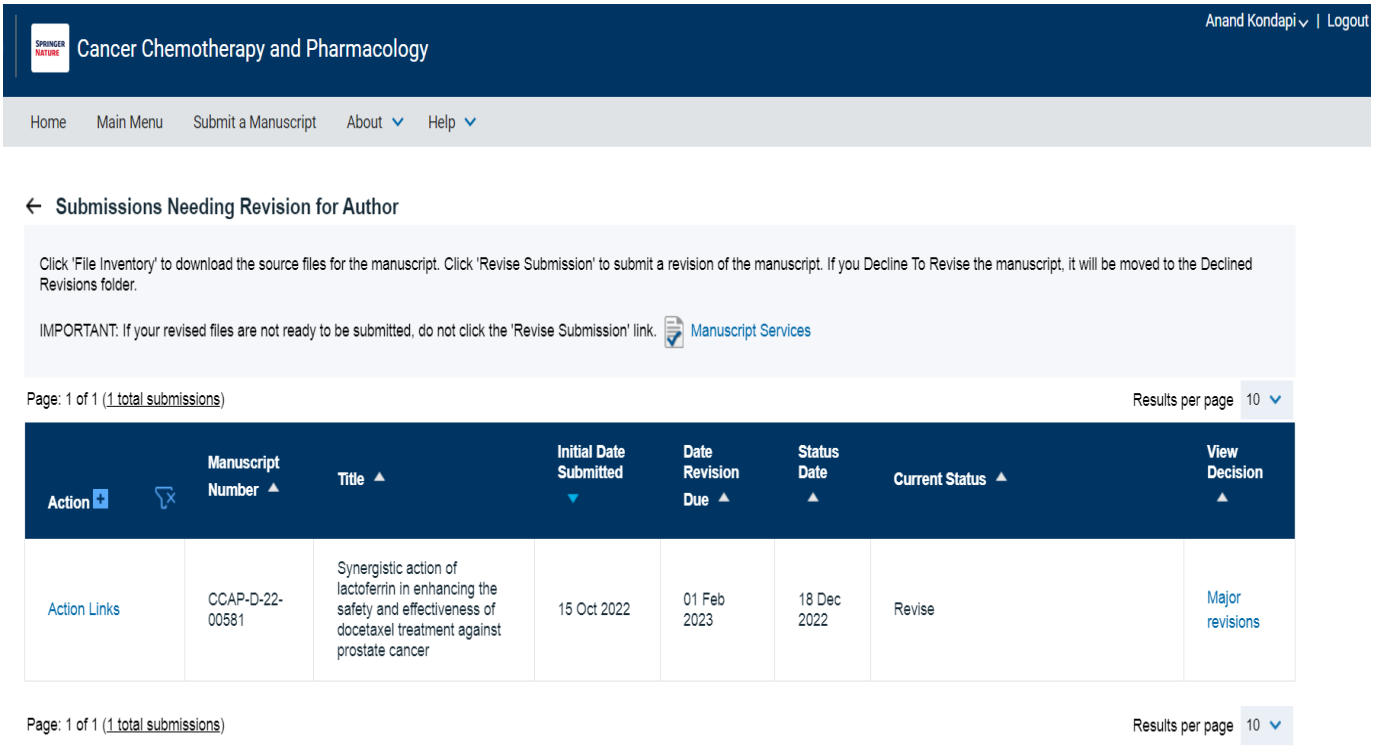

Cancer Chemotherapy and Pharmacology

Anand Kondapi | Logout

Home Main Menu Submit a Manuscript About Help

← Submissions Needing Revision for Author

Click 'File Inventory' to download the source files for the manuscript. Click 'Revise Submission' to submit a revision of the manuscript. If you Decline To Revise the manuscript, it will be moved to the Declined Revisions folder.

IMPORTANT: If your revised files are not ready to be submitted, do not click the 'Revise Submission' link. Manuscript Services

Page: 1 of 1 (1 total submissions) Results per page 10

Action	Manuscript Number	Title	Initial Date Submitted	Date Revision Due	Status Date	Current Status	View Decision
Action Links	CCAP-D-22-00581	Synergistic action of lactoferrin in enhancing the safety and effectiveness of docetaxel treatment against prostate cancer	15 Oct 2022	01 Feb 2023	18 Dec 2022	Revise	Major revisions

Page: 1 of 1 (1 total submissions) Results per page 10

An analysis of anticancer activities of drug- and DNA-loaded Nano formulations in vitro and in vivo

by Chukhu Muj

Submission date: 28-Dec-2022 04:01PM (UTC+0530)
Submission ID: 1987078710
File name: Chukhu_Muj_16LTPH03_Thesis_for_plagiarism.pdf (3.44M)
Word count: 21094
Character count: 112758

Prof. ANAND K. KONDAPI
Senior Professor
Dept. of Biotechnology & Bioinformatics
School of Life Sciences
University of Hyderabad
Gachibowli, Hyderabad-500 046.

An analysis of anticancer activities of drug- and DNA-loaded Nano formulations in vitro and in vivo

ORIGINALITY REPORT

7%	6%	5%	2%
SIMILARITY INDEX	INTERNET SOURCES	PUBLICATIONS	STUDENT PAPERS

PRIMARY SOURCES

1	www.nature.com Internet Source	2%
2	www.frontiersin.org Internet Source	<1%
3	Jiang Zhao, Chi Zhang, Weihao Wang, Chen Li, Xupeng Mu, Kebang Hu. "Current progress of nanomedicine for prostate cancer diagnosis and treatment", Biomedicine & Pharmacotherapy, 2022 Publication	<1%
4	Sonali Kumari, Anand Kumar Kondapi. "Receptor-mediated targeted delivery of DNA using Lactoferrin nanoparticles", International Journal of Biological Macromolecules, 2018 Publication	<1%
5	idoc.pub Internet Source	<1%
6	centaur.reading.ac.uk Internet Source	<1%

Prof. ANAND K. KONDAPI
Senior Professor
Dept. of Biotechnology & Bioinformatics
School of Life Sciences
University of Hyderabad
Gachibowli, Hyderabad-500 046.

7	Márcia Cristina Oliveira da Rocha, Patrícia Bento da Silva, Marina Arantes Radicchi, Bárbara Yasmin Garcia Andrade et al. "Docetaxel-loaded solid lipid nanoparticles prevent tumor growth and lung metastasis of 4T1 murine mammary carcinoma cells", Journal of Nanobiotechnology, 2020 Publication	<1 %
8	Zhu, Qian, Lixin Jia, Zhongfei Gao, Chunming Wang, Haoyang Jiang, Junfeng Zhang, and Lei Dong. "A Tumor Environment Responsive Doxorubicin-Loaded Nanoparticle for Targeted Cancer Therapy", Molecular Pharmaceutics, 2014. Publication	<1 %
9	iovs.arvojournals.org Internet Source	<1 %
10	Sonali Kumari, Anand K. Kondapi. "Lactoferrin nanoparticle mediated targeted delivery of 5-fluorouracil for enhanced therapeutic efficacy", International Journal of Biological Macromolecules, 2017 Publication	<1 %
11	www.wjem.org Internet Source	<1 %
12	baadalsg.inflibnet.ac.in Internet Source	<1 %

13	Song, Z.. "Curcumin-loaded PLGA-PEG-PLGA triblock copolymeric micelles: Preparation, pharmacokinetics and distribution in vivo", Journal of Colloid And Interface Science, 20110201 Publication	<1 %
14	cris.brighton.ac.uk Internet Source	<1 %
15	tessera.spandidos-publications.com Internet Source	<1 %
16	theses.gla.ac.uk Internet Source	<1 %
17	Sonali Kumari, Saad M. Ahsan, Jerald M. Kumar, Anand K. Kondapi, Nalam M. Rao. "Overcoming blood brain barrier with a dual purpose Temozolomide loaded Lactoferrin nanoparticles for combating glioma (SERP-17-12433)", Scientific Reports, 2017 Publication	<1 %
18	eprints.uanl.mx Internet Source	<1 %
19	Submitted to National University of Singapore Student Paper	<1 %
20	journals.plos.org Internet Source	<1 %

21	Sarah P. Sherlock, Hongjie Dai. "Multifunctional FeCo-graphitic carbon nanocrystals for combined imaging, drug delivery and tumor-specific photothermal therapy in mice", Nano Research, 2011 Publication	<1 %
22	Submitted to Spelman College Student Paper	<1 %
23	downloads.hindawi.com Internet Source	<1 %
24	escholarship.org Internet Source	<1 %
25	innovpub.org Internet Source	<1 %
26	tel.archives-ouvertes.fr Internet Source	<1 %
27	www.jimmunol.org Internet Source	<1 %
28	Submitted to King's College Student Paper	<1 %
29	T. Furuta, M. Fujita, R. Mukai, I. Sakakibara, T. Sata, K. Miki, M. Hayami, S. Kojima, Y. Yoshikawa. "Severe pulmonary pneumocystosis in simian acquired immunodeficiency syndrome induced by	<1 %

	simian immunodeficiency virus: its characterization by the polymerase-chain-reaction method and failure of experimental transmission to immunodeficient animals", Parasitology Research, 1993 Publication	
30	Submitted to University College London Student Paper	<1 %
31	Submitted to University of Sydney Student Paper	<1 %
32	etd.lib.metu.edu.tr Internet Source	<1 %
33	ijpsr.com Internet Source	<1 %
34	mdpi.com Internet Source	<1 %
35	urominas.com Internet Source	<1 %
36	Submitted to The University of Manchester Student Paper	<1 %
37	ntnuopen.ntnu.no Internet Source	<1 %
38	Submitted to Jawaharlal Nehru University (JNU) Student Paper	<1 %

39	Sonali Kumari, Dwaipayan Bhattacharya, Nandini Rangaraj, Sumana Chakarvarty, Anand K Kondapi, Nalam M Rao. "Aurora kinase B siRNA-loaded lactoferrin nanoparticles potentiate the efficacy of temozolomide in treating glioblastoma", Nanomedicine, 2018 Publication	<1 %
40	www.mdpi.com Internet Source	<1 %
41	www.science.gov Internet Source	<1 %
42	Yeruva Samrajya Lakshmi, Prashant Kumar, Golla Kishore, C Bhaskar, Anand K Kondapi. "Triple combination MPT vaginal microbicide using curcumin and efavirenz loaded lactoferrin nanoparticles", Scientific Reports, 2016 Publication	<1 %
43	polscientific.com Internet Source	<1 %
44	revistadechimie.ro Internet Source	<1 %

Exclude quotes On

Exclude matches < 14 words